

**IN VIVO VISUALIZATION OF NEURAL PATHWAYS IN THE RAT
SPINAL CORD USING VIRAL TRACING**

A Dissertation
Submitted to
the Temple University Graduate Board

In Partial Fulfillment
of the Requirements for the Degree
**DOCTOR OF PHILOSOPHY
OF BIOMEDICAL NEUROSCIENCE**

by
Kathleen M. Keefe
Diploma Date, August 2018

Examining Committee Members:

George Smith, PhD, Advisor, Shriner's Pediatric Research Center/Department of
Neuroscience

Wenhui Hu, MD, PhD, Committee Chair, Center for Metabolic Disease Research,
Department of Pathology and Laboratory Medicine

Barbara Krynska, MS, PhD, Shriner's Pediatric Research Center/Department of
Neuroscience

Shuxin Li, MD, PhD, Shriner's Pediatric Research Center/Department of
Neuroscience

Michel Lemay, PhD, External Examiner, Biomedical Engineering

©
Copyright
2018

by

Kathleen M. Keefe
All Rights Reserved

ABSTRACT

Much of our understanding of the fascinating complexity of neuronal circuits comes from anatomical tracing studies that use dyes or fluorescent markers to highlight pathways that run through the brain and spinal cord. Viral vectors have been utilized by many previous groups as tools to highlight pathways or deliver transgenes to neuronal populations to stimulate growth after injury. In a series of studies, we explore anterograde and retrograde tracing with viral vectors to trace spinal pathways and explore their contribution to behavior in a rodent model. In a separate study, we explore the effect of stimulating intrinsic growth programs on regrowth of corticospinal tract (CST) axons after contusive injury.

In the first study, we use self-complimentary adeno associated viral (scAAV) vectors to trace long descending tracts in the spinal cord. We demonstrate clear and bright labeling of cortico-, rubro- and reticulospinal pathways without the need for IH, and show that scAAV vectors transduce more efficiently than single stranded AAV (ssAAV) in neurons of both injured and uninjured animals. This study demonstrates the usefulness of these tracers in highlighting pathways descending from the brain.

Retrograde tracing is also a key facet of neuroanatomical studies involving long distance projection neurons. In the next study, we highlight a lentivirus that permits highly efficient retrograde transport (HiRet) from synaptic terminals within the cervical and lumbar enlargements of the spinal cord. By injecting HiRet, we can clearly identify supraspinal and propriospinal circuits innervating MN pools relating to forelimb and hindlimb function. We observed robust labeling of propriospinal neurons, including high fidelity details of dendritic arbors and axon terminals seldom seen with chemical tracers.

In addition, we examine changes in interneuronal circuits occurring after a thoracic contusion, highlighting populations that potentially contribute to spontaneous behavioral recovery in this lesion model.

In a related study, we use a modified version of HiRet as part of a multi-vector system that synaptically silences neurons to explore the contribution of the rubrospinal tract (RST) and CST to forelimb motor behavior in an intact rat. This system employs Tetanus toxin at the neuronal synapse to prevent release of neurotransmitter via cleavage of vesicle docking proteins, effectively preventing the propagation of action potentials in those neurons. We find that shutdown of the RST has no effect on gross forelimb motor function in the intact state, and that shutdown of a small population of CST neurons in the FMC has a modest effect on grip strength. These studies demonstrate that the HiRet lentivirus is a unique tool for examining neuronal circuitry and its contribution to function.

In the final study, we explore stimulation of the Phosphoinositide 3-kinase/Rac-alpha serine/threonine Protein Kinase (PI3K/AKT) growth pathway by antagonizing phosphatase and tensin homolog (PTEN), a major inhibitor, to encourage growth of CST axons after a contusive injury. We use systemic infusions of four distinct PTEN antagonist peptides (PAPs) targeted at different sites of the PTEN protein. We find robust axonal growth and sprouting caudal to a contusion in a subset of animals infused with PAPs targeted to the PTEN enzymatic pocket, including typical morphology of growing axons. Serotonergic fiber growth was unaffected by peptide infusion and did not correlate with CST fiber density. Though some variability was seen in the amount of growth within our animal groups, we find these PTEN antagonist peptides a promising and

clinically relevant tool to encourage CST sprouting, and a potentially useful addition to therapies using combinatory strategies to enhance growth.

These studies demonstrate that viral tracing is a powerful tool for mapping spinal pathways and elucidating their ability to reform spinal circuits after injury. Viral vectors can be used in both anterograde and retrograde tracing studies to highlight intricacies of neuronal cell bodies, axons and dendritic arbors with a high degree of fidelity. In the injured state, these tools can help identify pathways that contribute to spontaneous recovery of function by highlighting those that reform circuits past an injury site. In the uninjured state, these vectors can contain neuronal silencing methods that help define the contribution of specific pathways to behavior.

ACKNOWLEDGMENTS

I would like to acknowledge Dr. George Smith for supporting the work outlined in this thesis and for helping me achieve my dream of earning a doctorate of philosophy.

I would like to acknowledge all of the members of the Smith lab for their assistance over the years. Thank you to Yingpeng Liu for the surgical assistance and for helping me maintain my cool in the face of malfunctioning equipment. Thank you to Chidubem Eneanya, Ian Junker and Noelle Sterling for many hours of histology and microscope assistance. Thank you to Imran Sheikh for the commiseration.

I would like to acknowledge the members of my thesis committee for reading this extensive work – thank you for your time and energy.

I would like to acknowledge my fiancé Anthony Rubbo, who has been there to support me every step of the way, and has put up with all of the busy times.

I would like to acknowledge my friends Will and Sarah for always reminding me that I was capable of doing all of this.

I would like to acknowledge Shriner's Pediatric Research Center for supporting my work and fostering a welcoming and collaborative environment during my time as a graduate student.

TABLE OF CONTENTS

ABSTRACT.....	III
ACKNOWLEDGMENTS	VI
LIST OF FIGURES	IX
LIST OF ABBREVIATIONS	XI
CHAPTER 1. INTRODUCTION.....	1
Anatomy of the Spinal Cord	1
Descending Motor Pathways	6
Ascending Sensory Pathways	13
Propriospinal Interneurons.....	14
Spinal Cord Injury and its Effects.....	16
Why Do Neurons Fail to Regenerate?	25
The Rodent as a Model Organism for Spinal Cord Injury Studies	36
Using Viral Vectors for In Vivo Visualization and Regeneration Studies	40
CHAPTER 2. MAPPING SPINAL PATHWAYS VIA ANTEROGRADE TRACING WITH ADENO-ASSOCIATED VIRAL VECTORS	44
Introduction.....	44
Materials and Methods.....	46
Results.....	51
Discussion.....	56
CHAPTER 3. MAPPING SPINAL PATHWAYS AND ELUCIDATING THEIR CONTRIBUTION TO BEHAVIOR USING RETROGRADE TRACING WITH HIRET LENTIVIRUS	61
Introduction.....	61
Materials and Methods.....	68
Results.....	81
Discussion.....	93
CHAPTER 4. EXPLORING THE REGROWTH POTENTIAL OF SPINAL PATHWAYS AFTER INJURY.....	103
Introduction.....	103
Materials and Methods.....	105
Results.....	112

Discussion.....	123
CHAPTER 5. DISCUSSION	128
REFERENCES CITED	137

LIST OF FIGURES

Figure	Page
Figure 1. The structure of the vertebral column, spinal cord and spinal nerves.....	2
Figure 2. Segmental structure of the spinal cord, showing the attachment of the spinal roots.....	4
Figure 3 - Representation of Rexed Laminae	5
Figure 4. Location of Major Descending Motor Tracts in the Human Spinal Cord.....	7
Figure 5. Ascending Sensory Tracts in the Human Spinal Cord	14
Figure 6. Statistics on the Causes of Spinal Cord Injury	16
Figure 7. The Frequency of Spinal Cord Injury by Spinal Level	17
Figure 8. Blood Supply of the Spinal Cord.....	19
Figure 9. Retraction Bulbs in a Lesion Environment	23
Figure 10. Properties of the Lesion Environment.....	24
Figure 11. Ascending and Descending Tracts of the Rat Spinal Cord	37
Figure 12. Histological Features of a Contusive Injury.....	40
Figure 13. Specific neuronal transduction by recombinant scAAV2-GFP.....	52
Figure 14. GFP expression in the red nucleus and anterograde labeling of the rubrospinal tract	53
Figure 15. scAAV-GFP robustly labels axons at a lesion site.....	54
Figure 16. Anterograde labeling with AAV-mCherry.....	56
Figure 17. Experimental Details of the HiRet-GFP study	64
Figure 18. Schematic of the HiRet-TRE-eTeNT-eGFP vector.....	65
Figure 19. A double viral vector system for silencing neurons	65
Figure 20. HiRet/TetOn pilot study timeline	67
Figure 21. Timeline of HiRet/TetOn silencing experiment.....	67
Figure 22. Contusion Graphs from an Infinite Horizons Impactor.....	74

Figure 23. Extent of GFP-expressing neurons within the spinal cord in normal and T10 contused rats.....	84
Figure 24. GFP-positive neurons located within the brainstem after injection of HiRet-GFP into the lumbar spinal cord in uninjured and contused rats.....	87
Figure 25. Affected animal in the cylinder test.....	89
Figure 26. Animals injected with a multi-vector inducible system have profound forelimb deficits in the affected forelimb	89
Figure 27. Silencing of the Red Nucleus has no effect on behavior in uninjured animals.	91
Figure 28. Neuronal silencing of CST neurons affects grip strength.	93
Figure 29. Timeline of mTOR/STAT3 upregulation study	112
Figure 30. Increased growth of RST axons in animals treated with AAV-Rheb/STAT3	113
Figure 31. Axonal dieback is decreased in animals treated with a combination of AAV2-Rheb/STAT3.....	114
Figure 32. Behavioral assessments show mild proprioceptive recovery in animals treated with a combination of AAV-Rheb/STAT3.....	115
Figure 33. Experimental Timeline of PTEN Antagonist Peptide Study.....	116
Figure 34 – Increased CST axon density in a subset of animals treated with PAP2 and PAP3 knockdown peptides.	117
Figure 35 – CST axons in animals treated with PAP2 and PAP3 demonstrated typical profiles of sprouting or regenerative growth	118
Figure 36. Similar or lesser CST axon density was seen caudal to a contusion in animals treated with PAP1 or PAP4 peptides.	120
Figure 37. Serotonergic Fiber density was similar in all animal groups studied.....	122
Figure 38. No significant effect was seen on hindlimb locomotion in animals treated with PTEN antagonist peptides.....	123

LIST OF ABBREVIATIONS

5-HT – 5-hydroxytryptamine

AAV – Adeno Associated Virus

AchR – Acetylcholine Receptor

AKT – Rac-alpha serine/threonine Protein Kinase

ANOVA – Analysis of Variance

BBB – Beattie, Bresnahan and Basso

BDA – Biotinylated Dextran Amine

BDNF – Brain-Derived Neurotrophic Factor

BpV – Bisperoxovanadium

B-RAF – BRAF proto-oncogene

cAMP – Cyclic Adenosine Monophosphate

CMV - Cytomegalovirus

CNS – Central Nervous System

CPGs – Central Pattern Generators

CsCl – Cesium Chloride

CSF – Cerebrospinal Fluid

CST – Corticospinal Tract

DMSO – Dimethyl Sulfoxide

DNA – Deoxyribonucleic Acid

DRG – Dorsal Root Ganglion

eGFP – Enhanced Green Fluorescent Protein

eTeNT – Enhanced Tetanus Toxin

FMC – Forelimb Motor Cortex

FuG-B – Fusion Glycoprotein B

GAP-43 – Growth Associated Protein 43

GFAP – Glial Fibrillary Acidic Protein

GFP – Green Fluorescent Protein

GSK-3 – Glycogen synthase kinase 3

HEK – Human Embryonic Kidney

HiRet – Highly Efficient Retrograde Transport

HIV – Human Immunodeficiency Virus

IBB – Irvine, Beatties and Bresnahan

IH – Immunohistology

IHI – Infinite Horizons Impactor

IL-1 – Interleukin 1

kD – Kilodyne

LAPNs – Long Ascending Propriospinal Interneurons

LDPNs – Long Descending Propriospinal Interneurons

LMN – Lower Motor Neuron

LPN – Long Propriospinal Interneuron

MAG – Myelin-Associated Glycoprotein

MNs – Motor Neurons

MRF – Medullary Reticular Formation

mTOR – Mammalian Target of Rapamycin

NCAM – Neural Cell Adhesion Molecule

NeuN – Neuronal Nuclei

NGF – Nerve Growth Factor

Nogo – Neurite Outgrowth Inhibitor

NRG – Nucleus Reticularis Gigantocellularis

NT-3 – Neurotrophin-3

OMgp – Oligodendrocyte Myelin Glycoprotein

P75^{NTR} – P75 Neurotrophin Receptor

PAPs – Phosphatase and Tensin Homolog Antagonist Proteins

PBS – Phosphate Buffered Saline

PDH – Pyruvate Dehydrogenase

PDK1/2 – Phosphoinositide-dependent Kinase 1/2

PEG – Polyethylene Glycol

PEI - Polyethylenimine

PFA - Paraformaldehyde

PI3K – Phosphoinositide 3-kinase

PIP2 – Phosphatidylinositol bisphosphate

PIP3 – Phosphatidylinositol triphosphate

PNs – Propriospinal Interneurons

PNS – Peripheral Nervous System

PRF – Pontine Reticular Formation

PTEN – Phosphatase and Tensin Homolog

ReST – Reticulospinal Tract

Rheb – Ras Homolog Enriched in Brain

RN – Red Nucleus

RNA – Ribonucleic Acid

RST – Rubrospinal Tract

RTK – Receptor Tyrosine Kinase

RVG – Rabies Virus Glycoprotein

scAAV – Self-Complimentary Adeno Associated Virus

SCI – Spinal Cord Injury

SD – Standard Deviation

SEM – Standard Error of the Mean

SOCS3 – Suppressor of Cell Signaling 3

SPNs – Short Propriospinal Interneurons

ssAAV – Single Stranded Adeno Associated Virus

STAT3 – Signal Transducer and Activator of Transcription 3

TBS – Tris-Buffered Saline

TNF – Tumor Necrosis Factor

TRE – Tetracycline Responsive Element

TSA – Tyramide Signal Amplification

VSV-G – Vesicular Stomatitis Viral Glycoprotein

WGA – Wheat Germ Agglutinin

CHAPTER 1. INTRODUCTION

The spinal cord is an amazing anatomical structure that houses many of the cells and circuits ultimately responsible for human movement and sensation. Neurons in the spinal cord receive and integrate input from various sources, transmitting it to muscles to initiate both voluntary and involuntary actions. Understanding the flow of information into, out of and within the spinal cord is the key to realizing how these functions are controlled, and hopefully how to restore them if the circuits are damaged.

Anatomy of the Spinal Cord

The main function of the nervous system is to transmit information so we can decide on actions, direct the movement of our bodies and react to input from the environment. The central nervous system (CNS), which consists of the brain and spinal cord, is responsible for the decision to perform actions, the carrying out of those actions, and homeostasis, which allows the body to function properly. Generally, the brain is most active in making decisions and sending the necessary commands, and the spinal cord is the recipient of this input that then organizes and relays the information to the skeletal muscles, which carry out the actions.

More specifically, the spinal cord can be categorized as having three main functions: to conduct signals, to generate rhythmic patterns and to control reflex activity. The spinal cord conducts signals via the axons that run in fiber bundles throughout its length, either those that descend from the brain, or those that ascend from the periphery. Spinal cord segments can also connect with one another, allowing one segment to influence the activity in another. The experiments outlined here are most concerned with the ability of the spinal cord to conduct signals and generate rhythmic patterns.

In order to understand how the spinal cord conducts signals, one must understand its structure. The spinal cord is a thin rod of nervous tissue enclosed within the vertebral column, a series of segmented bones that descend on the dorsal aspect of a person, attaching rostrally to the skull and travelling caudally to the pelvis. In humans, the vertebral column is divided into 5 regions, which describe generally where the bones are located. There are seven cervical vertebrae located in the neck and shoulders, twelve thoracic vertebrae in the upper and mid back where the ribs attach, 5 lumbar vertebrae in the lower back, and 5 sacral and 4 coccygeal vertebrae in the pelvic and tailbone region. Figure 1 shows the vertebral column from a lateral view, with the first vertebral level of each segment marked (vertebral levels, left).

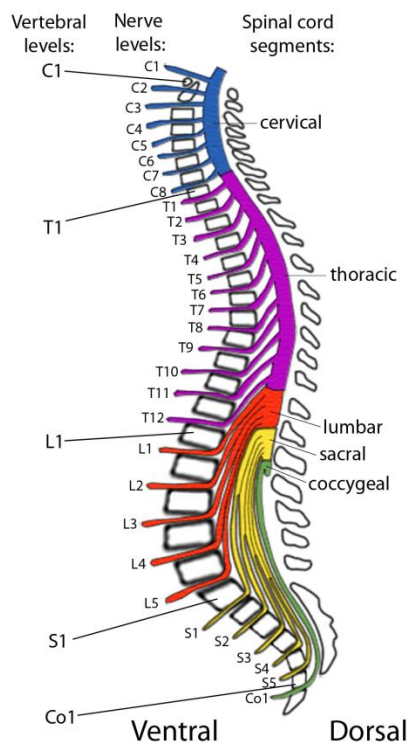


Figure 1. The structure of the vertebral column, spinal cord and spinal nerves - The spinal cord is shown in a lateral view encased within the segmented vertebral column. The five segments of the spinal cord are shown, as well as the location where each spinal nerve exits.

The nervous tissue of the spinal cord itself is not visibly segmented, but it is described as segmental in the same way as the vertebral column, with cervical, thoracic, lumbar, sacral and coccygeal regions. These regions are delineated by the 31 pairs of spinal nerves that exit the cord in regular intervals, one on each side. Early in development the spinal cord spans the entirety of the vertebral column, but as a fetus grows the rate of growth of the bones outpaces the rate of growth of the spinal cord, and thus in the adult human the main body of spinal tissue ends at about the L1 vertebrae, giving way to bundles of individual spinal nerves termed the *cauda equina*. Segments of actual spinal cord tissue are named according to where the roots attach to the body of the cord, which could be some distance away from where the nerves exit (Figure 1). In this document I will refer to spinal levels when speaking about injections or injuries made to the spine, by which I mean the segment of the nervous tissue itself, not the vertebrae.

In order to appreciate how information flows into and out of the spinal cord, it is helpful to observe a cross section of a single spinal segment. There are two distinctive types of tissue in the spinal cord, the gray matter and the white matter. The gray matter, which is named for its darker appearance, lies in the medial portion of the cord, in a distinctive 'H' or butterfly shape. This houses the cell bodies of neurons and glia, as well as the dendrites and proximal parts of axons making synaptic contact with gray matter neurons. White matter, which is lighter due to the presence of myelin, surrounds the gray matter and is composed of bundles of axons that carry information from one part of the CNS to another. Nerve roots attach to each side of the cord, some dorsally (the dorsal roots) and others ventrally (the ventral roots). These roots join together outside the spinal cord to become the spinal nerves for each segment (Figure 2).

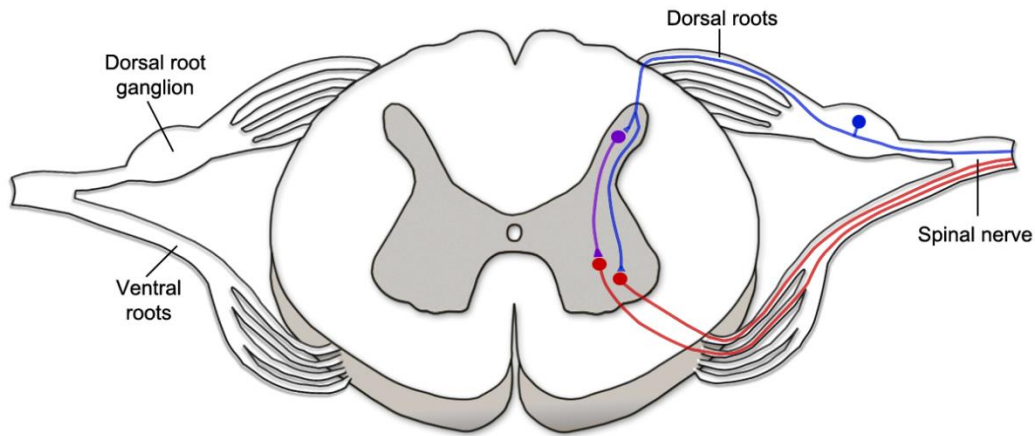


Figure 2. Segmental structure of the spinal cord, showing the attachment of the spinal roots - A drawing of a coronal section of the spinal cord demonstrates the location of the gray and white matter, and the attachment of the dorsal and ventral roots, which join together outside the spinal cord to form the spinal nerves. An example sensory neuron, with its cell body in the dorsal root ganglion (DRG), is represented in blue. A motor neuron (MN) is represented in red and an interneuron in purple.

The cell bodies of sensory neurons are housed in the DRG, a bulge seen in each dorsal root (Figure 2, blue neuron). These neurons receive information from the sensory receptors in the peripheral nervous system, such as those in the skin or muscle spindles, and relay that information into the spinal cord via their connections with MNs (red) or interneurons (purple). The axons of MNs travel through the ventral roots and out to the skeletal muscles, where their signals cause muscle contraction and directly affect movement. Thus, a general summary of information flow in the spinal cord could state that sensory information flows through the dorsal roots into the spinal cord, and motor information flows through the ventral roots and out of the spinal cord.

Locations in the spinal cord are often referred to with anatomical directions – white matter can be divided into dorsal, ventral or lateral columns, and gray matter into dorsal and ventral horns. As the gray matter houses the inherently interesting and diverse neuronal population, further divisions can be noticed due to cell type and density,

directional arrangement of processes and the concentration of synaptic connections in the region. A system of organization was first developed by neuroscientist Bror Rexed in 1952 (Rexed, 1952). He noticed that cells in the gray matter were arranged regularly in different zones if you were viewing the spinal cord in cross section, and that this organization was continuous along the entire length of the cord. He termed these regions ‘laminae’, which I have reproduced in Figure 3. Knowledge of Rexed laminae is especially important to studies that involve injection of fluid into the spinal cord. A successful experiment depends on correctly targeting the laminae of the desired neuronal or synaptic population with the needle that is infusing your virus or dye. Several studies contained within this work will refer to these laminar targets.

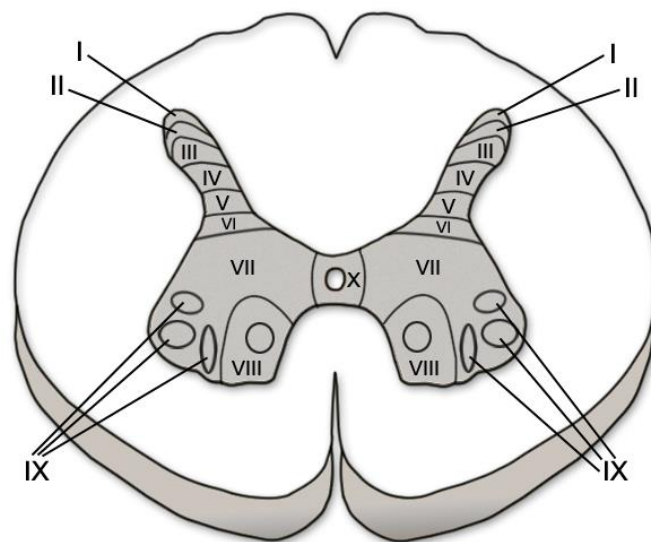


Figure 3 - Representation of Rexed Laminae

Understanding the structure of the spinal cord and the flow of information into and out of it is important when studying spinal cord injury (SCI) and nerve regeneration, as these details can reveal what types of information will be interrupted when an injury occurs and where regrowing axons may be likely to make reconnections. It is also

important to take into consideration the location and course of fiber bundles descending from the brain and how these form the spinal tracts.

Descending Motor Pathways

How does the brain influence movement? Groups of neurons are clustered together in structures called nuclei in the brain and brainstem. The axons of these clustered neurons travel together as they descend into the spinal cord, forming the descending motor pathways. Individual pathways often control specific types of movements, and the descending axons, which travel together in the white matter of the spinal cord, will at some point leave the white matter to synapse upon MNs in the gray matter that connect to the muscles associated with that type of movement. These gray matter neurons with direct connections to muscles are termed lower motor neurons (LMNs).

At the cervical spinal cord levels, descending motor axons synapse on the LMNs that innervate muscles of the neck and upper limbs. At the thoracic levels, the descending axons innervate LMNs that control trunk muscles, at lumbar and sacral levels LMNs innervate muscles that control the lower limbs, and at the coccygeal level the LMNs innervate muscles of the bowel and urogenital systems.

The majority of axons represented in descending motor pathways can be divided into two major groups: lateral pathways and medial pathways. These divisions refer to where the axonal fibers run in the spinal cord and what MNs they tend to synapse upon. These pathways cooperate in directing most movement, but their functions and locations are distinct from each other. The lateral pathways are so named because they descend in

the lateral portion of the white matter of the spinal cord, and synapse on more lateral MNs once they reach the gray matter. The target MNs of the lateral pathways control more distal musculature, such as distal limb muscles and muscles of the extremities. The main lateral tracts are the lateral CST, the RST and the raphespinal tract.

The second major group is the medial group, so named because their axons descend in the more medial portions of the spinal cord white matter, and tend to synapse on medial MNs in the spinal gray. These neurons control axial musculature such as proximal limb and trunk muscles. Medial pathways include the anterior corticospinal, tectospinal, medial & lateral reticulospinal, and the medial and lateral vestibulospinal tracts. Figure 4 outlines the location of the major lateral and medial descending tracts in the white matter of the spinal cord.

Understanding the positioning of these tracts is especially vital when studying SCI. The proximity of these tracts to each other often means that an injury can affect multiple tracts, and therefore multiple types of movement.

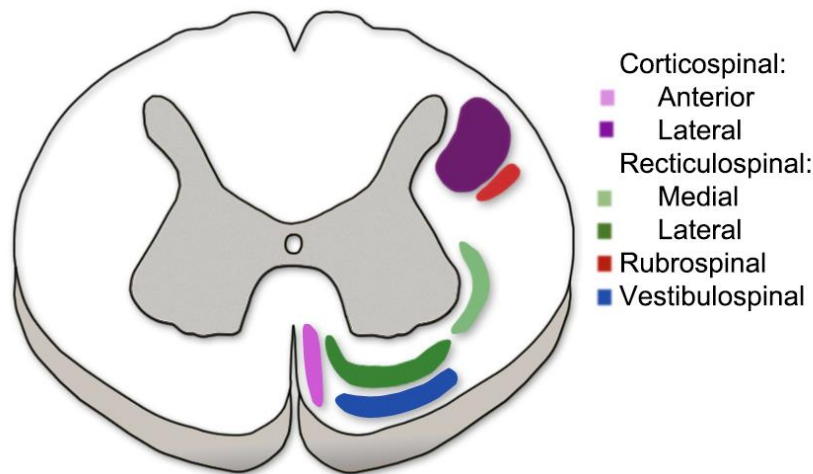


Figure 4. Location of Major Descending Motor Tracts in the Human Spinal Cord - The approximate locations of the major medial and lateral long descending motor tracts are shown in this representation of the human spinal cord. Tracts are shown as distinct for ease of viewing. In reality, there is no discrete border where one tract ends and another begins, and there is some natural overlap.

Below I have outlined salient facts about the motor tracts traced in these studies, including the types of movement they control, where they originate and what LMNs they innervate. It should be noted that nearly all spinal tracts actually contain a mixture of fibers, as a small amount of information about where the body is in space (proprioception) is intertwined with nearly every fiber tract. However, for simplicity's sake tracts are referred to by the type of movement that the majority of their fibers control.

The Corticospinal Tract

The CST originates in the cerebral cortex and descends via the internal capsule and cerebral crus into the medullary pyramids. In humans, about 85% of the fibers decussate at the pyramids and run in the lateral funiculus of the spinal cord as the lateral CST, and the remaining 15% run ipsilaterally as the anterior CST. Axons of both of these divisions terminate along the entire length of the spinal cord, but are most concentrated in the cervical and lumbosacral enlargements. The function of the CST is varied, and includes roles such as direct or indirect control of MNs, regulation of spinal reflexes, control of nociceptive (associated with pain stimulus) afferents and contribution to autonomic functions (Alstermark et al., 1992; Bacon and Smith, 1993; Cheema et al., 1984; Evarts and Tanji, 1976).

The CSTs role in voluntary control of large groups of musculature makes it one of the most clinically important pathways. The lateral CST is especially important in control of the extremities such as the hands and fingers, and more specifically in fractionating

finger movement (the ability to move the fingers individually) and in precision grip. The anterior CST is associated with control of bilateral trunk muscles. The origins of the CST in the cortex include multiple areas in the parietal lobe. The most important of these is the primary motor cortex, which is the origin of half of all CST fibers, and which is interconnected with the other cortical areas of CST origin, such as the premotor and supplementary motor areas. The primary motor cortex is considered responsible for carrying out voluntary movement while the associated areas are involved in planning movement sequences (supplementary motor area), and sensory guidance of movement (premotor areas) (Lemon and Griffiths, 2005; Lemon, 2008).

Synaptic terminals of corticospinal neurons can make direct connections onto MNs that control voluntary movement, as well as connections to spinal interneurons that integrate signals from various descending tracts. Some percentage of CST terminals are also present in the dorsal horn, where they may contribute to the regulation of sensory input (Canedo, 1997; Wall and Lidieth, 1997).

The Rubrospinal Tract

The RST originates in the red nucleus (RN), a large nucleus located in the tegmentum of the midbrain. In humans, the RN is divided into distinct magnocellular and parvocellular divisions. These divisions are named because of the majority cell types within them – medium and small cells are found in the parvocellular division, while large cells are found in the magnocellular division. These divisions are less clear in lower species, where there is overlap of cellular types (Massion, 1967). The divisions are thought to have different functions, though the exact function of the RN, its divisions and the RST are still under investigation.

RST axons originate from the magnocellular division. The majority of these axons decussate immediately upon exiting the RN in the ventral tegmental decussation, and travel caudally just ventral to the spinal trigeminal nucleus. This tract runs the length of the spinal cord in the dorsolateral funiculus. Though the majority of RST axons run contralaterally, there is a small uncrossed component found in the rat and certain other species (Antal et al., 1992; Holstege, 1987; Shieh et al., 1983).

Although the function of the RST, especially in humans, is not completely understood, the many connections received by the RN make it an intriguing anatomical area. The parvocellular RN receives major input from the cerebellum and the cerebral cortex, and additional projections to both divisions also arise from areas such as the posterior thalamic nuclei, the central pontine grey, the raphe nucleus and several reticular nuclei (Massion, 1967; Roger and Cadusseau, 1987; Stanton, 1980). RN circuitry connected with the cerebellum and inferior olivary nucleus may contribute to motor learning and the formation of motor memories via error detection and mental rehearsal of movement (Kennedy, 1979; Gilbert and Thach, 1977).

Research in cats found that flexion of the contralateral hind limbs (especially hip joints and overall limb movements) during the swing phase of locomotion occurred with electrical stimulation of the RN (Orlovsky, 1972), though others found that destruction of the RN did not result in a decrease in flexor activity during locomotion (Ingram et al., 1932; Tsukahara et al., 1964). Some theorize that the RN may be responsible for adjustments of the level of activity of different flexors, functioning in the correction of movements (Massion, 1967). This may make deficits associated with RST impairment more subtle and harder to analyze by many behavioral measures. Indeed, studies from

labs such as the Whishaw group that use more granular analyses have shed some light on subtle functions of the RN and RST. Kinetic analysis of locomotion after excitotoxic lesions of the RN detected an asymmetric gait with abnormal kinematics due to slightly adjusted timing and placement of the impaired limbs, especially the forelimb. This suggested to them that the RST may participate in continual step-to-step adjustments occurring during locomotion (Muir and Whishaw, 2000).

RN ablation studies analyzing contribution to forelimb function from that same group have revealed subtle defects during certain aspects of reaching and grasping (Whishaw et al., 1990; Whishaw et al., 1998). When a rat reaches for a food pellet, it first brings its elbow to the midline of the body to assist in aiming. The arm and paw are then extended with the palm of the paw facedown. The paw is brought over the pellet and the fingers move to grasp the pellet in a staggered motion called an ‘arpeggio’ movement. Once the pellet is grasped, the arm is brought back towards the mouth and the paw is turned into a supine position in order to eat the pellet. Excitotoxic lesions of the RN interfere with the aiming, arpeggio movement and supination steps of the reaching program described above. Lesions specific to the magnocellular division, where the RST originates, effect only the arpeggio movement (Morris et al., 2015).

This contribution of the RST to movements of distal and intermediate muscles of the forelimb is also supported by studies in cats and monkeys that found direct synapses of the RST onto distal forelimb MNs (Kuchler et al., 2002; Fujito and Aoki, 1995). This is notable because the majority of RST axons do not make direct connections onto MNs, but instead synapse on interneurons in laminae V, VI and VII, with a large population of

terminals in the cervical and lumbosacral enlargements (L. T. Brown, 1974; Antal et al., 1992).

The Reticulospinal Tract

The reticulospinal tract (ReST) is classified as a medial motor pathway as its fibers run medially in the white matter. It is divided into a medial ReST, and, somewhat confusingly, a lateral ReST. This terminology simply refers to their relative positions to each other, with the lateral tract running more laterally than the medial tract.

Reticulospinal fibers originate in the scattered brainstem nuclei referred to as the reticular formation. Rostral reticular nuclei in the midbrain contribute to alertness, consciousness and respiratory control. As you descend to the pons and medulla, the nuclei contribute to motor functions such as preparation for movement and postural control over limb and trunk muscles.

The medial ReST originates in the pontine reticular formation (PRF), and mainly provides support against gravity for standing by enhancing extensor muscle tone. This tract is greatly ipsilateral, running medially in the brainstem and remaining uncrossed to run in the ventromedial spinal cord. The lateral ReST originates in the medullary reticular formation (MRF) of the medulla. The MRF contains the nucleus reticularis gigantocellularis, which is known for integration of motor commands from the mesencephalic motor region and other areas (Alstermark et al., 1992). This tract contributes to preparation for movement through the Nucleus Reticularis Gigantocellularis (NRG), as well as adjustment of muscle tone during postural movements and inhibition of axial muscles during locomotion to achieve smooth movement. ReST fibers are found throughout the spinal cord, with characteristic terminations in laminae VII and VIII on interneurons and long propriospinal neurons.

Ascending Sensory Pathways

The studies outlined here deal mostly with motor behavior, targeting motor tracts and their contributions to movement. However, spinal cord injuries are by their nature diffuse injuries, and they often involve deficits in sensory modalities. A brief outline of important ascending tracts, which carry sensory information, is worth reviewing for their potential contributions to both deficit and recovery.

The largest ascending fiber tracts are the dorsal column pathways. These travel from peripheral sensory receptors to nuclei in the caudal medulla, where they decussate and ascend to the thalamus and then to the cerebral cortex. Some collaterals also enter the gray matter of the spinal cord to synapse on interneurons or MNs. Dorsal column pathways can be divided into two regions – the fasciculus gracilis and the fasciculus cuneatus. These fibers carry information concerning proprioception, as well as vibration sense and fine touch, which is the ability to both realize a touch sensation and localize it. The fasciculus gracilis transmits information from the mid-thoracic spinal cord levels (about T7) and below, dealing with information from the lower limbs and trunk. It takes up the majority of the dorsal white matter of the spinal cord until about T6, where it is pushed to the dorsomedial aspect by the fasciculus cuneatus. Cuneatus fibers carry information from the upper limbs, trunk and neck (Figure 5).

The spinothalamic tract carries information about pain and temperature, and controls different types of touch sensations, such as crude (or non-discriminative) touch (touch sensation without localization), light touch, tickle and itch. It runs close to the ventral horn of the spinal cord, ascending to synapse in thalamic nuclei. The spinocerebellar pathway transmits information about unconscious proprioception, such as

the relative position of your joints, to the cerebellum. It runs in a rim in the lateral aspect of the white matter, ascending to synapse in the deep cerebellar nuclei.

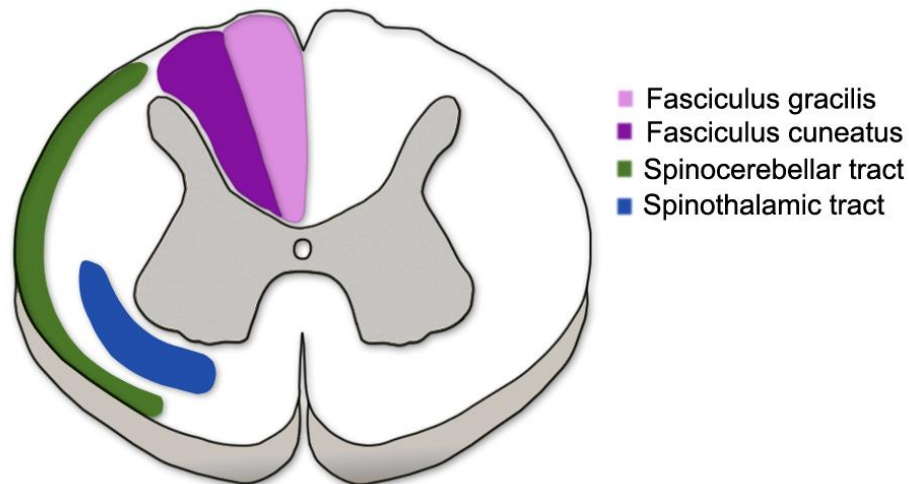


Figure 5. Ascending Sensory Tracts in the Human Spinal Cord – This schematic reflects a spinal cord segment above T6, since both dorsal column pathways are present.

Propriospinal Interneurons

The final neuronal population that needs mentioning is the propriospinal interneurons (PNs). These are neurons with their cell bodies entirely within the spinal cord. These cells were originally defined by Sir Charles Scott Sherrington and E.E. Laslett in the early 1900s when they were searching for intrinsic spinal pathways that would explain electrophysiological data contradicting their current doctrines of tracts descending entirely from the brain. They discovered neurons which connected spinal segments to each other, and suggested there were two groups – those with long fibers connecting distant segments to each other, and those with shorter fibers connecting closer segments. It was suggested that these fibers participated in motor reflexes (Sherrington and Laslett, 1903).

Later, it was confirmed via electrophysiology that a group of long PNs connect the lumbar and cervical segments of the spinal cord and that these neurons receive

sensory input so that they can regulate rhythmicity of movement by their connection to the central pattern generators (CPGs) (Jankowska et al., 1967; Kostyuk and Vasilenko, 1979). Both long and short PNs work together with MNs, integrating information from descending and ascending pathways to generate smooth and appropriate movement and control spinal reflexes. PNs are also referred to based on the direction that the axons run, either ascending or descending (Alstermark et al., 1987).

Short PNs (SPNs) are defined as those that connect six or fewer spinal segments. Their cell bodies are located in most laminae throughout each segment of the spinal cord (excluding lamina IX), though the majority are located in intermediate lamina VII. SPN axons surround the gray matter, running at the gray-white matter interface (Flynn et al., 2011; Menetrey et al., 1985; Matsushita, 1970; Sterling and Kuypers, 1968). Included in the category of SPNs are the thoracic PNs (TPNs), which connect segments of the thoracic spinal cord to lumbar segments.

Long PNs (LPNs) connect spinal segments separated by more than six segments, and include inter-enlargement connections. The long descending PNs (LDPNs) have their cell bodies in the cervical enlargements, with axons that reach the lumbar enlargement, and the long ascending PNs (LAPNs) have their cell bodies in the lumbar enlargement, with axons that project rostrally. The axons of LPNs run along the lateral and ventral outer edges of the white matter. PNs are a hotly researched topic at this moment, as recent evidence suggests that these pathways can be used as relays to bypass injured tissue and forge functional connections in the spinal cord (Bareyre et al., 2004; Courtine et al., 2008; Asboth et al., 2018; Kinoshita et al., 2012; Filli et al., 2014; Filli and Schwab, 2015).

Spinal Cord Injury and its Effects

An injury to the spinal cord is devastating because the severing of axons traveling in the white matter tracts mentioned and the destruction of neurons in the gray matter interrupt the signals being propagated. In the case of a complete injury, this means that muscles below the damaged area are unable to receive the signals needed to contract, resulting in paralysis below the injury. Ascending sensory tracts are also affected, meaning that sensation below the level of injury is deficient.

As of 2017, there are approximately 285,000 persons living with SCI in the United States, with approximately 17,000 new cases per year. Injury is most often caused by vehicular accidents or falls, which generate a blunt force impact to the spinal column (Figure 6). This impact fractures or dislocates the vertebral bodies, which in turn severs or compresses spinal cord tissue.

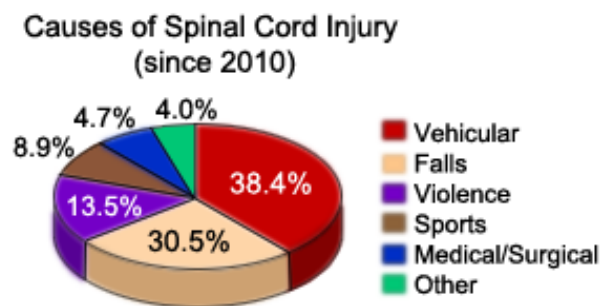


Figure 6. Statistics on the Causes of Spinal Cord Injury - Percentages reflect causes of SCI in America. Numbers can vary by country, though car accidents and falls are often the top two causes of injury. *Modified from National Spinal Cord Injury Statistical Center's 'Spinal Cord Injury Facts and Figures at a Glance'*

SCI occurs most frequently at the cervical level (~60%), followed by the thoracic (32%), then lumbosacral levels (9%), as represented in Figure 7 (Chen et al., 2016). The cervical vertebrae are some of the thinnest and most delicate bones in the axial skeleton,

which contributes to the higher frequency of injury. An injury can be classified as complete or incomplete, depending on the amount of damage done to the spinal cord tissue. The majority of injuries are incomplete, meaning that some neurons and axons at the site of the lesion are spared. Spared tissue may allow some signals to bypass the injury, allowing limited muscle function or sensation below the injury.

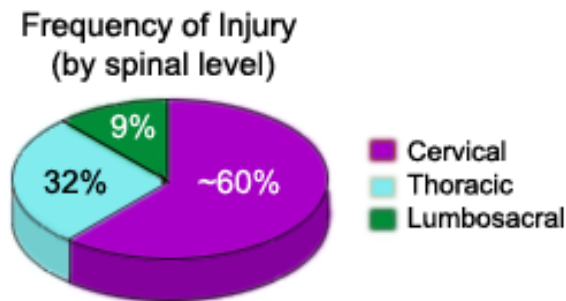


Figure 7. The Frequency of Spinal Cord Injury by Spinal Level

The mechanical trauma caused by impact to the spinal cord is a massive shock to the system, and this primary trauma initiates a cellular cascade which can damage the tissue around the impact area even further. These processes fundamentally change the structure of the affected spinal cord, not only due to the severed axons and damaged neurons, but also via formation of fluid-filled cavities and cellular barriers initiated by the immune system. The primary and secondary injury phases are followed by a more stable chronic injury phase.

Primary Injury

When the tissue of the spinal cord is damaged by blunt force or laceration a cascade of neurological damage occurs. The immediate damage to the tissue is termed the **primary injury**. Primary injury encompasses the death of neurons and glia at the site of

impact, the severing of the axons that conduct electrical signals to targets such as muscles or organs, and the interruption of the blood supply that nourishes the area via damage to the blood vessels. Primary injury is often referred to as a mechanical injury as it is caused by forces outside the body. This is in contrast to biochemical injury, which is injury caused by the body itself via chemical cascades and activation of the immune system. The shock of a primary injury causes a biochemical cascade termed **secondary injury**, which can begin minutes after the initial damage, and last for weeks. These cascades can cause progressive cell death and expand the area of the initial damage.

Secondary Injury

Major events of the secondary injury phase include vascular changes, invasion by immune system cells, additional cell death of neurons and glia surrounding the injury, demyelination and degeneration of axons, and structural remodeling of the tissue to form a glial scar and cystic cavities (for review, see (Ahuja et al., 2017)). Secondary injury represents a push-pull scenario where the body is trying to destroy dead tissue and isolate areas that might cause further damage to healthy tissue, and simultaneously promote as much survival of damaged and struggling areas as it can. This is reflected in the regulation of genes at the time of injury – in the early stages genes involved in transcription and inflammation are upregulated, while many genes involved in manufacturing structural proteins and proteins involved in neurotransmission are downregulated. This may represent the attempt to isolate and destroy unhealthy tissue. In later stages, upregulation of genes associated with growth factor expression, angiogenic factors and axonal guidance factors represent an attempt for growth and repair, while downregulation of cytoskeletal proteins and upregulation of proteases discourage growth

(Bareyre and Schwab, 2003). Due to the potential for further damage from secondary injury cascades, immediate treatment is critical to maintain spared sections of tissue around the impact area. An old adage in the clinical community is ‘time is spine’, referring to the rush to save spared tissue.

Vascular Changes

The major blood supply of the spinal cord is provided by the anterior and posterior spinal arteries, which branch to perfuse both the white and gray matter (Figure 8). The gray matter especially is rich in capillaries, which provide the necessary nutrients to neuronal and glial cell bodies.

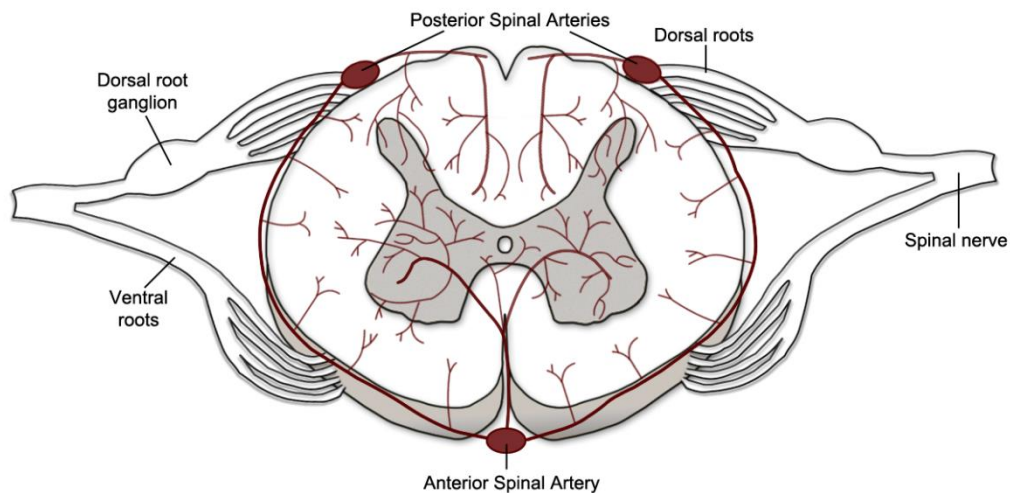


Figure 8. Blood Supply of the Spinal Cord

After an initial blunt impact, bleeding (hemorrhage) will occur into the spinal cord tissue from broken blood vessels and capillaries. In the following hours, this hemorrhage slowly enlarges. Pinprick (petechial) hemorrhages appear around the site of injury first, and then in more distant areas (Kawata et al., 1993). These hemorrhages coalesce,

expanding the damaged area three dimensionally. This is especially true if the injured area encompasses the gray matter. Secondary injury cascades can cause capillaries to undergo a delayed structural failure, breaking them apart in a phenomenon called progressive hemorrhagic necrosis (Guth et al., 1999; Simard et al., 2007). Those blood vessels whose structural integrity wasn't immediately compromised by the primary injury can suddenly constrict (vasospasm), causing a reduction in diameter of the vessel, and reducing the rate of blood flow. This can cause death of neurons and glia as they are deprived of their nutrients and unable to recycle waste.

Immune System Activation and Invasion

SCI results in the immediate activation of cells of the immune system. Microglia and astrocytes at the lesion site can become activated, releasing pro-inflammatory cytokines such as interleukin 1 (IL-1) and tumor necrosis factor (TNF). IL-1 and TNF aid in further recruitment of immune cells to the area by modulating cell adhesion molecules, which allow leukocytes to exit from blood vessels and infiltrate tissue (Sroga et al., 2003). At different time points during the injury cascade, neutrophils, macrophages and T cells are attracted to the lesion area (Sroga et al., 2003; Bareyre and Schwab, 2003). These cells can release further cytokines, affecting the lesion environment (Pineau and Lacroix, 2007). Cytokines can be toxic to neurons and glia, causing demyelination and further axon damage (for reviews see (Allan and Rothwell, 2001; Tator and Fehlings, 1991).

Cell Death and Apoptosis

Death of neurons and glia can happen after the initial mechanical trauma. Disruption of cell membranes causes an ionic imbalance in the environment as ions that were once inside cells spill out. Disruption of the ionic balance of K^+ , Na^+ and Ca^{2+} leads to depolarization of cell membranes, failure of ATPase pumps and activation of proteases. Further downregulation of genes associated with Na^+ , K^+ , Na^+/Ca^{2+} and Na^+/HCO_3^- transporter synthesis means that the cell may not be able to recover, and could trigger self-destruction protocols (apoptosis) (Stys et al., 1998; G. Song et al., 2001; Lumb, 2017). Activation of apoptotic programs occur in both neurons and glial cells and may continue for many weeks after injury. Evidence for apoptosis after SCI exists in humans, monkeys and rodents (Beattie et al., 2000; Crowe et al., 1997; Emery et al., 1998).

Demyelination and Axon Degeneration

Apoptosis of the oligodendrocytes that enwrap CNS axons contributes to demyelination that occurs after the initial SCI. Proteins associated with myelin such as neurite outgrowth inhibitor (Nogo), myelin-associated glycoprotein (MAG), and oligodendrocyte myelin glycoprotein (OMgp) inhibit axon outgrowth and induce growth cone collapse in the axon (Domeniconi et al., 2002; M. Li et al., 1996; GrandPre et al., 2000; Prinjha et al., 2000; K. C. Wang et al., 2002).

The axons themselves undergo several processes, both death-related and later, growth-related. Segments of severed axons closest to the lesion environment experience cytoskeletal breakdown, undergoing fragmentation in a process known as Wallerian

degeneration. This process simultaneously affects all injured axons in the area, and has been potentially attributed to dysfunctional autophagy or the lack of transport into the axon of a “survival signal” (for review see (Conforti et al., 2014)). Axons shortened because of fragmentation are referred to as having “died back”.

Another hallmark of axons in the lesion environment is retraction bulbs (Hill et al., 2001; S. R. Y. Cajal et al., 1991). These are swollen endings of axons which contain disrupted cytoskeletal proteins and accumulations of membrane parts and organelles present because of impaired transport or growth cone collapse (Kamber et al., 2009; Tom et al., 2004; Erturk et al., 2007; Bresnahan, 1978). These bulbs are most prevalent closest to the lesion site and may persist for months (Hill et al., 2001) or even years after injury (Ruschel et al., 2015). The presence of retraction bulbs can reflect axons attempting to regenerate by forming new growth cones, but failing due to the hostile lesion environment (Davies et al., 1999). Figure 9 demonstrates examples of retraction bulbs in a lesion environment.

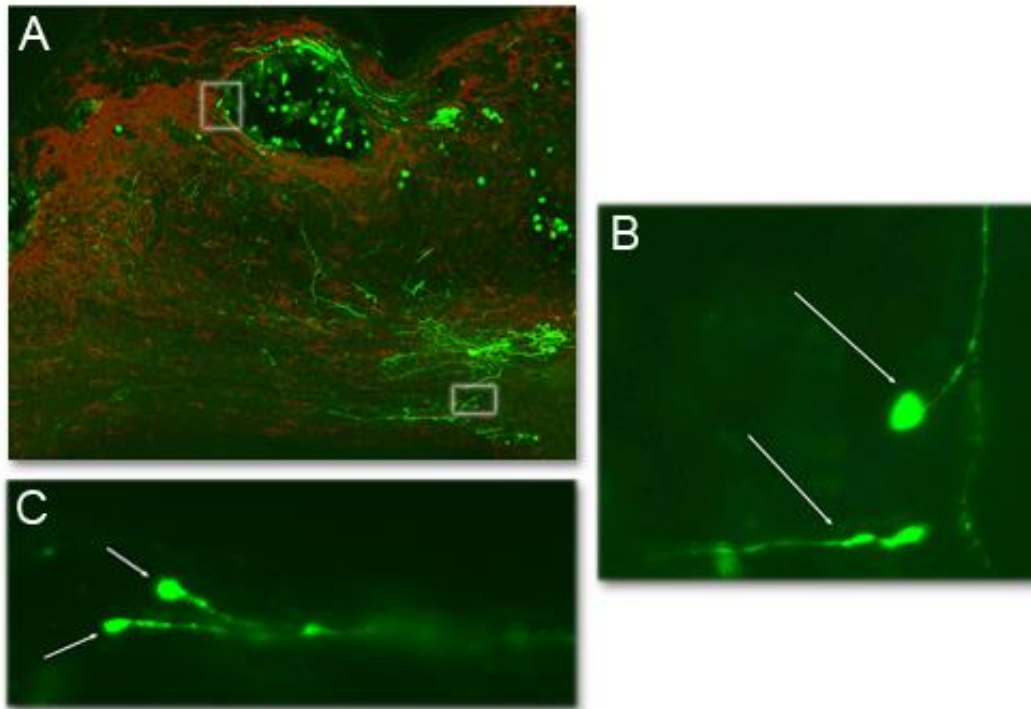


Figure 9. Retraction Bulbs in a Lesion Environment – An injured spinal cord is pictured with examples of axons ending in retraction bulbs. A) Low magnification shows necrotic areas and strong Glial Fibrillary Acidic Protein (GFAP) staining (red) denoting astrocytic scarring. Retraction bulbs are seen approaching areas of cavitation (upper box, high magnification B), and in adjacent tissue (lower right box, high magnification in C).

Cystic Cavities and the Glial Scar

In the majority of human spinal cord injuries, fluid filled cavities form in the injured area. These cavities are cordoned off by the action of reactive astrocytes in the area. The astrocytes interweave their processes to form a dense barrier termed the glial scar. During the first few days, signaling from activated microglia and invading macrophages cause the addition of extracellular matrix proteins such as Chondroitin Sulfate Proteoglycans to the scar (Ahuja et al., 2016; McKeon et al., 1991). These proteins act as inhibitory factors to axon regeneration, and, in combination with the physical barrier of the astrocytes, make it very difficult for axons to cross the scar border.

Despite the inhibitory properties of the glial scar, complete removal of key components of this barrier can also have detrimental effects after an injury. The scar serves the purpose of barricading the cystic cavity, preventing the spread of cytotoxic molecules and inflammatory factors (M. A. Anderson et al., 2016; Wanner et al., 2013). It also seems to be important in the repair of the blood brain barrier, as complete removal of reactive astrocytes causes impaired barrier repair, massive influx of inflammatory cells and increased neuronal death (Okada et al., 2006; Faulkner et al., 2004). Figure 10 summarizes many of the important characteristics of the lesion environment.

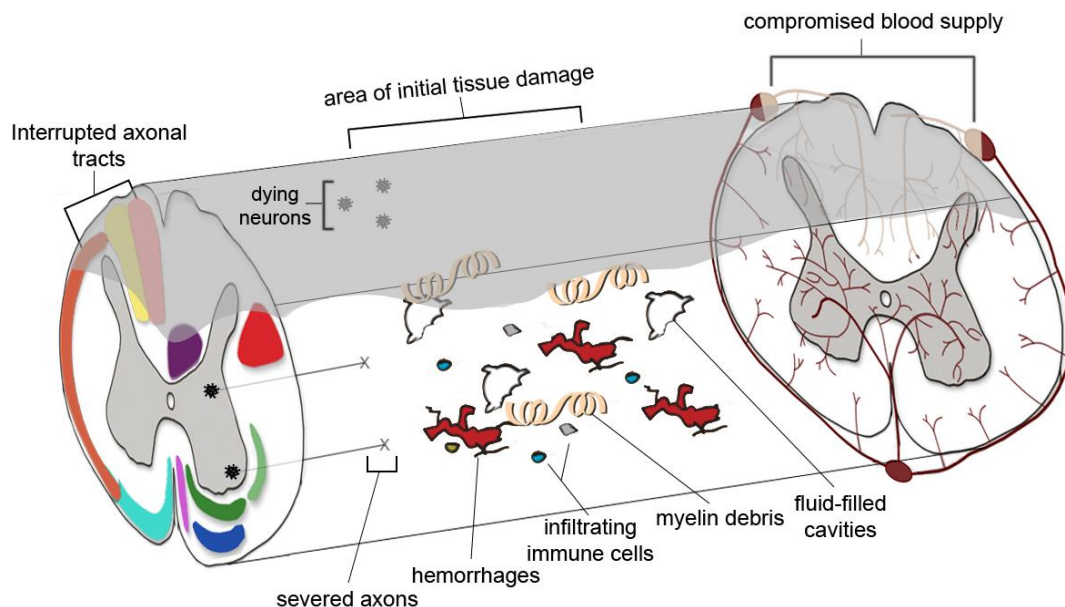


Figure 10. Properties of the Lesion Environment – The initial area of tissue damage results in dead and dying neurons and glia, severed axons that interrupt spinal pathways and a compromised blood supply. Shortly thereafter blood vessel hemorrhages occur, cells of the immune system invade and a glial scar begins to form. The gray area is loosely representative of a contusive injury.

Spinal Shock

One last effect of SCI of interest is the phenomenon of spinal shock. This is a state of temporary additional impairment that includes flaccid paralysis, loss of sensation,

decreased reflexes and loss of bladder control (Ditunno et al., 2004). It is seen in 50% of human subjects, and a correct injury diagnosis cannot be made until this effect resolves itself. Spinal shock also happens in rats, and empirical observations suggest that the affected percentage is higher than 50%. After a contusive injury at the thoracic level, the majority of animals will have complete or very severe paralysis of the hind limbs, lack of the hindlimb pinch reflex, and loss of bladder control requiring manual bladder expression. This generally resolves itself in 5-10 days, and animals will be able to move their hind limbs, and begin to regain stance and stepping, depending on the severity of the injury.

The mechanisms behind spinal shock are not completely understood. Potential causes include breakdown of membrane potential, excessive amounts of neurotransmitter, or loss of modulating signals that regulate the excitability of the neuron (Onifer et al., 2011). Recovery could be due to restoration of membrane potential, or synaptic plasticity of modulating fibers. When studying behavioral phenomenon surrounding SCI, it is important to consider spinal shock so that a sudden behavioral improvement in this time period is not attributed to an experimental treatment.

Why Do Neurons Fail to Regenerate?

Neurons of the CNS are known to be especially poor at regenerating their axons after an injury (Schwab and Bartholdi, 1996). As discussed in the previous section, there are many inhibitory elements in the lesion environment, and this is responsible for some of the failure to regrow. However, many studies in embryonic or very young animals have demonstrated that young neurons are able to overcome environmental factors and regenerate with more alacrity than mature ones (Nogradi and Vrbova, 1994; Wictorin and

Bjorklund, 1992; Shimizu et al., 1990), and thus it is apparent that the environment is not the only limiting factor.

Comparative genetic studies of neurons of different ages reveal that as a neuron matures, there is a rapid switch from a ready state of robust growth capacity to a more quiescent state where many genes associated with growth are downregulated (P. N. Anderson et al., 1998; Caroni et al., 1997). In the case of an injury, some neurons can revert to this ready state, upregulating important proteins that allow for regenerative growth after injury such as those associated with the formation of new growth cones and the production of proteins that assist in axonal elongation (Schreyer and Skene, 1991; Tetzlaff et al., 2011). However, CNS neurons do not do this as well as their peripheral counterparts, and it is apparent that only a small fraction of injured CNS cells can revitalize their growth programs (Jung et al., 1997; Schaden et al., 1994; Tetzlaff et al., 1991). Those that do upregulate these important proteins are correlated with more successful axonal regeneration (Skene, 1989). These cellular states are not completely understood, but several pathways or proteins associated with active growth have been identified, such as growth associated protein-43 (GAP-43), Cyclic Adenosine Monophosphate (cAMP), or the PI3K/AKT pathway (Hannila and Filbin, 2008; Smith and Skene, 1997; P. N. Anderson et al., 1998; Bush et al., 1996; Caroni et al., 1997; De la Monte et al., 1989; D. A. Guertin and Sabatini, 2007).

For many years, SCI research was focused mainly on enabling neurons to regenerate. However, studies that encourage growth do not always cause significant regeneration, and even when some regeneration does occur, a functional connection to a previous target does not happen often, especially if the target is long distance. Luckily,

there are other methods of growth possible for neurons that may be more promising for recovery than long-distance regeneration.

Regeneration versus Sprouting

Regeneration is defined as growth of a cut or damaged axon. It can refer to the growth of the severed end of the damaged axon or growth of a branch extending from a different part of that same axon. The latter case is sometimes referred to as ‘regenerative sprouting’. True regeneration has been something the SCI field has chased for decades with only modest success.

Another type of growth is termed sprouting, or sometimes, plasticity. These terms are often used interchangeably to refer to a number of different types of growth (for review, see (Filli and Schwab, 2015)). Plastic changes include synaptic reorganization, supraspinal reorganization, or compensatory plasticity from spared fibers. Synaptic reorganization can include strengthening or reorganization of existing fibers on connected targets or upregulation of post-synaptic receptors on MNs to increase the strength of the signal.

Plastic changes can also happen in the brain (supraspinal reorganization) when descending tracts rewire in an attempt to compensate for lost connections by synapsing onto neurons connected to areas below the injury. For example, CST fibers can sprout into brainstem nuclei such as the RN to take advantage of intact connections of the RST (Belhaj-Saif and Cheney, 2000; Nishimura and Isa, 2009). Other studies in monkeys missing part of their forelimbs show that cortical territories associated with intact limbs enlarge and sprout into areas associated with the missing part. So, for example, areas that

were formerly devoted to the missing part of the limb could now affect movements of a remaining part of the limb or the shoulder (Qi et al., 2000). This also happens in the human brain in individuals with SCI, who exhibit extensive changes in the mapping of cortical areas (Bruehlmeier et al., 1998; Levy et al., 1990; Topka et al., 1991). Spared fibers from descending tracts, sensory fibers or PNs can also make compensatory plastic changes by sprouting and innervating damaged tissue. Some spared fibers can cross the midline to make connections onto contralateral descending tracts in an attempt to make bypass circuits (Cafferty and Strittmatter, 2006; Rosenzweig et al., 2010).

One of the most exciting things about plastic growth is the potential for creating a bypass circuit in the spinal cord that can restore function in individuals with SCI. Even if regenerative growth can be jumpstarted, it takes time for a nerve fiber to regrow. It is estimated, for example, that axonal elongation of a peripheral nerve can proceed at a rate of between 0.25 – 6 mm per day, depending on the hostility of the growth environment, the distance of the axon from the cell body and the presence of other confounding factors (Armantrout, 2017; Jain and Gupta, 2007; S. R. Y. Cajal et al., 1991). CNS neurons may grow at an even slower pace. If local circuits can be taken advantage of to restore function, this may be a much more efficient process. Encouraging the growth that a neuron can realistically achieve may be the key to restoring function in those with SCI.

Encouraging neuronal growth in the literature

For as long as the scientific community has understood how to target damaged neurons, there have been studies attempting to encourage regeneration. Modest success is observed protecting neurons from cell death or coaxing them to regenerate or sprout by making the environment more permissive. For example, degradation of molecules

inhibitory to axonal elongation such as the CSPGs or myelin-associated proteins can encourage growth (Houle et al., 2006; Lee et al., 2010; Schwab and Strittmatter, 2014; Fitch and Silver, 2008; Filbin, 2003), (see (Filbin, 2003; Fitch and Silver, 2008) for review).

Another popular method to make the environment more permissive is to insert a cellular graft or bridge into the lesion cavity. Schwann cell grafts, peripheral nerve grafts, olfactory ensheathing cells, neural or glial progenitor cells, and bone marrow stem cells have all caused modest axonal growth (Guest et al., 1997; Martin et al., 1993; Ruitenberg et al., 2005; Ogawa et al., 2002; Okada et al., 2005; Bambakidis and Miller, 2004; Deng et al., 2008; Cizkova et al., 2006; Tetzlaff et al., 2011). These grafts give the axons a substrate to grow upon, and some cells may secrete neurotrophins that can target growth or serve as protection for the axon (Sasaki et al., 2009; Weidner et al., 1999; Y. H. Ma et al., 2010).

Neurotrophins are a family of proteins that regulate neuronal survival, synaptic function, and neurotransmitter release. During development, growth-permissive neurotrophic factors allow axons to lengthen and extend towards appropriate targets in the correct numbers. However, the expression of many neurotrophic factors is greatly reduced within the adult CNS. Exogenous application of factors such as brain-derived neurotrophic factor (BDNF), neurotrophin-3 (NT-3) or nerve growth factor (NGF) can elicit plasticity and growth of axons within the adult central and peripheral nervous system (Novikova et al., 2000; Schreyer and Jones, 1982; Tuszynski et al., 1996; N. R. Kobayashi et al., 1997; Ye and Houle, 1997; Schnell et al., 1994; Kromer, 1987), see (Keefe et al., 2017) for review).

Another major focus of neural growth studies is the attempt to restart internal growth programs by upregulating regeneration associated genes such as GAP-43 or molecules such as cAMP. The GAP-43 gene, which codes for components of the growth cone, was one of the first genes shown to be active during axonal regeneration (Benowitz and Lewis, 1983; Kalil and Skene, 1986; Skene and Willard, 1981). Upregulation of GAP-43 can enhance sprouting, but is unable to trigger regeneration by itself, even in a permissive environment (Aigner et al., 1995; Neumann and Woolf, 1999). cAMP is a signal transduction molecule shown to influence attractive growth cone guidance cues and also neuronal response to myelin inhibition during injury (Ming et al., 1997; H. J. Song et al., 1997). Reductions in the endogenous levels of cAMP during embryonic development coincide with the onset of growth failure when encountering the inhibitory myelin proteins mentioned above (Cai et al., 2001). Studies elevating cAMP via conditioning lesion found increased regeneration in transected sciatic nerves and DRG neurons (Kilmer and Carlsen, 1984; Qiu et al., 2002), and interganglionic cAMP elevation can induce regeneration of sensory nerves after a dorsal column lesion (Neumann et al., 2002).

These studies show that individual molecules associated with an active embryonic growth state hold promise for increasing axonal growth after injury. Even more promising may be a pathway that can both activate protein synthesis in the cell body and influence local growth in the axon. The PI3K/AKT signaling pathway has many downstream molecules involved in multiple aspects of growth. PI3K is known to mediate signaling during the formation of new growth cone proteins and influence polarized outgrowth, as well as acting as a key regulator of cellular responses to growth factors

(Adler et al., 2006; D. A. Guertin and Sabatini, 2005; Hay, 2005; Tee and Blenis, 2005). Activation of this pathway is a demonstrated requirement for neurotrophin-induced cell survival and distal axon growth in sympathetic neurons. Glycogen synthase kinase 3 (GSK-3), which is downstream of AKT, is implicated in microtubule polymerization (Yoshimura et al., 2005; Fukata et al., 2002), a key component in rapid growth cone formation. Mammalian target of rapamycin (mTOR), another downstream target of AKT, regulates protein translation and ribosome biogenesis by phosphorylating substrates that initiate cap-dependent protein translation (Park et al., 2008; X. M. Ma and Blenis, 2009; D. A. Guertin and Sabatini, 2007), and contribute to the formation of new growth cones (Verma et al., 2005). mTOR is also shown to be significantly down-regulated in injured CNS neurons, but not in peripheral nervous system (PNS) neurons (Park et al., 2008), which are known to be better regenerators. In several studies in chapter 4, the influence of mTOR upregulation or PTEN inhibition on growth is examined in the RST or CST of rats with a SCI.

Regrowth Studies of Descending Tracts and Propriospinal Neurons

There have been many studies exploring the growth properties of the neuronal populations outlined in this document. Corticospinal neurons are of great interest since they are important in humans for fine motor movement. The CST is notoriously poor at regenerating (Thallmair et al., 1998; Cafferty and Strittmatter, 2006; Case and Tessier-Lavigne, 2005), but there is ample evidence for sprouting of CST fibers (Schnell et al., 1994; Cafferty and Strittmatter, 2006; Rosenzweig et al., 2010; Bareyre et al., 2004). Injury-induced sprouting is evident in both severed and spared CST axons at both days and weeks post-injury, and both near and far away from the injury site (Fouad et al.,

2001; Hill et al., 2001; Bareyre et al., 2004; Onifer et al., 2011; Carmel and Martin, 2014; Nakagawa et al., 2015; Asboth et al., 2018; Zareen et al., 2017; Z. H. Liu et al., 2015; Du et al., 2015). Changes in dendritic spines of CST neurons suggest that they can revert to an adaptable and immature pattern of synaptic connectivity (Kim et al., 2006).

Sprouting over the midline to innervate intact circuitry can be important if an injury spares tissue on one side of the cord. Certain studies have found substantial spontaneous CST sprouting over the midline after unilateral hemisections in both rodents and primates, accompanied by some restoration of fine motor movement or locomotion (Rosenzweig et al., 2010; Cafferty and Strittmatter, 2006). CST fibers in the brain can sprout onto brainstem nuclei or onto PNs in the spinal cord in an attempt to create bypass circuits (Bareyre et al., 2004; Lemon and Griffiths, 2005).

Although the RST is rudimentary in humans, there is interest in this population of neurons for several reasons: studies in primates show it has the potential to create important compensatory locomotor circuits during CST injury because of its close association with the CST (Lemon and Griffiths, 2005; P. T. Williams et al., 2014; Z'Graggen et al., 1998), it has shown greater responsiveness to experimental manipulation than many other tracts (Y. Liu et al., 1999; Tuszynski and Steward, 2012; Tobias et al., 2003), it has a distinct and relatively easy-to-access population of neurons in the RN, and it is an important controller of motor movement in rats (L. T. Brown, 1974), though its exact contribution to behavior is somewhat controversial.

RN remodeling can be seen in the human brain, with significantly increased fiber density found in stroke patients with infarcts in the internal capsule, where CST axons run (Takenobu et al., 2013). In rodents, extensive sprouting of rubrospinal projection onto

the raphe nucleus correlated with recovery of some motor function (Siegel et al., 2015). RST axons were found to increase their innervation onto ventral horn MNs usually associated with CST axons after pyridotomy. This was correlated with recovery of precision grip in the forepaw (Raineteau and Schwab, 2001). They can also sprout onto PNs (Bareyre et al., 2004; Raineteau and Schwab, 2001; Raineteau et al., 2002). Regeneration and sprouting of the RST has been shown in cell transplantation studies and after peripheral nerve graft (Jin et al., 2002; Richardson et al., 1984), even one year after axotomy (Kwon et al., 2002).

ReST axons may also grow into cellular grafts such as Schwann cells, (Menei et al., 1998; Takami et al., 2002), olfactory ensheathing cells (Plant et al., 2003) or fibroblasts (Blesch and Tuszynski, 2009; Jin et al., 2002). And have been associated with spontaneous recovery after injury by compensatory sprouting (Ballermann and Fouad, 2006, Filli et al., 2014). Increased projection fibers from the NRG were found when retrograde tracer was injected into the cervical cord after injury, and increased arborization of these fibers occurred at the lesion site (Filli et al., 2014). ReST fibers are shown to sprout onto cervical PNs, and make midline crossings. This correlated with spontaneous recovery of locomotion (Filli et al., 2014). Encouraging the growth of reticulospinal axons is especially interesting because their location in the ventral spinal cord white matter means that they are often spared in contusive injuries.

PNs may be a critical population of neurons that contribute to spontaneous recovery, that is, the behavioral recovery seen after SCI with no treatment. Spontaneous recovery of some function after SCI is a known phenomenon, and many individuals with SCI experience some recovery from the first clinical assessment (Taccola et al., 2018).

This is most common in the first three months, but may be observed for up to a year (Waters et al., 1992; Kirshblum et al., 2004; Fawcett et al., 2007). The amount of recovery is inversely correlated to the severity of injury (Marino et al., 1999), with incomplete injuries showing more recovery. Spontaneous recovery is also apparent in lower species such as cats and rodents (Schwab and Bartholdi, 1996; Rossignol, 2000). The mechanisms are not completely understood, but many involve recovery from spinal shock (Hiersemenzel et al., 2000; Holaday and Faden, 1983), remyelination (Schwab and Bartholdi, 1996; Gensert and Goldman, 1997), and axonal sprouting. Evidence of sprouting of descending tracts onto PNs has been demonstrated after injury in animal models (Bareyre et al., 2004; Courtine et al., 2008). CST axons sprout onto both long and short PNs, and maintain synaptic contacts with LDPNs over a 12-week period (Bareyre et al., 2004). Due to their location and ubiquitous nature, PNs likely contribute to formation of bypass circuits that drive spontaneous recovery.

A complete transection of the spinal cord will result in complete and irrevocable paralysis as all descending supraspinal input is severed. However, very interestingly, if half of the cord is cut at one level, and the other half of the cord cut at a lower level, spontaneous recovery of function can still occur over a period of time if a large enough tissue bridge exists in between the cut segments. A study done by the Courtine lab found that some spontaneous recovery occurred after a unilateral spinal cord lesion, which was then abolished by a second staggered lesion on the contralateral side. This suggested that reformed connections that had crossed the midline were likely responsible for this recovery, instead of any axons that might have regenerated across the lesion on the ipsilateral side. After a short time, the animals had some recovery of function from the

second lesion, which was then again abolished when neurons of the connecting tissue bridge were ablated (Courtine et al., 2008). This suggested that neurons in the tissue bridge, many of which would be propriospinal in nature, were sprouting to form new functional connections to intact circuitry, creating bypass relays that restored some degree of supraspinal input.

The potential creation of bypass relays has made the study of PNs and their regenerative abilities a current hot topic. Research has begun into specific populations of these cells and their contributions after injury. For example, studies following injury at the thoracic level, demonstrate that TPNs can undergo plasticity to re-innervate lumbar MNs and function as endogenous detours to restore locomotion (van den Brand et al., 2012; Courtine et al., 2009). Several studies by Stelzner's group have examined TPNs and cervical LDPNs in regards to axotomy and retrograde cell death following thoracic SCI, finding that these populations upregulate genes differently and have different survival rates (Conta Steencken et al., 2011; Conta Steencken and Stelzner, 2010; Siebert, Middleton et al., 2010; Conta and Stelzner, 2004).

Why do PNs exhibit substantial plasticity after injury? One reason may be the location of their cell bodies – meaning that in contrast to neurons of descending tracts, the cell bodies of PNs are much closer to the lesion. This gives them increased access to the cellular proteins needed to elongate their axons (Fernandes et al., 1999). Additionally, some populations of PNs may upregulated growth programs after injury, demonstrating increased expression of GAP-43, neurotrophic factors, and neuroprotective proteins (Siebert, Middleton et al., 2010). Several studies in this document explore connections of

descending tracts and PNs after SCI in the rat. The next section briefly explores why rats are used as an injury model.

The Rodent as a Model Organism for Spinal Cord Injury Studies

A diverse range of model organisms are used to study the spinal cord and its functions, including worms, lamprey, cats, sheep, monkeys, rodents and many others. Mice and rats are used frequently because their nervous systems have a great deal of similarity to humans, they breed prolifically and are relatively inexpensive to maintain. There is also a well-developed suite of histological and behavioral analysis available in the rodent model, making data analysis relatively simple. Rats are especially useful for spinal cord studies because the nature of their injuries resemble a human injury more closely than other rodents. For example, rats develop cavitation in the injured areas similar to humans, where mice have more cell proliferation into the lesion, and do not display cystic cavities (Onifer et al., 2011; Bunge et al., 1993; Bunge et al., 1997). A comparative electrophysiological study between humans and rats with similar SCIs demonstrated similar latencies and reduced amplitudes of motor evoked potentials, which correlated with degree of impaired locomotion (Metz et al., 2000). Rats also have a similar pattern of spinal shock and recovery to humans (Basso et al., 1996).

Anatomical Differences in the Rat Spinal Cord

The structure of the spinal cord in rats is similar to what I have thus far described, including the location of vertebrae, spinal nerves, and white and gray matter. Rats have minor differences corresponding to a more flexible spine. For example, spinal cord tissue itself is more slender than in humans, and some vertebrae in rats are found to be slimmer

and more elliptical. Cervical vertebrae also have a greater width-to-depth ratio, which may reflect differences in neck musculature and head movement (Jaumard et al., 2015).

Rats also display certain differences in the location of descending and ascending white matter tracts. Considering descending fibers, the major difference lies in what is referred to in the CST. This tract follows a similar path in rats from the brain, until it arrives in the spinal cord, where its positioning is quite different. What was previously referred to as the lateral CST in humans is now a very small percentage of fibers, comprising only about 3% running in the lateral funiculus. The vast majority of fibers run in the dorsomedial funiculus in the rat, at about 95% (Lemon and Griffiths, 2005). This component is referred to as the dorsal CST (Figure 11). The anterior CST occupies similar real estate to humans, running in the ventromedial cord, but comprises about 1-2% of CST fibers (Joosten et al., 1987; Joosten et al., 1992; Brosamle and Schwab, 1997; Terashima, 1995).

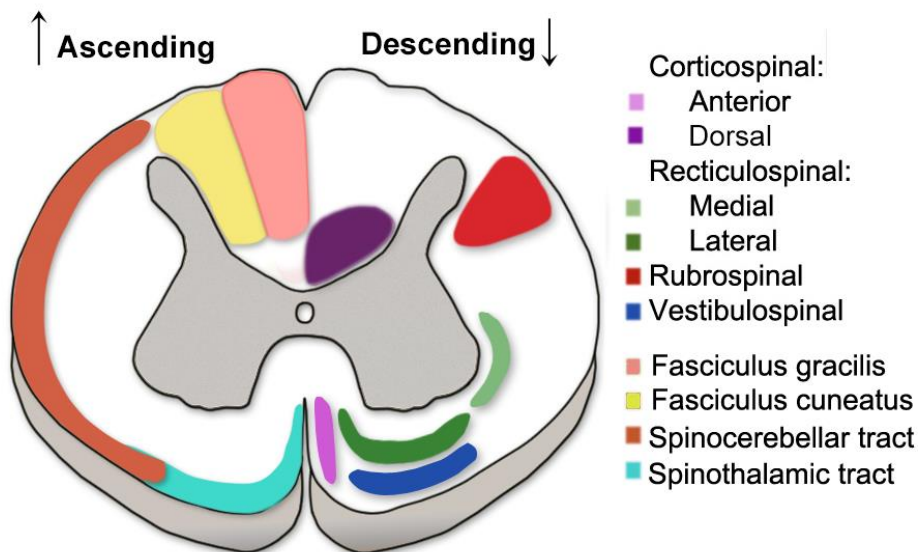


Figure 11. Ascending and Descending Tracts of the Rat Spinal Cord

The dorsal columns, one of the major ascending tracts, gives up the dorsomedial territory taken up by the dorsal CST, as pictured above. The spinothalamic tract also differs slightly, as it runs at the ventral most aspect of the white matter, further from the ventral horn.

Specific Injury Models

There are three main injury types seen in SCI studies. These are cut injuries, compression injuries and contusive injuries (for review see (Rosenzweig and McDonald, 2004; Kjell and Olson, 2016)). Cut injuries such as complete transections where all fibers are severed, or hemisections where a certain portion of the spinal cord is severed by a sharp instrument are often used in regeneration studies. Cutting the entirety of the spinal cord, or at least one entire tract, makes it possible to conclude that fibers are de novo regenerators instead of sprouting from spared fibers. One study in this document focused on regeneration uses a lateral hemisection model.

Compression injuries are performed by squeezing the spinal cord with forceps or clips, and are often used to model an injury where both spinal cord tissue and spinal roots are affected (Rivlin and Tator, 1978; Vanicky et al., 2001; Blight, 1991). Perhaps the mostly clinically relevant model of SCI is the contusion model. Human SCIs are mainly generated due to blunt force trauma to an area of the spinal cord after a car accident, fall or sports injury. In this work, contusive injury is used as the model in many studies.

Historically blunt force trauma was replicated by dropping a weight from a vertical distance, relying on gravity to apply force to the tissue (Allen, 1911). Surgery of experimental lesion of spinal cord equivalent to crush injury of fracture dislocation of spinal column (Khan et al., 1999). Parameters that were measured during this type of

injury were distance the weight traveled before impact, the amount of weight used and the resistance encountered while the weight is falling (Dohrmann and Panjabi, 1976; Dohrmann et al., 1978). This model helped to create a more clinically relevant injury, but had a few drawbacks. It was difficult to measure precisely how much force was applied to the spinal cord and how much displacement of the cord was occurring. This made determining the severity of injury difficult, and reproducibility between animals was inexact (Blight, A. (1996), Experimental SCI models. In: *Neurotrauma*. R.K. Narayan, J.E. Wilberger, and J.T. Povlishock (eds), McGraw-Hill: New York, pps. 1367–1379; (Falconer et al., 1996)).

To improve upon the weight-drop model, impactor machines with software interfaces were designed that used force as the variable to define the severity of injury. This allowed the user to control the force applied to the tissue, allowing for a more repeatable injury assuming all other factors were correct. The impactor that has gained the most popularity, and the one used in these experiments, is the Infinite Horizons Impactor (IHI) (Precision Systems, Inc.). This device contains the “stepping motor” technology linked to a piston and a force sensor, which allows for a precise amount of force to be applied to the tissue. When the user defines the force to be applied, the motor ‘steps’ by moving the tip downward and immediately thereafter measuring the force applied between the impactor and the tissue. If the force is less than what is desired, the motor takes another step. These steps and samplings are so fast that the piston appears to move smoothly and without pause. When the force measured equals the desired force, the motor withdraws the piston (Scheff et al., 2003).

The software interface of the impactor immediately displays actual force applied to the tissue after impact, as well as plotting changes in both displacement and force as a function of time. The subtleties of the graphs can also reveal if the piston has hit bone (i.e. if the laminectomy did not expose sufficient cord) or if the animal was not secured in the spinal holder correctly. Analyzing these parameters can aid in making a pool of animals with similar injuries. As represented in the schematic in Figure 10, contusive injuries do the most initial damage to the dorsal portions of the spinal cord. This can create a large cavity or necrotic area. Figure 12 demonstrates histological features of a contusive injury. In a coronal section in Figure 12A, bright spots in the damaged area inside the arrows are likely macrophages, which can auto fluoresce when viewed under a microscope. In 12B, a sagittal section demonstrates several linked contusion cavities spanned by thin tissue bridges, and a thick band of spared fibers in the ventral portion of the cord.

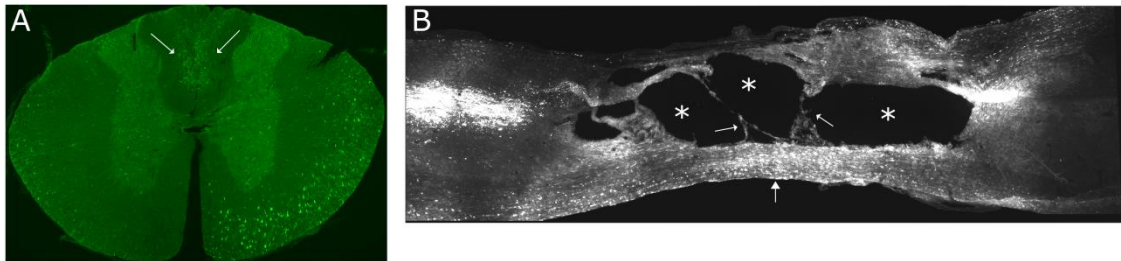


Figure 12. Histological Features of a Contusive Injury – A) A coronal section of a spinal cord stained with GFP shows a damaged area in the dorsal white matter (arrows). B) A sagittal section demonstrates fluid filled cavities (*), thin tissue bridges that span cavities (arrows) and a thick band of spared fibers in the ventral portion of the cord (arrowhead)

Using Viral Vectors for In Vivo Visualization and Regeneration Studies

Some of the first studies outlining the intricate circuitry of the brain and spinal cord were done in the 1900s by Santiago Ramon Y Cajal, who pioneered a method of

infusing cells with silver stains. The dyes he used accumulated inside neurons and diffused through cellular processes, revealing the structure and connections of layers of cells in the cortex, and many other areas of the brain (R. Y. Cajal, 1909). Cajal used post-mortem tissue and relied on diffusion of the dyes for labeling. As time progressed tracing tracts of fibers in living tissue was developed, including an adaptation of the silver stain (Nauta, 1952; Fink and Heimer, 1967).

In the 1970s it was discovered that it is possible to take advantage of the machinery of the cell to transport dyes or chemicals (Kristensson et al., 1970). If a molecule is introduced into the vicinity of the cell membrane, it may be taken into the cell via endocytosis or active transport. Cellular cargo can be transported away from the cell body (anterograde) or towards the cell body (retrograde). This is an incredibly useful tool because tracers can fill a neuronal cell body, attached dendrites, axon and synaptic terminals, identifying the origin of the cell, the course of its axon and its termination. Because of this many of the details of spinal tracts have been elucidated through tracing studies (Rexed, 1952; Liang et al., 2011; Brichta and Grant, 1985; Watson et al., 2009).

Popular chemical tracers used to highlight neuroanatomical pathways include biotinylated dextran amines (BDA) (Veenman et al., 1992) cholera toxin beta subunit (Trojanowski et al., 1982; Luppi et al., 1990) fluorogold (Schmued and Fallon, 1986), and microbeads (Katz et al., 1984; Katz and Iarovici, 1990). BDA and fluorogold became gold standard for many experiments, but they do have certain disadvantages. BDA can be taken up by damaged axons in the injection area, or by axons in passage in the white matter surrounding an injection site (Geed and van Kan, 2017; Brandt and Apkarian, 1992; Reiner et al., 2000). This may lead to incorrect interpretations of neuronal

numbers or connecting pathways, and could also be a drawback in studies examining axon regeneration if BDA is absorbed by damaged or severed axons, since they could be mistaken for regenerating fibers (Steward et al., 2007).

Another method for tracing pathways was introduced in the late 1970s when several different labs exploited the power of viruses to introduce proteins of interest into cultured cells (Ganem et al., 1976; Nussbaum et al., 1976; Goff and Berg, 1976). Viruses have evolved specialized mechanisms to maximize the propagation of their genetic material by hijacking cellular machinery. Many can efficiently infect cells, continually propagate within them, and use their transport mechanisms. Viral vectors are tools derived from viruses that keep the genetic material of the virus needed to infect cells and use their transport machinery, but often replace the part of the genome required for viral replication with proteins of interest to researchers. Making the vector replication deficient increases safety and guarantees the virus won't spread beyond the injected tissue. Vectors can also be manipulated to exhibit cell type specificity, or to express antibiotic resistance for convenient use in cell culture (for review see (Bouard et al., 2009)).

Considering the promising nature of viral vector-mediated delivery of transgenes to specific neuronal populations, viral gene delivery is used here in both anterograde and retrograde tracing experiments to highlight distinct spinal pathways and their connections to the brain. Chapter 2 describes AAV vectors as classic tools for anterograde tracing studies, and demonstrates the novel usage of a scAAV vector to highlight long descending pathways in the spinal cord. This vector provided superior transduction efficiency over ssAAV vectors, and bright labeling without the need for immunohistology (IH) was seen in RST and CST axons. Chapter 3 explores retrograde

tracing with the HiRet lentiviral vector in order to focus on pathways that may contribute to spontaneous behavioral recovery after a thoracic contusion by reforming connections with spared circuitry. The RST, CST and ReST are established as potential contributors due to their connections to areas below the injury. This chapter also introduces synaptic silencing of neuronal populations in the RST and CST in the uninjured state, in order to explore the contribution of these tracts to forelimb motor behavior. The RST is found to have no effect on gross forelimb behavior in an uninjured rat, whereas a small population of CST neurons may be involved in grip strength and digit wrapping. Chapter 4 explores regrowth of CST axons in a contusive injury model by using classical tracer BDA to highlight axons of the CST after treatment with PAPs. Systemic infusion of PAPs targeted at the enzymatic pocket of the PTEN protein cause substantial growth of CST axons in a subset of treated animals.

CHAPTER 2. MAPPING SPINAL PATHWAYS VIA ANTEROGRADE TRACING WITH ADENO-ASSOCIATED VIRAL VECTORS

Introduction

AAV is a member of the *Parvoviridae* family of Deoxyribonucleic Acid (DNA) viruses, originally discovered in the 1960's as a contaminant in a preparation of simian adenovirus (Atchison et al., 1965). AAV is not known to be pathogenic, and causes very little immune response in currently studied species (Samulski and Muzyczka, 2014). It can infect terminally differentiated cells, and its ability to integrate into the host genome allows it to persist at a high level of expression in many different tissues (Maeda et al., 1997; Herzog et al., 1997; Snyder et al., 1997; Kaplitt et al., 1994; Xiao et al., 1997).

These advantages, along with AAVs strong preference for neuronal transduction, makes transgene transfer by AAV vector an attractive candidate for the clinic. Building the initial AAV vector initially posed a few difficulties, as this virus cannot replicate without the presence of adenovirus as a helper. A group at the University of Florida took the first step in 1982 by cloning the intact AAV genome into a bacterial plasmid, and then rescuing the recombinant plasmid after transfection into human cells (Samulski et al., 1982). Further groups then worked to increase the efficiency of packaging, and cement the production of this vector in the absence of adenovirus (Ferrari et al., 1996; Xiao et al., 1998).

Viruses by nature are highly mutable. Antigens on the surface can vary, causing diversity in interactions with cell receptors. Fundamentally similar viruses with different surface antigens are termed serotypes. AAV currently has 13 widely-available serotypes, many of which are being tested in animal models (Samulski and Muzyczka, 2014; Zincarelli et al., 2008). Serotype can have different tissue tropisms, or even specific

tropisms within a tissue type. For example, a systematic study using AAV2 determined that the virus transduced the hippocampus, inferior colliculus and piriform cortex robustly, whereas expression was dampened in the olfactory tubercle, and reduced still further in the striatum (Tenenbaum et al., 2004). AAV2 is known to preferentially transduce neurons, and has been used successfully to infect neuronal cell bodies and transport to axon terminals, allowing the entirety of the neuron and axon to be labeled (R. Williams et al., 2012; Chamberlin et al., 1998; Xiao et al., 1997; Kells et al., 2009). In our experiments that involve AAV, the AAV2 serotype affords the best expression in the areas of interest in the brain and spinal cord.

Since AAV vectors have been ubiquitously used in scientific studies for some years, ideas that maximize efficient usage of this vector, or correct certain limitations it possesses, are well sought after. For example, conventional AAV vectors are single-stranded DNA viruses that rely on host-cell machinery to synthesize the complimentary DNA strand in order for the transgene to express. This rate-limiting step can make transduction less efficient (Ferrari et al., 1996). A group from the University of North Carolina offered a solution to this problem in a series of studies in the early 2000s that introduced the scAAV vector (McCarty et al., 2001).

A traditional AAV vector can hold a transgene insert of up to ~5kb (Salganik et al., 2015). These vectors package single-stranded genomes and use the infected cells machinery to synthesize the complimentary strand. However, if the included genome is half the size of wild-type (~2.4kb), then AAV can package two copies. These copies will be dimeric inverted repeats which can spontaneously reanneal, and thus the vector does not need to use the host cell to synthesize the second strand of DNA, and will be

immediately ready for replication and transcription. This increases the transduction efficiency of the scAAV vector by 5-140 fold over the traditional vector, and leads to faster expression of the transgene (McCarty et al., 2001).

As GFP is a small transgene insert, scAAV-GFP seems perfect for tracing studies. Our 2014 paper explored the use of scAAV-GFP in labeling long projection axons in the CST, RST, and central axons of the DRG, and if expression was consistent in lesioned animals (Y. Liu et al., 2014). My part of the study, which is presented here, explores scAAV-GFP labeling of the RST.

Additional studies described in this document required multiple viral tracer injections – whether to simultaneously target multiple pathways, or to guarantee neuronal specificity of targeting by introducing one vector at a synapse and another at the cell body. Supplementary data in this chapter demonstrates AAV2-mCherry efficiency as an anterograde tracer, for use when an additional fluorescent marker was needed. mCherry is a fluorescent marker derived from the sea anemone *Discosoma*, which has been manipulated to increase photo stability. It produces a red color (Shaner et al., 2004).

Materials and Methods

Animals

All surgical and animal care protocols were approved by the Temple University Lewis Katz School of Medicine's Institutional Animal Care and Use Committee, and performed per the National Institutes of Health *Guide for the Care and Use of Laboratory Animals*. All rats were housed two per cage, on a 12-hour light-dark cycle with food and water provided *ad libitum*. Animals were allowed 7 days of acclimatization prior to any experimental procedure.

For the initial scAAV-GFP study, female Fischer 344 rats (175-200g, Harlan Laboratories) were used. After several studies with these animals and discussions with other laboratories, it was apparent that the Sprague-Dawley breed of rat was better suited for our purposes, and all subsequent studies were performed on female Sprague-Dawley rats (200-224 g; Harlan Laboratories). Animals were split into the following groups for the data displayed in this chapter: 1) three female Fischer 344 rats were injected unilaterally into the RN with scAAV-GFP to label axons of the RST; 2) four female Sprague-Dawley rats were given a unilateral hemisection lesion at spinal level T8, and then injected one week later with scAAV-GFP into the contralateral RN; 3) four female Sprague-Dawley rats received unilateral injections of scAAV-mCherry into the FMC; 4) six female Sprague-Dawley rats received unilateral injections of ssAAV-mCherry-P2A-WGA into the RN; and 5) three female Sprague-Dawley rats received unilateral injections of ssAAV-mCherry-P2A-WGA into the PRF.

Viral Vector Construction and Production

The AAV2 vector was generated by transfecting human embryonic kidney (HEK) 293 T cells (American Type Culture Collection) with a three-plasmid helper-virus free system. Cells were grown to 70–80% confluence, and then transfected with two packaging plasmids using polyethylenimine (PEI, linear, MW-25 k, Warrington, PA). One plasmid contained AAV *rep* and *cap* genes and the other the adenovirus helper functions. ssAAV and scAAV are type 2 vectors carrying either the enhanced GFP (eGFP) or mCherry gene, and driven by the chicken beta actin promoter. Three days post-transfection, cell lysates and supernatants were harvested and 40% polyethylene glycol (PEG) 8000 added for 2 hours to precipitate crude virus. Crude virus was purified by

double-centrifugation with cesium chloride (CsCl) and dialyzed in 0.1 M Phosphate Buffered Saline (PBS)/5% sorbital overnight (Ayuso et al., 2010). The titer of AAV vectors was determined by infecting fibroblast cells. Serial dilutions of virus were added to a 24-well plate seeded with 0.5×10^5 fibroblast cells per well. After one day, cells expressing fluorescence were counted under a microscope to determine infectious titer (TU/ml) and multiplying by the multiplicity of infection (10^3) to convert to genomic copy titer (GC/mL). scAAV2-GFP titer was estimated at 1.66×10^{12} GC/mL. The mCherry used in supplementary material in this chapter was either scAAV2-mCherry or ssAAV2-mCherry, depending on the study. scAAV2-mCherry titer was estimated at 1.4×10^{12} GC/ml or ssAAV2-mCherry at 1.5×10^{12} GC/ml.

Surgical Procedures

Rats were weighed and anesthetized by intraperitoneal injection of ketamine at 67 mg/kg and xylazine at 6.7 mg/kg dosage. The target area was shaved and disinfected thoroughly with iodine and 70% ethanol. Ophthalmic ointment was applied to the eyes to prevent drying. During all procedures, animals were monitored for depth of anesthetic plane and booster shots of ketamine/xylazine were given if breathing became too rapid or whisking occurred. After surgery, rats were placed on a temperature controlled heating pad and administered 10 ml of saline (0.9% NaCl, Baxter Healthcare Corp.) to combat dehydration and 10 mg/ml of cefazolin antibiotic (West-Ward Pharmaceutical Corp.) to combat infection. Rats were monitored until wakeful and then transferred to their home cages, where they were provided with analgesics in the form of 2mg Rimadyl tablets (Bio Serv, Flemington, NJ).

Stereotactic Brain Injections

For the scAAV anterograde tracing study, scAAV2-GFP was injected into the RN by placing the animals into a stereotactic frame (David Kopf Instruments, Tujunga, CA) and exposing the skull via a skin incision. After clearing the connective tissue over the skull with a scalpel, a burr hole was made in the skull with a dental drill to expose the brain dorsal to the RN at A/P: 26.1 mm; L: 0.6 mm; D/V: 7.2 mm (injection 1) and A/P: 25.88 mm; L: 0.6 mm; D/V: 7.2 mm (injection 2). Coordinates were determined using a rat brain atlas, and by drawing on previously established protocols (Watson and Paxinos, 2007; Ziemba et al., 2008). A micromanipulator (Narishige International) was employed for precise measurements. One microliter of scAAV-GFP was injected into each set of coordinates with a 30 G steel needle attached to a 10ml Hamilton syringe (Hamilton, Reno, NV). After the needle was lowered to the appropriate depth, the vector was infused by manually moving the plunger to inject 0.2ul, then pausing for 30 seconds to allow for diffusion. This was repeated until 1ul total volume was injected. After injection the needle was left in place for 5 min to allow for sufficient diffusion away from the injection site. Skin over the skull was then closed with wound clips (CellPoint Scientific, Inc., Gaithersburg, MD). For studies involving mCherry injections, the procedure was performed as above, with the following exceptions: for injections into the FMC, windows were made in the skull and injections performed at A/P: 0.4 mm; M/L: 2.8 mm and D: 2.0 mm (injection 1) and A/P: 1.3 mm; M/L: 2.8 mm and D: 2.0 mm (injection 2); for injections into the reticular formation, injections were performed at A/P: 9.2 mm; M/L: 0.7 mm; D: 8.7 mm (injection 1) and A/P: 10.3; M/L: 0.7 mm; D: 8.7 mm (injection 2). Cortical and reticular formation injections were performed with a glass micropipette

pulled to a diameter of 30-40 μm connected to a nanoliter injector (Nanoject, Drummond Scientific).

Unilateral Hemisections

A skin incision was made in the back and the fat pad separated to reveal the musculature dorsal to the T6-T7 vertebrae. Musculature was carefully incised on either side of the spinous processes, and cleared between each process. Hemi-laminectomies of vertebrae were performed to expose the T8 spinal cord. The dura on the appropriate side was scored to increase traction, and a cut was performed to sever the hemichord with a pair of iridectomy scissors. Scissors were passed through the entirety of the hemichord just lateral to the midline to avoid the posterior spinal artery. Scissors were then closed to cut the hemichord. Following this, a needle was scraped up the inside of the vertebrae in the wound to sever any residual fibers.

Tissue processing

At the completion of each experiment, animals were sacrificed by injection of Fatal-Plus (Dearborn, MI) and transcardially perfused with 0.9% saline, followed by a 4% paraformaldehyde (PFA) solution in 0.1M phosphate buffer (pH 7.4). Brain and spinal cord tissue was dissected, post-fixed in 4% PFA at 4°C overnight and then transferred to a 30% sucrose solution for 2-3 days. Blocks of tissue were then embedded in M-1 Embedding Matrix (Kalamazoo, MI) and quick frozen on dry ice. Serial sections were cut coronally at 30 μm on a cryostat, stained as free floating sections for maximum antibody penetration, and mounted on slides.

Immunofluorescence

For the scAAV-GFP study, staining with Neuronal Nuclei antibody (NeuN) was performed to demonstrate that the GFP signal was contained within neuronal cells, or with GFAP to show the astrocytic scar at the lesion site. Floating sections were first washed with 0.1 M PBS to remove cryoprotectant storage solution, then incubated for one hour in 0.3% Triton X-100 and 5% normal goat serum in 0.1 M PBS to block non-specific antigen sites. The tissue was then incubated overnight at 4°C with rabbit-anti-NeuN antibody (1:400, Millipore, Temecula, CA) or rabbit-anti-GFAP antibody (1:500, Dako Agilent Pathology Solutions, Santa Clara, CA). The next day primary antibody was washed from the tissue thoroughly with 0.1 M PBS and incubated with goat-anti-rabbit Texas Red (1:400, Jackson Labs, Sacramento, CA).

For studies involving ssAAV-mCherry, staining was performed as above with the following exceptions: tissue was incubated with rabbit-anti-DsRed primary antibody (1:400, Takara Bio USA, Mountain view, CA), and donkey-anti-rabbit AF594 secondary (1:400, Jackson Labs, Sacramento, CA).

Results

Anterograde Tracing with scAAV-GFP

In order to determine whether scAAV-GFP could label long projection axons in the RST, virus was injected into the RN, which is the origin of these fibers. Animals were sacrificed at either 2 weeks or 8 weeks, and fluorescent signal was analyzed in the midbrain, medulla and cervical spinal cord.

Viral Transduction was Specific to Neurons in the Red Nucleus

Injection of scAAV2-GFP into the RN produced a bright fluorescent signal that was specific to neurons (Figure 13). GFP signal is shown in a cluster of neurons, with evident decussating axons (Figure 13A, higher magnification in B). To verify that the cells analyzed were neuronal in nature, tissue was probed with NeuN. A high percentage of NeuN (red) signal (Figure 13C) was found to colocalize with the green fluorescence from the scAAV2-GFP (Figure 13D). To determine the sustainability of expression of the scAAV2-GFP signal, GFP expression level was analyzed at 2 weeks and 8 weeks post-injection. No significant difference was found in the number of GFP-positive neurons or in the brightness of the signal, demonstrating that GFP expression levels are stable over time (data not shown).

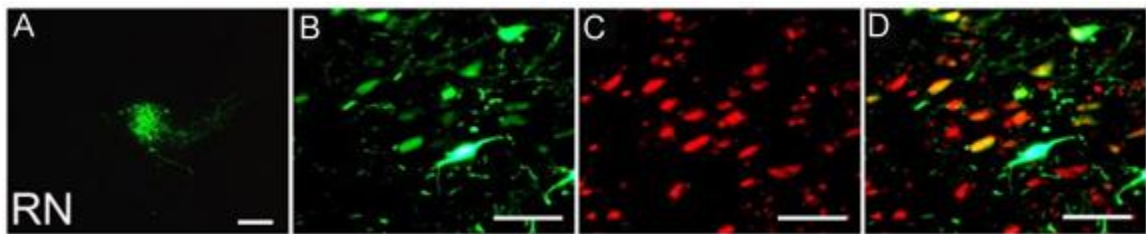


Figure 13. Specific neuronal transduction by recombinant scAAV2-GFP. Following injections of scAAV2-GFP into the RN, strong expression of GFP (green) was detected (A, higher magnification in B). Sections were stained for NeuN (red) to demonstrate neuronal specificity (C and D). Scale Bars: 500 μ m (A) and 200 μ m (B-D).

Labeling of the Rubrospinal Tract in the Brain and Spinal Cord

Stereotactic injections of scAAV2-GFP were made unilaterally into the RN, where the RST originates. The course of the tract was then analyzed at 2 weeks post-injection at the RN, its decussation (as it exits just inferior to the RN); through the medulla and into the lateral funiculus of the spinal cord (Figure 14). Cells transduced by

scAAV2-GFP had a neuronal morphology, with long GFP-positive axons decussating into the contralateral brain (Figure 14, A-C). Coronal sections through the medulla show axonal labeling in the ventrolateral tissue (Figure 14, D-E). In coronal sections of the spinal cord, strongly-labeled bundles of fibers were seen in the lateral funiculus at the expected site of the RST (Figure 14, F-G). In sagittal sections, a robust signal is seen in a straight and well-grouped bundle (Figure 14, H-I).

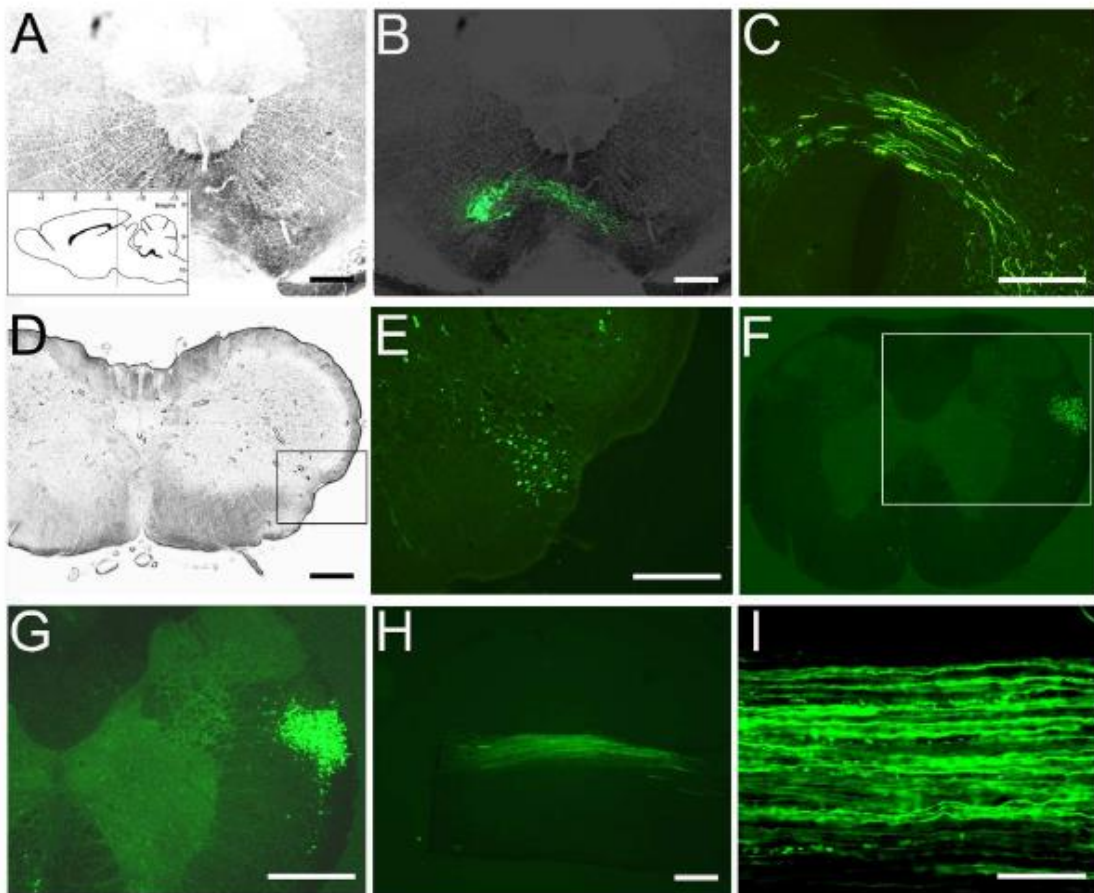


Figure 14. GFP expression in the red nucleus and anterograde labeling of the rubrospinal tract – GFP-positive expression (green) was observed in the RN following scAAV2-GFP injection, as illustrated in coronal sections (A and B). The schematic inset in panel A illustrates the coordinates and levels of this section. Higher magnification images demonstrate anterograde transport of GFP to the contralateral side I, medulla (D and E) and cervical spinal cord in coronal (F and G) and sagittal sections (H and I). Box frames in panels D and F represent the regions magnified in panels E and G, respectively. Scale Bars: 500 μ m (AH), 200 μ m (I).

scAAV-GFP Successfully Labels Rubrospinal Tract Axons at a Lesion Site

To determine whether scAAV-GFP could successfully label RST axons in an injured animal, rats were given a unilateral hemisection lesion at T8 spinal level. This lesion severs all axons on one side of the spinal cord, as represented in Figure 15A. GFP expression in the RN, medulla and spinal cord rostral to the lesion was comparable to that seen in uninjured animals (data not shown). At the lesion site, bright axons were seen approaching the lesion cavity (15B).

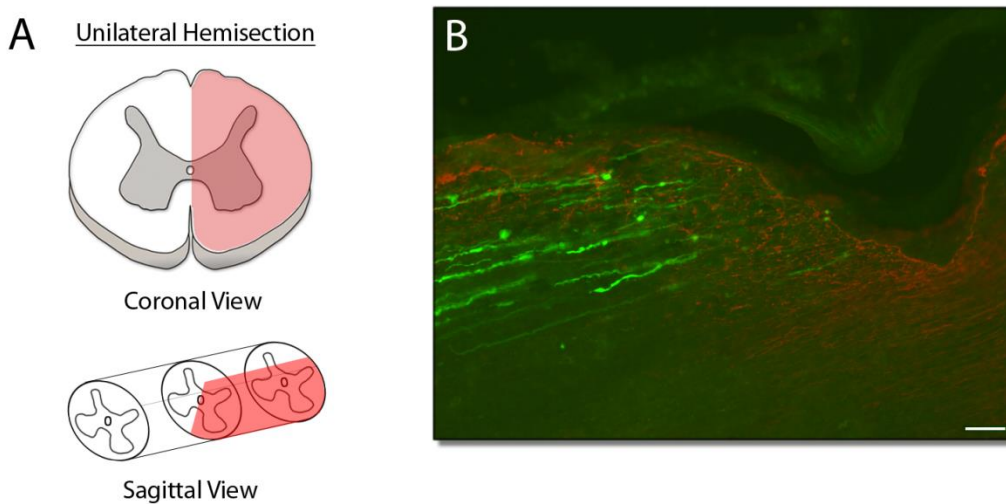


Figure 15. scAAV-GFP robustly labels axons at a lesion site – A) Coronal and Sagittal cartoons of the spinal cord show the area of tissue damaged during a lateral hemisection in red. B) Axons, shown in green, are seen approaching a lesion site, which is stained with GFAP (red), to outline the astrocytic scar. Scale bar: 50 μ m.

Anterograde Tracing with AAV2-mCherry

A number of additional studies described here required use of several fluorescent tracers simultaneously. When an alternative anterograde tracer was needed, AAV2-mCherry was used, either as a self-complementary vector (scAAV2-mCherry) or as a single-stranded vector (ssAAV2-mCherry). The single-stranded vector was employed

when additional elements were needed in the vector, such as wheat germ agglutinin (WGA), which potentially makes the fluorescent proteins travel trans-synaptically.

mCherry successfully labels long descending spinal cord tracts

mCherry was used in conjunction with several studies employing retrograde GFP tracers. In Figure 16, mCherry is shown labeling the FMC (Figure 16A), with axons of the CST apparent in the dorsomedial spinal cord (16B). In 16C neurons of the RN are labeled with mCherry. Axons that run in the ventrolateral spinal cord and synapse onto the intermediate zone of the gray matter are apparent in the spinal cord of the same animal (16D). In Figure 16E the PRF was targeted to label ReST neurons. It is known that tracer injections targeting reticular nuclei may also label other brainstem nuclei (Tuszynski and Steward, 2012). Neurons expressing mCherry are located in the vestibular nuclei (Figure 16E, arrowhead). In the spinal cord of the same animals, axons labeled with mCherry are present in the ventral-most white matter, and are likely a mixture of both reticulo- and vestibulospinal axons.

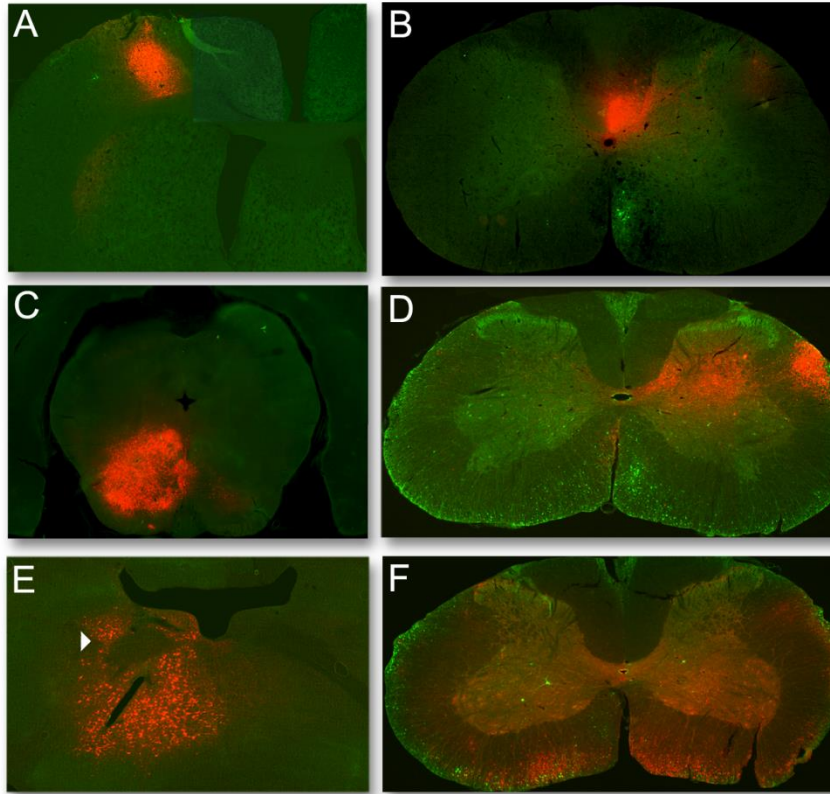


Figure 16. Anterograde labeling with AAV-mCherry – AAV-mCherry (red) efficiently labels neurons in the motor cortex (A), RN (C), and PRF (E). In (E) some diffusion to vestibulospinal neurons is seen (arrowhead). In the spinal cord, axons of the CST (B), RST (D) and ReST (F) are seen, as well as some vestibulospinal axons in (F). The GFP (green) channel is included here only to enhance visualization of the anatomy of the spinal cord.

Discussion

In these studies AAV2 vectors are explored as tools useful for tracing long descending axonal tracts in the CNS. We demonstrate ssAAV-mCherry labeling neurons of the RN and reticular formation, as well as RST and ReST axons. ssAAV vectors have contributed to the treatment of CNS disorders such as Parkinson’s disease (Kaplitt et al., 2007; LeWitt et al., 2011; Marks et al., 2010), Alzheimer’s disease (Ryan et al., 2010; Mandel, 2010; Azzouz et al., 2000) and lysosomal storage diseases (Fu et al., 2002). These studies demonstrate the potential of this vector for human gene therapy, and clinical trials involving AAV vectors have been active since 2002 (Janson et al., 2002).

AAV is considered safe in clinical trials for patients with hemophilia (Nathwani et al., 2011), inherited blindness (MacLaren et al., 2014; Maguire et al., 2008), cystic fibrosis (Wagner et al., 1999) and neurological disorders such as Parkinson's and Alzheimer's disease (Mandel et al., 1997; Bartus et al., 2013; Azzouz et al., 2000).

Self-Complimentary Vectors in Research

Self-complimentary vector are recently developed modifications of the single-stranded AAV vector, which are used in these experiments to label the RN and FMC, as well as RST and CST axons. scAAV produces an intense fluorescent signal without the need for IH procedures, and is neuron-specific. It labels axons close to an injury site (Figure 15), which is supported by additional data in dorsal root crush and dorsal column lesion injuries from our lab (Y. Liu et al., 2014). Our 2014 paper also demonstrated greater transduction efficiency with faster expression of scAAV-GFP in DRG neurons when compared with ssAAV-mCherry. This increased transduction efficiency may mean that lower viral titers or a decreased viral load can suffice when using this vector for treatment. This may translate to reduced immune system reactions when used in human patients (Clement et al., 2009). Indeed, clinical trials have already begun using scAAV vectors for treatment of spinal muscular atrophy and giant axonal neuropathy (Intrathecal administration of scAAV9/JeT-GAN for the treatment of giant axonal neuropathy (2017; Gene transfer clinical trial for spinal muscular atrophy type 1 (2017)).

Our 2014 study also demonstrates co-injection and labeling of scAAV and ssAAV vectors in DRG neurons. Successful co-injection of self-complimentary vectors means that these viruses can serve as useful tools in studies delivering transgenes to neuronal populations for treatment. The packaging capacity of scAAV may be relatively small compared to other vectors, but it can still hold a transgene encoding 40-55 kD of proteins, with 500-1000bp reserved for other transcription elements such as promoters

and polyadenylation signals. Additionally, scAAV could expression cassettes for ribonucleic acid (RNA) cargoes, such as short hairpin RNAs, small interfering RNAs or micro RNAs (Xu et al., 2005). Several studies have used this vector to down-regulate pyruvate dehydrogenase, creating an animal model of Pyruvate Dehydrogenase (PDH) deficiency (Han et al., 2008; Ojano-Dirain et al., 2010), and scAAV vectors have been used to inhibit hepatitis C replication in liver cells (Yang et al., 2010).

Recent studies have also demonstrated that the 2.2kB packaging capacity may be modifiable. Wu et al. successfully packaged 3.3kB into the scAAV vector before it started to create more single stranded genomes than double, and further demonstrated that the modified vectors retain increased transduction efficiency in culture. Furthermore, the use of modified helper plasmids that discouraged production of the single-stranded genomes may stretch that limit to 6.6kB (J. Wu et al., 2007). The mechanism of a modifying packaging capacity is not completely clear, but it has also been demonstrated in ssAAV (Dong et al., 1996; Hermonat et al., 1997; Grieger and Samulski, 2005). Others have found that distinct AAV serotypes can have widely different packaging capacities (Allocca et al., 2008), with AAV5 ranging up to 8.9kb. It may be that as scAAV technology is improved, this vector will become even more useful for studies in the CNS.

There is also work demonstrating that scAAV vectors can infect cells that are relatively non-permissive to ssAAV. In mouse hepatocytes *in vivo*, equivalent doses of scAAV and ssAAV transduced cells at rates of 90% and 2%, respectively (Z. Wang et al., 2003). Cells of the trabecular meshwork (in the eye) were found to be highly permissive to scAAV transduction, and non-permissive to ssAAV (Borras et al., 2006), likely due to downregulation of DNA replication in these cells (Fisher et al., 1996). Additional studies showing administration through the cerebrospinal fluid (CSF) show that many more cells

are infected with scAAV than ssAAV, such as cells lining the ventricles and parenchymal cells close to the periphery of the ventricles (McCarty, 2008).

In summary, self-complimentary AAV2 vectors carrying either GFP or mCherry reporter genes can efficiently transduce neurons in the motor cortex, RN and reticular formation, and intensely label their axonal fibers without the need for IH practices. These vectors can be co-injected with other viruses and used in the injured or uninjured state, making them useful tools in tracing or regeneration studies in long descending tracts of the spinal cord.

Pitfalls of anterograde tracing

The mCherry labeling data presented here affords the opportunity to mention one of the pitfalls of anterograde tracing, especially when the target neuronal population is physically small. The RN, for example, is a roughly ovular three-dimensional structure in the rat brain approximately 1.2 mm x 1 mm x 0.8 mm in size (Reid et al., 1975). Performing a stereotactic injection that hits this structure exactly is very challenging, especially since the coordinates taken from a rat atlas cannot take into consideration individual differences in size or brain structure.

Figure 16C demonstrates another issue – even when the initial targeting is appropriate, the volume of injection must be tightly regulated, as virus infusing too large of a surrounding areas has the potential to infect glia in the area, or even to transport to other tracts and cause off-target effects. This is also seen in the reticular formation labeling in Figure 16E, which has likely diffused to neurons outside of the ReST. In the next chapter, retrograde tracing is used as a tool to achieve greater specificity of labeling. Since a retrograde tracer is taken up at the synapse of the neurons analyzed and travels

some distance to the cell body, there is little chance that cells expressing tracer in a given area are glial. To increase specificity further, a system is employed that requires simultaneous infection of two viral vectors, ensuring that only one tract will be traced.

CHAPTER 3. MAPPING SPINAL PATHWAYS AND ELUCIDATING THEIR CONTRIBUTION TO BEHAVIOR USING RETROGRADE TRACING WITH HIRET LENTIVIRUS

Introduction

Retrograde tracing is a key facet of neuroanatomical studies involving long distance projection neurons. Allowing a virus to be taken up at the synapse allows exploration of synaptic connections of spinal tracts, and reduces the potential for infection of glial cells in the injection area. Previous studies have utilized a variety of tools ranging from classical chemical tracers to viruses intended for gene delivery. Here, the usage of a lentivirus that permits highly efficient retrograde transport from synaptic terminals within the lumbar region of the spinal cord is highlighted. HiRet is used to identify supraspinal and propriospinal circuits innervating MN pools relating to hindlimb locomotion. We also examine changes in interneuronal circuits after a thoracic contusion, highlighting populations that potentially contribute to spontaneous behavioral recovery. In a separate study, a double-viral vector system incorporating HiRet to synaptically silence neurons of the RN or FMC is used in order to explore their contribution to skilled forelimb behavior in the uninjured state.

Retrograde Tracing with the HiRet lentiviral vector

Lentiviral vectors have been used in many studies involving gene therapy, as they provide stable, long-term expression in neuronal populations (B. D. Brown et al., 2007; Adjali et al., 2005; Malik et al., 2005; Lo Bianco et al., 2004; Pawliuk et al., 2001; G. Wang et al., 1999). These vectors are often based on human immunodeficiency virus (HIV), and packaged with vesicular stomatitis viral glycoprotein (VSV-G), which is

simple to concentrate and creates a high-titer product. VSV-G, however, can limit retrograde transport of the transgene, and are toxic to some mammalian cells if constitutively expressed (Liang et al., 2012). VSV-G can also trigger an immune response directed against the envelope protein when used *in vivo* (DePolo et al., 2000; Higashikawa and Chang, 2001).

Immune system reactivity caused by VSV-G has been alleviated in some cases via chemical modification of the envelope glycoprotein, such as conjugation with PEG (Croyle et al., 2004). To improve retrograde transport, Kato and colleagues have modified the envelope by pseudotyping with a fusion glycoprotein (FuG-B) of rabies virus to produce a highly-efficient retrograde transport vector termed HiRet (Hirano et al., 2013; Kato, Kobayashi et al., 2011). HiRet lentivirus has been used to specifically target C3-C4 PNs in the macaque in combination with AAV2 expressing TetOn for reversible synaptic silencing experiments (Tohyama et al., 2017; Kinoshita et al., 2012).

This vector seems to be an excellent choice for mapping CNS pathways because of the advantages outlined in this document: it does not negatively impact the survival or function of infected neurons, and it is stable, long-lasting and easily detectable. Although HiRet is not entirely specific to neurons, as it also labels astrocytes at the injection site, it does show selective uptake at the synapse of neurons, and it does not spread into injured axons or unrelated cells regardless of the dosage or time course of the study (Morcuende et al., 2002; Ugolini, 1995). In addition, coupling HiRet lentivirus containing a tetracycline-inducible promoter to drive transgene expression (HiRet-TRE-eTeNT-eGFP) with a second virus, AAV2-TetOn, allows very tight retrograde labeling of specific neuronal populations. In this study constitutively active HiRet-GFP was used to map

supraspinal and propriospinal connections terminating in the lumbar regions of the rat spinal cord. The advantages this lentivirus provides for mapping studies in the CNS and in the context of thoracic SCI is highlighted.

An IHI was used to deliver a severe contusion (200 kD) to the T10 spinal cord of an adult rat. This injury affects hindlimb locomotion, which is measured by observing the animals' locomoting across a flat plane, and analyzing the details of stepping, weight bearing, correct foot placement, posture and coordination with the BBB scale (Basso et al., 1995). Rats initially lose the ability to bear weight and step, but after several weeks they begin to recover, even without treatment. A plateau of this spontaneous behavioral recovery was observed at about 4 weeks, and therefore this time point was chosen to inject constitutively active HiRet-GFP tracer into the spinal cord, to map reformed connections. HiRet-GFP was injected into the L1-L4 cord, below the lesion, to facilitate uptake by neurons forming connections with lumbar circuitry (Figure 17). This region of the lumbar cord was chosen because of its involvement in hindlimb locomotion, and specifically because the lumbar CPGs are known to reside in these segments (P. A. Guertin, 2013; T. G. Brown, 1914). The intermediate grey matter was targeted to infect a dense population of TPNs and LDPNs (see (Blight, 2004) for review) to determine whether these populations were involved in the spontaneous behavioral recovery seen.

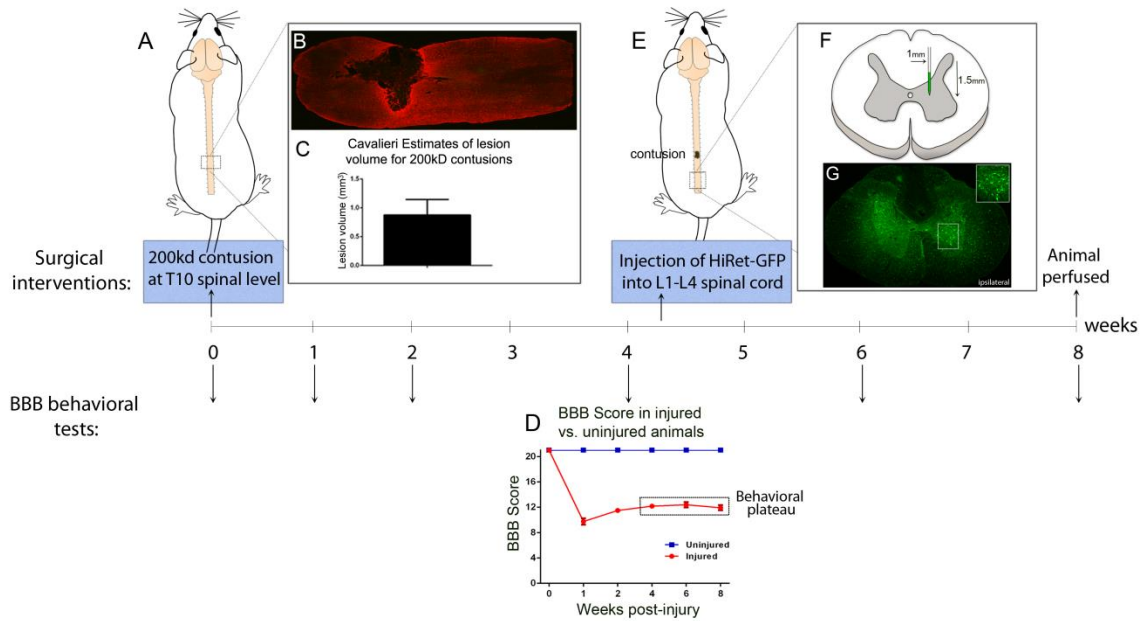


Figure 17. Experimental Details of the HiRet-GFP study. To map neurons that survive and reconnect to the lumbar spinal cord after an injury, a severe contusion was performed at the T10 spinal level (A). (B) A sagittal section of the lesion area shows a large cavity surrounded by an astrocytic scar (red: GFAP). (C) Cavalieri estimates reveal an average lesion volume of 0.9 mm³. (D) Analysis of locomotion via the BBB scale reveals a plateau of spontaneous behavioral recovery at 4 weeks post injury. HiRet-GFP was injected at this time point into the L1-L4 spinal cord, below the lesion area (E). (F) Virus was injected into the intermediate grey matter (schematic) to reach a dense population of PNs (G). (G) Histology at the lesion site shows robust neuronal expression (GFP in green) in the ipsilateral cord, with spread to a few neurons in the medial grey matter of the contralateral side.

Neuronal Silencing with HiRet and TetOn

In a separate study, the HiRet retrograde vector is utilized in combination with a tetracycline inducible system to effect neuronal silencing and explore the contribution of the RST and CST to forelimb motor behavior in uninjured animals. HiRet lentivirus was modified to introduce a tetracycline responsive element (TRE) that transcribes Tetanus toxin and enhanced GFP proteins when in the presence of a tetracycline transactivator protein and doxycycline, a tetracycline derivative (schematic in Figure 18).



Figure 18. Schematic of the HiRet-TRE-eTeNT-eGFP vector – The tetracycline inducible element pictured in yellow (TRE) will cause transcription of eGFP and TeNT when bound with the appropriate complex.

HiRet-TRE-eTeNT-eGFP is introduced at the synapse, where it is taken up and transported to the cell body of a target neuron. A second vector encoding the tetracycline transactivator protein (AAV-CMV-rtTAV16) is delivered to the cell body of the target neuron. When doxycycline is introduced via systemic injection, it can bind to the transactivator protein, and this complex can then bind to the tetracycline inducible element in the HiRet-TRE-eTeNT-eGFP vector (Figure 19). In this way, only cells doubly-infected with the two viruses will transcribe the eGFP and tetanus toxin. Tetanus toxin/eGFP is then transported to the synapse, where it cleaves vesicle docking proteins and prevents neurotransmitter release, effectively ‘silencing’ the neuron and highlighting axons (Figure 19).

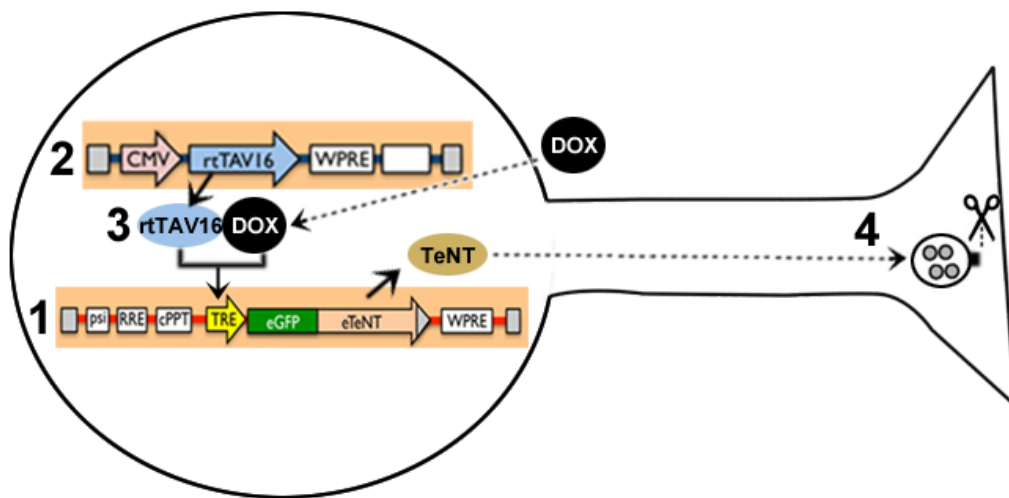


Figure 19. A double viral vector system for silencing neurons – When a neuron is doubly-infected with both the HiRet-TRE-eTeNT-eGFP (1), and AAV-CMV-rtTAV16

(2) vectors, and doxycycline is introduced into the system, a complex will form between doxycycline and the protein product of AAV-CMV-rtTAV16 (3). This complex can bind with the tetracycline element of the HiRet vector, causing transcription of tetanus toxin tagged with eGFP. eTeNT is then transported to the synapse, where it will cleave vesicle docking proteins and prevent neurotransmitter release (4).

Injecting the HiRet vector at the synapses of RST and CST neurons in the C6-T1 spinal areas will specifically target neurons that interact with forelimb musculature such as the wrist, digit, biceps, triceps and shoulder muscles of the animal. This will allow us to observe the effect of neuronal silencing on these neurons when the animals are engaged in tasks using these muscles, such as manipulating food objects, exploratory paw placements during rearing, digit wrapping, and applying forelimb strength while gripping. The behavioral tests described in this chapter are designed to measure these specific behaviors and assess the function of the animal.

In a small pilot study, this multi-vector system was used to express Tetanus toxin in the synapse of rubrospinal neurons in the cervical spinal cord. HiRet-Tre-eTeNT-eGFP was injected into the C5-C7 spinal cord unilaterally targeting laminae VI and VII, where axons of the RST synapse on interneurons. A few days later, TetOn was injected into the RN on the contralateral side and three weeks were given for the virus to transport and express for a maximum number of doubly-infected cells. After 3 weeks doxycycline was given by subcutaneous injection for 7 days, and behavior tested during that period at 2, 4, and 7 days. A one week period of recovery was then allowed to guarantee that doxycycline was washed out of the system, and the last behavioral tests were performed. Doxycycline was then administered for one week prior to perfusion so that histology could be visualized (Figure 20).



Figure 20. HiRet/TetOn pilot study timeline

In a follow-up study, the pilot study is repeated with a few refinements and additions (Figure 21). A lesser volume of HiRet virus was injected and a slightly adjusted targeting scheme was applied to maximize injection into spinal segments associated with forelimb musculature (Takahashi and Nakajima, 1996). Mainly, HiRet was injected into the C6-T1 area instead of C4-C6. Behavioral tests such as the grip strength and IBB tests were added to focus more finely on forelimb motor function. Animal groups were added with AAV-TetOn injections into the FMC, to explore silencing of neurons of the CST, and control groups were added for comparative data.



Figure 21. Timeline of HiRet/TetOn silencing experiment

Materials and Methods

Animals

All surgical and animal care protocols were approved by the Temple University Lewis Katz School of Medicine's Institutional Animal Care and Use Committee, and performed per the National Institutes of Health *Guide for the Care and Use of Laboratory Animals*. Female Sprague-Dawley rats (200-224 g; Harlan Laboratories) were used. Female rats were chosen for studies involving contusive injuries because their bladders are easier to express, which must be done twice a day for 5-10 days following injury. All rats were housed two per cage, on a 12-hour light-dark cycle with food and water provided *ad libitum*. Animals were allowed 7 days of acclimatization prior to any experimental procedure.

For the HiRet-GFP tracing study, animals were divided into two groups: 1) Five animals received 200kD contusions at T10 spinal level. Four weeks later, HiRet-GFP was injected into the L1-L4 spinal cord; 2) Four animals had control laminectomies at the T10 spinal level. Four weeks later, HiRet-GFP was injected into the L1-L4 spinal cord. BBB behavioral tests were performed prior to surgery, and at 1, 2, 4, 6 and 8 week time points. All animals were perfused eight weeks from the first surgery.

For the HiRet/TetOn pilot study, five animals were given unilateral injections with HiRet-TRE-eTeNT-eGFP into the C5-C7 spinal area. A few days later, AAV2-CMV-rtTAV16 was injected into the contralateral red nucleus. Cylinder and horizontal ladder behavioral tests were performed prior to surgery, 1 week post-TetOn injection, at days 2, 4, and 7 of doxycycline injection, and at 1 and 2 week after doxycycline injections were terminated.

For the HiRet/TetOn follow up silencing experiment, animals were divided into four groups: 1) five animals were given unilateral injections with HiRet-TRE-eTeNT-eGFP into the C6-T1 spinal area. A few days later, AAV2-CMV-rtTAV16 was injected into the contralateral RN; 2) Four animals were given unilateral injections with HiRet-TRE-eTeNT-eGFP into the C6-T1 spinal area. A few days later, saline was injected into the contralateral RN; 3) Four animals were given unilateral injections with HiRet-TRE-eTeNT-eGFP into the C6-T1 spinal area. A few days later, AAV2-CMV-rtTAV16 was injected into the contralateral FMC; 4) Four animals were given unilateral injections with HiRet-TRE-eTeNT-eGFP into the C6-T1 spinal area. A few days later, saline was injected into the contralateral FMC. Cylinder, IBB and grip strength behavioral tests were performed prior to surgery, at days 2, 4, and 7 of doxycycline injection, and 1 week after doxycycline injections were terminated.

Viral Vector Construction and Production

Lentiviral Vectors

Constitutively active HiRet lentiviral vector (HiRet-GFP) was constructed by packaging a GFP plasmid (pCSC-SP-PW-GFP, Addgene plasmid #12337, a gift from Inder Verma) (Marr et al., 2004) with rabies virus fusion envelope glycoprotein G (FuG-B; provided by Dr. Kobayashi) and plasmids pMbl and pRev. HiRet-TRE-eTeNT-eGFP was constructed similarly, with plasmid pLV-TRE-eTeNT-eGFP (also provided by Dr. Kobayashi) replacing the GFP plasmid. The vector and packaging plasmids were transfected into HEK293T cells using the CaPO₄ method, supernatants were collected and virus was concentrated via centrifugation. Purified virus was suspended in a Tris

buffer containing rat albumin and mannitol. Lentiviral titers were determined using a P24 HIV-1 ELISA kit and were estimated at 2×10^7 TU/mL infectivity.

AAV Vectors

The AAV2-TetOn vector (AAV2-CMV-rtTAV16) was generated in a similar manner as above. The plasmid pAM-rtTAV16 was generously provided by Dr. Kobayashi and was packaged using the helper-free method as reported previously (Ayuso et al., 2010; Y. Liu et al., 2014). In brief, HEK293T cells at 70 – 80% confluency were transfected with two packaging plasmids, one carrying AAV rep and cap, the other with AAV helper functions and the transgene using PEI (MW 25k, Warrington, PA). Three days post transfection, cell supernatant and lysates were harvested. 40% PEG 8000 was added to precipitate crude virus for 2 hours. AAV samples were double-ultracentrifuged in a CsCl gradient with isolated viral fractions dialyzed in 0.1 M PBS/0.5% sorbital overnight (Y. Liu et al., 2014; Ayuso et al., 2010). Purified fractions were added to HEK293T cells previously transduced with HiRet-TRE-eTeNT-GFP to verify function. On the third day doxycycline was added to induce GFP expression, and cells were analyzed on the fourth day for fluorescence. Titer for the AAV2-CMV-rtTAV16 vector was estimated at 1.3×10^{12} GC/ml and the HiRet-TRE-eTeNT-GFP vector at 6.7×10^6 TU/ml.

Surgical Procedures

Rats were weighed and anesthetized by intraperitoneal injection of ketamine at 67 mg/kg and xylazine at 6.7 mg/kg dosage. The target incision area was shaved and disinfected thoroughly with iodine and 70% ethanol. Ophthalmic ointment was applied to

the eyes to prevent drying. During all procedures, animals were monitored for depth of anesthetic plane and booster shots of ketamine/xylazine were given if breathing became too rapid or whisking occurred. After surgery, rats were placed on a temperature controlled heating pad and administered 10 ml of saline (0.9% NaCl, Baxter Healthcare Corp.) to combat dehydration and 10 mg/ml of cefazolin antibiotic (West-Ward Pharmaceutical Corp.) to combat infection. Rats were monitored until wakeful and then transferred to their home cages, where they were provided with analgesics in the form of 2mg Rimadyl tablets (Bio Serv, Flemington, NJ).

Spinal Cord Injections

For the HiRet-GFP retrograde tracing study, HiRet-GFP lentivirus was injected into the L1-L4 spinal cord to target the synaptic terminals of PNs with connections to lumbar circuitry. A skin incision was first made on the back and the fat pad separated to reveal the musculature. Musculature was cleared from the T11-T13 vertebral bodies, and hemi-laminectomies performed to expose the L1-L4 spinal cord. It is well established that the spinal cord does not extend the entire length of the vertebral column and L1 – L4 spinal cord lies directly under the T12 –L1 vertebrae (Gelder and Chopin, 1977). Targeting of correct vertebral levels was done with the assistance of rat spinal cord atlas and a previous study outlining landmarks in the mouse (Harrison et al., 2013; Watson et al., 2009). HiRet-GFP was injected with a beveled pulled glass needle with an aperture of 30-40 μm into 6 evenly spaced sites (1 mm) along this length. Injections were made lateral to the midline at 0.8 mm. Virus was injected at 3 separate depths of 0.5 mm, 1.0 mm, and 1.5 mm, for a total volume of 2 μl per site (0.7 μl at each depth). All injections

were done using a nanoliter injector (Nanoject, Drummond Scientific) attached to a micromanipulator (Narishige International) for precise measurements.

In the TetOn studies, HiRet-TRE-eTeNT-eGFP was injected into either the C4-C6 (pilot study) or C6-T1 (follow-up study) spinal cord to target synaptic terminals of RST and CST neurons that may influence the forelimb muscles. A 0.5 cm incision is made through the dorsal skin above vertebra C4 – C6 to target the C4-C6 spinal cord, or C5-C7 to target the C6-T1 spinal cord. The skin is retracted to expose the underlying muscle. The exposed spinotrapezius muscle is cut along the midline with scissors, and then spread with a small Alm retractor. The muscles are freed from the cervical vertebrae with scissors and the right dorsal vertebral arch and the dorsal spinous process are carefully removed from the vertebra, so as to not damage the spinal cord. Precise injections into the intermediate zone of the spinal cord were performed according to previously established protocols (Y. Liu et al., 2016; Kelamangalath et al., 2015; Tang et al., 2007; Romero et al., 2001). This was done using a beveled glass micropipette pulled to a diameter of 30-40 μm connected to a nanoliter injector (Nanoject, Drummond Scientific). Coordinates were determined using a rat spinal cord atlas, previously established protocols and a micromanipulator (Narishige International) for precise measurements (Tang et al., 2007; Watson et al., 2009). All coordinates were taken from the midline or surface of the spinal cord. The midline was determined either by the position of the posterior spinal artery or the midpoint between the entry zones of the dorsal roots. Unilateral injections of HiRet-TRE-eTeNT-eGFP { 1 μL /injection (pilot study) or 0.5 μL /injection (follow-up study); 8 injection sites at 0.5 mm apart } were made at respective spinal levels targeting the intermediate grey matter at laminae V-VII; 0.8 mm lateral to

the posterior sulcus and 1.5 mm from the dorsal surface of the spinal cord, based on ours and others previously published reports (Watson et al., 2009; Filli et al., 2014). All injections were done using a nanoliter injector (Nanoject, Drummond Scientific) attached to a micromanipulator (Narishige International) for precise measurements.

Contusion injuries

An IHI was used to deliver a 200 kilo dyne (kD) severe contusion to the T10 spinal cord. A skin incision was made in the back and the fat pad separated to reveal the musculature dorsal to the T7-T9 vertebrae. Musculature was carefully incised on either side of the spinous processes, and cleared between each process. Laminectomy was performed to expose the T10 spinal cord, being careful to clear a wide enough margin so that the impactor piston was not in danger of hitting bone. The animal was then placed into a spinal holder. Forceps on the holder hook into the ventral notches in between the vertebrae to secure the animal tightly so that a secondary injury will not occur if the animal bounces back into the piston.

The spinal holder was then slid into the IHI stage and secured with clamps. The piston was positioned at 4mm above the target and the software engaged to deliver a 200kD blow. The software interface is pictured below with example graphs from an experimental animal that has just been contused (Figure 22).

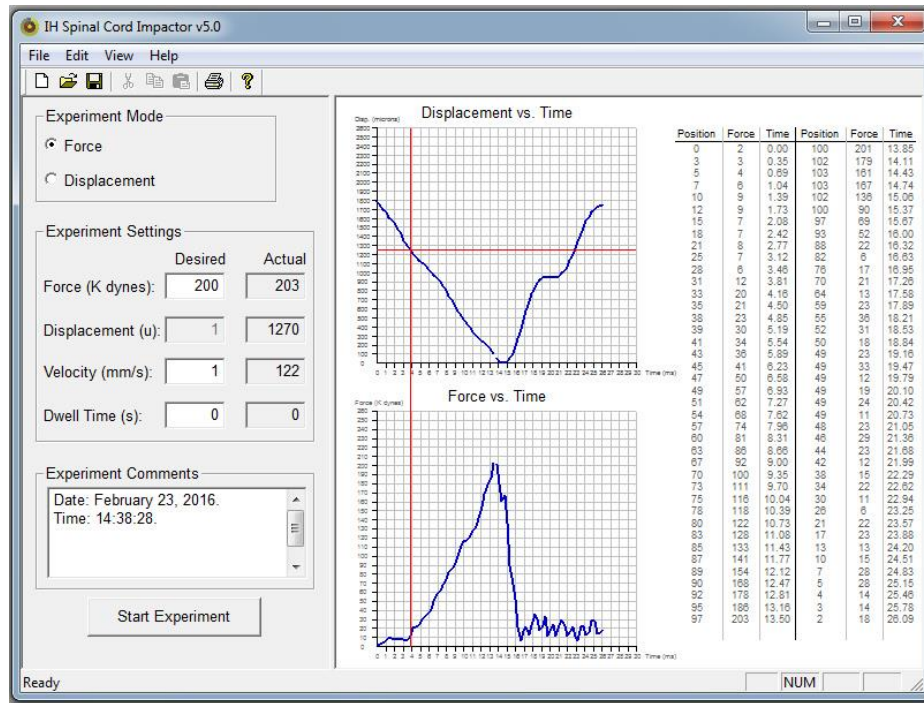


Figure 22. Contusion Graphs from an Infinite Horizons Impactor – A 200kD contusion on the animal above produced an actual hit force of 203kD, a Displacement vs. Time graph that shows smooth stepping and withdrawal, and a Force vs. Time graph that shows a single significant peak, representing the contusive hit.

Stereotactic Brain Injections

For the TetOn neuronal silencing study, AAV-CMV-rtTAV16 (TetOn) was injected into either the RN or FMC by placing the animals into a stereotactic frame (David Kopf Instruments, Tujunga, CA) and exposing the skull via a skin incision. After clearing the connective tissue over the skull, a burr hold was made in the skull with a dental drill to expose the brain dorsal to the RN at A/P: -6.1 mm; M/L: 0.6 mm; D/V: -7.2 mm (injection 1) and A/P: -5.88 mm; M/L: 0.6 mm; D/V: -7.2 mm (injection 2) or the FMC at A/P: +0.2 mm; M/L: 2.8 mm; D: 1.6 mm (injection 1), A/P: +0.2 mm; M/L: 3.2 mm; D: 1.6 mm (injection 2), A/P: -1.4 mm; M/L: 2.8 mm; D: 1.6 mm (injection 3) and A/P: -1.4 mm; M/L: 3.2 mm; D: 1.6 mm (injection 4).

For RN injections, two microliters of TetOn was injected into each set of above coordinates with a 30 G steel needle attached to a 10ml Hamilton syringe (Hamilton, Reno, NV). After the needle was lowered to the appropriate depth, the vector was infused by manually moving the plunger to inject 0.2ul, then pausing for 30 seconds to allow for diffusion. This was repeated until 2ul total volume was injected. After injection the needle was left in place for 5 min to allow for sufficient diffusion away from the injection site. For cortical injections, a beveled pulled glass needle with an aperture of 30-40 μm was used to inject 2ul of solution into each coordinate using a nanoliter injector (Nanoject, Drummond Scientific) attached to a micromanipulator (Narishige International) for precise measurements. After injection the needle was left in place for 5 min to allow for sufficient diffusion away from the injection site.

Drug administration

During the experiments using the TetOn system, doxycycline was administered four weeks after injections of HiRet-TRE-eTeNT-eGFP and AAV2-TetOn to activate this inducible system. Drug was injected subcutaneously at 30mg/kg once a day for seven days. Doxycycline was also administered for one week prior to perfusion to visualize GFP signal during histological preparations.

Tissue processing

At the completion of each experiment, animals were euthanized by injection of Fatal-Plus (Dearborn, MI) and transcardially perfused with saline (0.9% NaCl), followed by a 4% PFA solution in 0.1M phosphate buffer (pH 7.5). The brain and spinal cord were promptly dissected. Spinal cord samples were dissected with dorsal roots intact for

identification of each spinal level. Samples were post-fixed in 4% PFA overnight at 4°C. Tissue samples were then transferred to 30% sucrose for an additional 3 days prior to sectioning. The spinal cord was cut into blocks encompassing the appropriate spinal segments by counting the attached dorsal roots from well-established landmarks (Gelderd and Chopin, 1977) and cut into regions using a 1mm rat brain matrix (Ted Pella, Reading, CA). Brain and brainstem blocks were carefully identified based on the rat brain atlas (Watson and Paxinos, 2007). The medulla was isolated by first placing a single edge razor blade through the slot closest to the back of the cerebellum, and the next blade six millimeters rostral. The pons was isolated from the next 3mm slice, extending to about the middle of the inferior colliculus. The midbrain was the next rostral 3mm section extending to just anterior to the superior colliculus. Serial sections were cut coronally at 30 (spinal cord) or 60 μm (brain) on a cryostat, stained as free floating sections for maximum antibody penetration, and mounted on slides.

Immunofluorescence

To amplify GFP fluorescence, every fifth section was permeabilized in 0.3% Triton X-100 with 5% normal donkey serum to block non-specific binding sites. Spinal cord samples were then incubated with chicken-anti-GFP primary antibody (1:1000; Aves Labs Inc., Tigard, OR) overnight at 4°C. The next day, samples were incubated with donkey-anti-chicken-AlexaFluor 488 secondary antibody (1:400, Jackson ImmunoResearch Laboratories, Inc., West Grove, PA), mounted and photographed using Axiovision software (Carl Zeiss Microscopy, Thornwood, NY). Brain sections were co-stained with NeuN for easier identification of groups of neurons. The same procedure as above was used, with primary incubation in rabbit-anti-NeuN antibody (1:400, Millipore,

Temecula, CA)/chicken-anti-GFP primary antibody (1:1000; Aves Labs Inc., Tigard, OR), and secondary incubation in goat-anti-rabbit Texas Red (1:400, Jackson Labs, Sacramento, CA)/donkey-anti-chicken-AlexaFluor 488 secondary antibody (1:400, Jackson ImmunoResearch Laboratories, Inc., West Grove, PA).

Stereology

Unbiased stereological estimates of GFP-positive neurons were performed as previously described (West et al., 1991). Systematic random samplings of GFP-positive neurons were acquired using Stereo Investigator (MicroBrightField, Inc., Williston, VT). Spinal cord sections were identified prior to tissue cryosectioning and the contours between grey and white matter identified by differential phase or dark field imaging. The laminae of Rexed were identified as illustrated in our previous publications (Tang et al., 2007; Rexed, 1952). Boundaries were drawn around regions of interest in the grey matter of C4-C7 or T5-T8. Ipsilateral and contralateral grey matter was generally determined by density of GFP signal in axons in the corresponding white matter.

Brain sections were processed as follows: midbrain sections identified containing the RN were quantified from bregma -5.20 mm to -6.70 mm (Watson and Paxinos, 2007). The RN was identified within this region as an almost circular cluster of neurons ventrolateral to the periaqueductal grey and bounded medially by the medial raphe nucleus and laterally by the medial lemniscus as described in earlier studies (X. Wang et al., 2011; Y. Liu et al., 2014). Neurons within the caudal PRF were quantified from bregma -9.10 mm to -10.3 mm. The boundaries indicated in Figure 22 were identified to be dorsal to the ventral pontine nuclei, lateral to the raphe nuclei, and medial to the

subcoeruleus nuclear cluster (Watson and Paxinos, 2007). Neurons within the gigantocellular region of the MRF were quantified from bregma -11.0 mm to -12.5 mm. These nuclei were lateral to the medial lemniscus/spinotectal tract, dorsal to the pyramidal tract and medial to the intermediate reticular formation (Watson and Paxinos, 2007). A 350 x 350 μm random sampling grid was placed on all regions of interest for spinal cord grey matter, RN and brainstem. Guard zone height was 5 μm (top and bottom) with a sampling brick depth of 20 μm for spinal cord or 40 for μm brain areas. Z-stacks were taken at each region of interest with at 40x objective using a Leica fluorescent microscope. GFP-positive neurons were marked if inside a counting frame (75 x 75 μm for spinal cord; 100 x 100 μm for brain) using the optical fractionator workflow. Total estimates of neurons labeled in the C4-C7 and T5-T8 spinal cord, RN and reticular formation (pontine and medullary) ipsilateral and contralateral to the injection site were reported.

Behavioral Assessments

For the HiRet-GFP contusion studies, several behavioral tests were administered to measure the degree of spontaneous recovery in these animals. The Beattie, Bresnahan and Basso (BBB) hindlimb locomotor scale was used to analyze stepping, weight bearing and coordination during locomotion, and the horizontal ladder test was used to determine recovery of proprioception, as described below. Baseline behavior was measured before any surgical intervention, and then again at 1, 2, 4 and 6 weeks post-contusion. All behavioral assessments are conducted while blinded to the treatment groups.

For the TetOn inducible vector studies, which focused on forelimb function, behavioral methodology included the cylinder test (sometimes referred to as the limb asymmetry test), the grip strength test, and forelimb function measurement via the Irvine, Beatties and Bresnahan scale (IBB). The cylinder test measures the use of each forepaw during normal exploratory rearing. Grip strength measures the amount of force that an animal can exert while gripping a metal rod, and the IBB scale measures precision grip and digit function.

BBB hindlimb locomotor test

The hindlimb locomotor test is a measure of success and accuracy of gait in the hind limbs while an animal locomotes across a flat plane. Gross measures such as the ability to step on the plantar surface of the paw, support the body weight and walk with a coordinated gait can be measured. Additionally, fine motor skills such as stability of the trunk, position of the tail, lateral paw placement and ability to walk without dragging the toes are measured. Animals were analyzed by two investigators trained in this method for a 4 minute time period, and a score was given on the 21 point BBB scale (Basso et al., 1995).

Cylinder test

The cylinder test is performed by placing an animal into a Plexiglas cylinder approximately 20cm high x 20cm diameter and recording exploratory rearing during a 5 minute period, as previously described (Gensel et al., 2006). During this time the animal will naturally rear up onto its hind limbs and explore the side of the cylinder with its forepaws. Videos are later scored in slow motion by counting the number of left and right

forepaw placements versus the number of times the animal placed the forepaws simultaneously on the side of the cylinder. Simultaneous placement is defined as both limbs contacting the side of the cylinder within 0.5 sec or less of each other.

Grip strength test

The grip strength test is performed on a specially designed force meter (Dunnet Style, Linton Instruments) that contains small metal bars that an animal can grip onto with their forepaws. This is designed to take advantage of the natural instinct of a rat to grip onto something when they are being lifted from a surface. Animals are gently encouraged to grip onto the metal bars, which are attached to force transducers. The animal is then pulled slowly away from the bars until they release their grip. Scores are assessed as an average force at release over 5 trials (Strong et al., 2009; M. A. Anderson et al., 2016).

Horizontal Ladder

Assessment for recovery of proprioceptive axons was measured by recording the accuracy of paw placement on a horizontal grid as described by Kunkel-Bagden et al., al. and modified by the Whishaw group (Kunkel-Bagden et al., 1993; Metz and Whishaw, 2009). Rats are videotaped walking for a minimum of 30 steps across a 6-foot horizontal grid contained randomly spaced pegs, each of which are 4–8 cm apart. The videos are then scored by dividing the number of correct foot placements by the total steps taken, to achieve a percentage of correct steps. Different categories of incorrect placements are also noted (misses, slips and touches), as each is indicative of a slightly different type of deficit.

IBB test

The IBB scale measures intricacies of forelimb movement and precision grip of an animal while it is eating (Irvine et al., 2010; Irvine et al., 2014). Animals are given two different shapes of cereal – a donut shape and a sphere. This allows for different types of movement with the digits during consumption. During the test, movements of the shoulders, forearms and digits are scored, as well as the angle of the forelimbs and the ability of the animal to open and close the paw. Cereal is given once a day for one week prior to testing to acclimate the animals. Animals are then placed in a Plexiglas cylinder and videotaped eating two pieces of each shape of cereal. Videos are replayed in slow motion and scored according to the 10 point scale.

Statistical analysis

All statistical analysis was performed using GraphPad Prism 6 (GraphPad Software, Inc., La Jolla, CA). Statistical evaluations of stereological data were analyzed by two-way analysis of variance (ANOVA) followed by a Sidak post-hoc test for statistical significance. All morphological analysis is represented as mean \pm standard deviation (SD), all behavioral data is reported as mean \pm standard error of the mean (SEM).

Results

Retrograde Tracing with the HiRet lentiviral vector

As discussed previously, retrograde tracing is a key method for targeting neurons with specificity by introducing viral vectors into the area of a neuronal synapse, where

they are taken up and transported to the cell body. In this study, our purposes were two-fold: to explore the properties of the HiRet vector as a retrograde tracer and to map neurons that survive and make reconnections to the lumbar spinal cord after a contusive injury.

HiRet-GFP labels descending pathways into the L1-L4 spinal cord

GFP-positive labeling of neurons was analyzed within the thoracic and cervical spinal cord, as well as brain nuclei such as the RN and reticular formation, both in the uninjured state and 8 weeks after a severe thoracic contusion. In the thoracic grey matter, the neuronal population expressing HiRet-GFP in uninjured animals amounted to $7,401 \pm 1,744$ neurons on the side ipsilateral to the injection, and $3,526 \pm 344$ neurons in the contralateral cord (Figure 23A, quantified in 23E). The majority of neurons were clustered in laminae V – VII, though scattered neurons were seen in laminae IV, VIII, IX and X. Stereological counts 8 weeks after spinal cord contusion showed GFP-positive labeled neurons were reduced to $1,211 \pm 653$ in the ipsilateral cord and 871 ± 883 in the contralateral cord, representing a 75-80% total loss of signal. Nearly all remaining neurons were located in laminae V-VII of the thoracic cord (Figure 23B, quantified in 23F).

The cervical spinal cord is known to have significant connections with the lumbar spinal cord due to relays between the two CPGs (Holstege, 1987; Zorner et al., 2014). In agreement with this possibility, a greater proportion of GFP-positive labeled neurons were observed within the cervical cord compared to the thoracic spinal cord. There were $18,777 \pm 8,144$ neurons seen on the side ipsilateral to the injection and $13,742 \pm 5,719$ in

the contralateral cord in uninjured animals (Figure 23C, quantified in 23F). As with the thoracic cord, there was a significant loss of GFP-positive labeled neurons in contused animals, though it was significantly less than that observed in the thoracic region.

Contusion resulted in an approximately 60% loss ($7,572 \pm 3,621$ neurons) and about a 40% loss ($8,407 \pm 4,602$ neurons) of GFP-positive labeled neurons within the ipsilateral or contralateral spinal cord, respectively (Figure 23D, quantified in 23F). In uninjured rats, the greatest concentration of neurons occurred in laminae V – VII, with just a few isolated neurons in laminae IX and X; whereas, after contusion the expression was primarily localized to laminae VI and VII, with a few cells in laminae V.

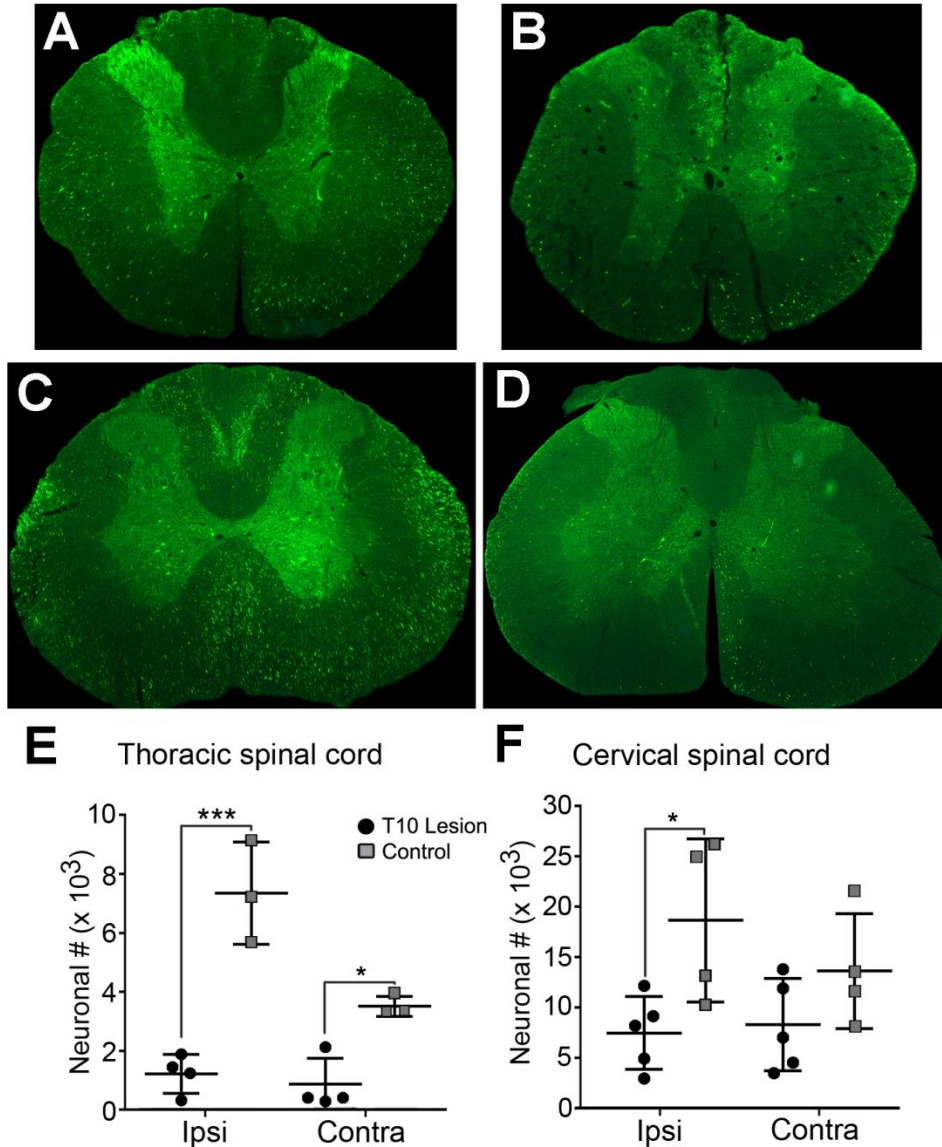


Figure 23. Extent of GFP-expressing neurons within the spinal cord in normal and T10 contused rats – Injection of HiRet-GFP into the non-injured lumbar spinal cord labels many axons and neurons bilaterally within the T7 (A) and C4 (C) regions of the spinal cord. Injection of HiRet-GFP into the lumbar spinal cord 8 weeks after a 200kD contusion injury to T10 showed a dramatic reduction in the numbers of axons within white matter tracts and neurons within the gray matter at T7 (B) or C4 (D) when compared to the GFP-labeling in normal rats. Stereological estimate of HiRet-GFP expressing neurons between the non-injured (control) and 8 weeks post-injury (lesion) shows a significant reduction in the numbers of bilateral thoracic propriospinal neurons (E) or ipsilateral cervical neurons (F). Comparisons in both graphs by two-way ANOVA ($F(1,12) = 9.181, p=0.0105$ (cervical) or $F(1,10)=68.70, p<0.0001$ (thoracic); Sidak multiple comparisons post-hoc test, $p=0.0263$ (cervical), $p<0.0001$ ipsi, $p=0.011$ contra (thoracic); * = $p < 0.05$, **** = $p < 0.0001$) Data are mean \pm SD. N = 5 injured, n=4 control. Scale bars: 500 μ m.

Connections from the lumbar cord to supraspinal nuclei

Retrogradely labeled GFP-positive neurons were also analyzed in the brainstem, midbrain, and cortex to observe expression in nuclei associated with locomotion, and to look for connections that may have been rerouted to unexpected areas.

Reticular Nuclei

GFP-positive neurons were localized within several regions of the brainstem and midbrain, most notably the pontine (caudal part) and medullary reticular nuclei and the R. In the MRF in uninjured animals, 1665 ± 532 GFP-positive neurons were labeled on the ipsilateral side, and 728 ± 153 on the contralateral side (Figure 24A, quantified in 24G). Eight weeks after contusion, GFP-positive neuronal numbers dropped by about 40% to 708 ± 116 on the ipsilateral side and by 80% to 155 ± 24 on the contralateral side (Figure 24D, quantified in 24G).

A similar density of GFP-positive labeled neurons was found in the caudal pontine reticular nuclei. In uninjured animals, 1403 ± 433 neurons were labeled on the ipsilateral side, and 492 ± 71 on the contralateral side (Figure 24B, quantified in 24H). Four weeks after contusive injury, GFP-positive neuronal numbers decreased 70% to 412 ± 211 neurons on the ipsilateral side and about 75% to 130 ± 36 on the contralateral side (Figure 24E, quantified in 24H).

The Red Nucleus

The RN is a midbrain structure whose total contribution to rodent behavior is not completely clear. Recent evidence from the Wishaw group suggests a role in the arpeggio movement associated with forelimb reaching and grasping, which was hindered

when a focused lesion was made in the magnocellular region of the nucleus, the area that gives rise to the RST (Whishaw et al., 1990). The RST's contribution to hindlimb locomotion is less clear. RST fibers are known to contact the lumbar spinal area, especially in laminae V and VI, and innervate interneuron pools (Wanner et al., 2013; K. D. Anderson et al., 2007). Thus, the RN was examined for GFP-positive labeling after injection of HiRet-GFP into lumbar spinal cord terminals.

A small population of GFP-positive labeled neurons was seen in the RN in both injured and uninjured animals. RST axons decussate almost immediately upon exiting the RN, and thus more signal can be expected on the side contralateral to the injection site (Bareyre et al., 2011). In uninjured animals, 315 ± 337 neurons were found on the contralateral side and 61 ± 106 neurons were found on the ipsilateral side (Figure 24C, quantified in 24I). Interestingly, there was no significant loss of neurons seen in contused animals, with 314 ± 283 neurons seen on the contralateral side, and 109 ± 163 neurons quantified on the ipsilateral side (Figure 24F, quantified in 24I).

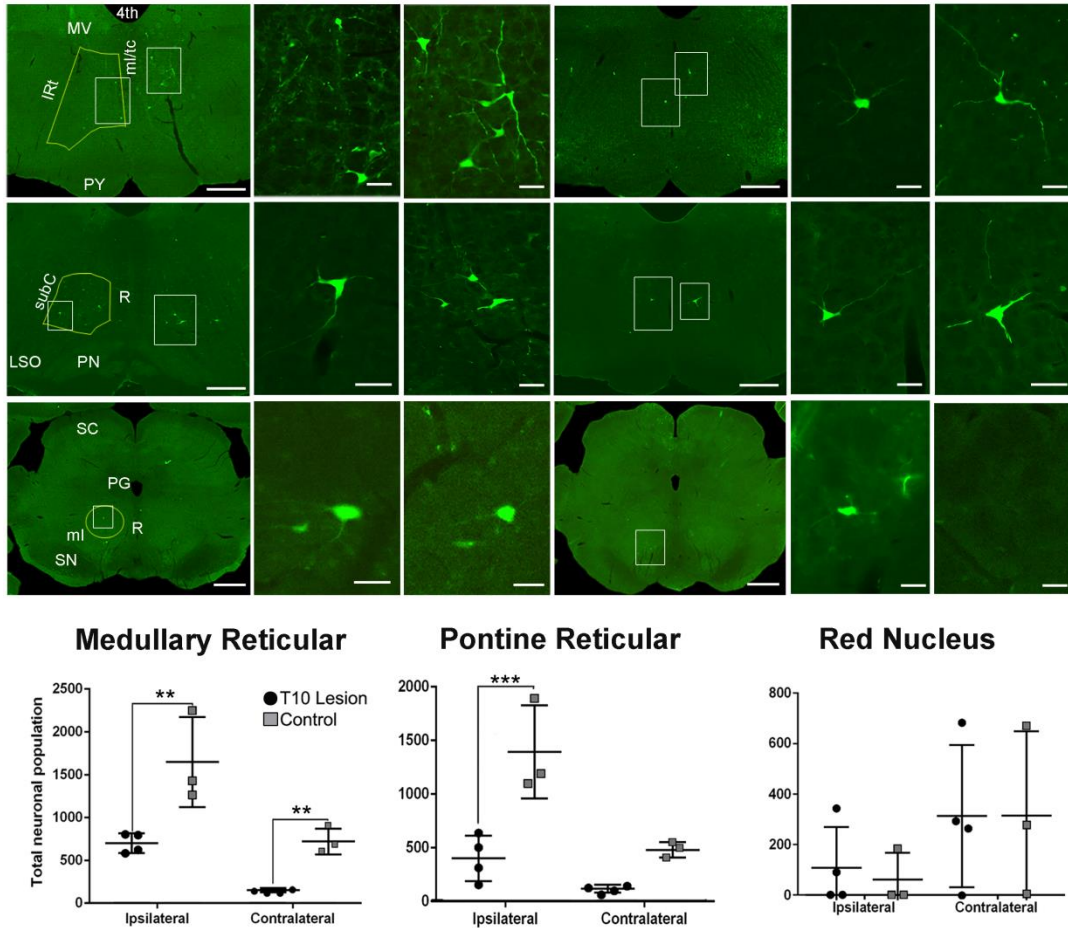


Figure 24. GFP-positive neurons located within the brainstem after injection of HiRet-GFP into the lumbar spinal cord in uninjured and contused rats – Representative images of GFP-expressing neurons within the MRF (A, A', A''), PRF (B, B', B''), and RN (C, C', C'') from HiRet-GFP injections into the non-injured lumbar spinal cord. Higher magnification from white boxed inserts from panels A, B, and C showing GFP-positive neurons contralateral (A', B', C') or ipsilateral (A'', B'', C'') to the injection site. Representative images of GFP-expressing neurons (white boxes) within the MRF (D, D', D''), PRF (E, E', E''), and RN (F, F', F'') from HiRet-GFP injections 878 into the lumbar spinal cord 8 weeks after T10 200kD contusion injury. Higher magnification from respective images showing GFP-positive neurons contralateral (D', E', F') or ipsilateral (D'', E'', F'') to the injection site. Stereological estimates of neuronal numbers within the MRF (G), PRF (H) and RN (I) from non-injured and contused spinal cord. Yellow lines represent regions that were chosen for stereological assessments. Contusion injury significantly reduced the number of GFP-positive neurons within the brainstem. 4th = fourth ventricle; MV = medial vestibular nucleus; IRT = Intermediate Reticular nucleus; ml/tc = medial lemniscus/tectospinal tracts; PY = pyramidal tract; subC = Subcoeruleus nucleus; R = raphe; PN = pontine nuclei; SC = superior colliculus; PG = periaqueductal gray; SN = substantia nigra. Comparisons in both graphs by two-way ANOVA ($F(1,10) = 30.03, p=0.0003$ (PRF) or $F(1,10) = 30.64, p=0.0002$ (MRF);

Sidak multiple comparisons post-hoc test $p=0.0004$ (PRF) or $p=0.013$ ipsi and 0.0298 contra (MRF) $** = p < 0.01$; $* = p < 0.05$) Data are mean \pm SD. N = 5 injured, n=4 control. Scale bars: (A), (B), (C), (D), (E), (F) = 1mm; (A'), (A''), (B'), (B''), (C'), (C''), (D'), (D''), (E'), (E''), (F'), (F'') = 50 μ m.

Silencing Neurons of the Red Nucleus with TetOn

The function of the RST is not completely understood. This is partially due to the difficulty of creating a lesion that will sever RST fibers without affecting other tracts. By using the inducible multi-vector TetOn system to shut down the synaptic function of rubrospinal neurons specifically, we helped determine their effect on behavior in an uninjured animal.

The HiRet/TetOn System produces a profound deficit in forelimb function in an uninjured animal, with inducibility issues

A profound effect on forelimb function was observed in the affected limb in animals tested in the HiRet/TetOn pilot study. In the cylinder paw preference test, for example, animals explored with the affected forelimb in a curled position while rearing, as pictured in Figure 25.



Figure 25. Affected animal in the cylinder test – The right paw of the pictured animal remained curled throughout natural rearing, and was not used to explore.

This caused significant deficits in individual forelimb usage during this test (Figure 26A). There were also significantly more misses and foot slips while locomoting on the horizontal ladder (Figure 26B), and a trend towards impairment in the grooming and inclined plane tests (data not shown).

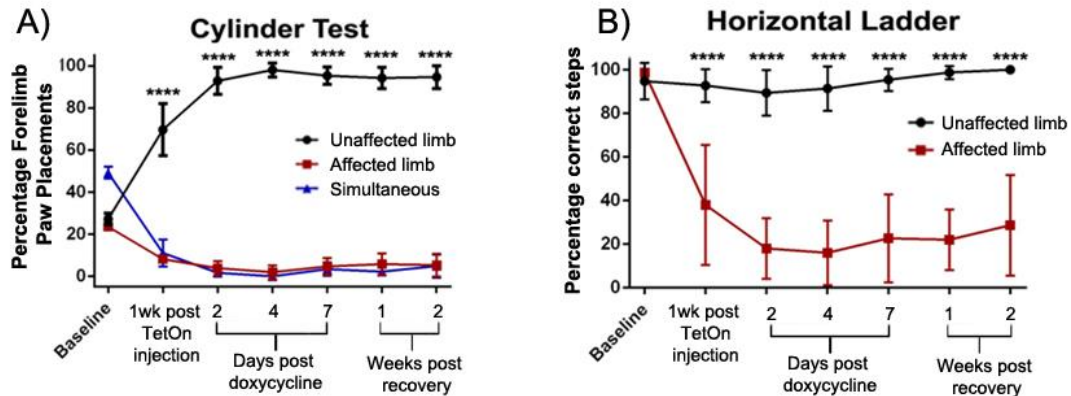


Figure 26. Animals injected with a multi-vector inducible system have profound forelimb deficits in the affected forelimb – A) the percentage of independent placements of the affected forelimb and simultaneous forelimb placements during exploratory behavior is significantly decreased in animals treated with HiRet/TetOn. B) the percentage of correct affected forelimb placements is significantly decreased in the horizontal ladder test in animals treated with HiRet/TetOn. Comparisons by two way ANOVA, *****: $p < 0.0001$, Data are mean \pm SEM.

One major issue with this study was the inducibility of the system. As you can see from the graphs in Figure 26, deficits to forelimb usage appeared before doxycycline was injected, and no recovery of function occurred during the recovery period. However, it is important to show this data as evidence that synaptic silencing was occurring. Several troubleshooting studies occurred after this pilot study, including conversations with other labs that had the same issue with this system, and suggested a lower volume of HiRet injected to solve the problem. In the data immediately following, you will see that no behavioral change occurs before doxycycline is administered.

Silencing of neurons of the red nucleus does not affect skilled forelimb motor behavior in an intact rat

Robust and specific expression of GFP was seen in cells of the RN (Figure 27A and B). Clear associated axons and expression of NeuN in these cells revealed them to be neuronal (Figure 27C). As the GFP and Tetanus toxin proteins are transcribed together, robust GFP expression should indicate robust expression of Tetanus toxin, and therefore neuronal silencing. Silencing these neurons had no discernible effect on digit wrapping and forelimb muscle strength in the grip strength test (Figure 27D), or fine manipulation of food in the IBB test (Figure 27E). There was also no effect on paw preference and natural exploratory behavior in the cylinder test (Figure 27F).

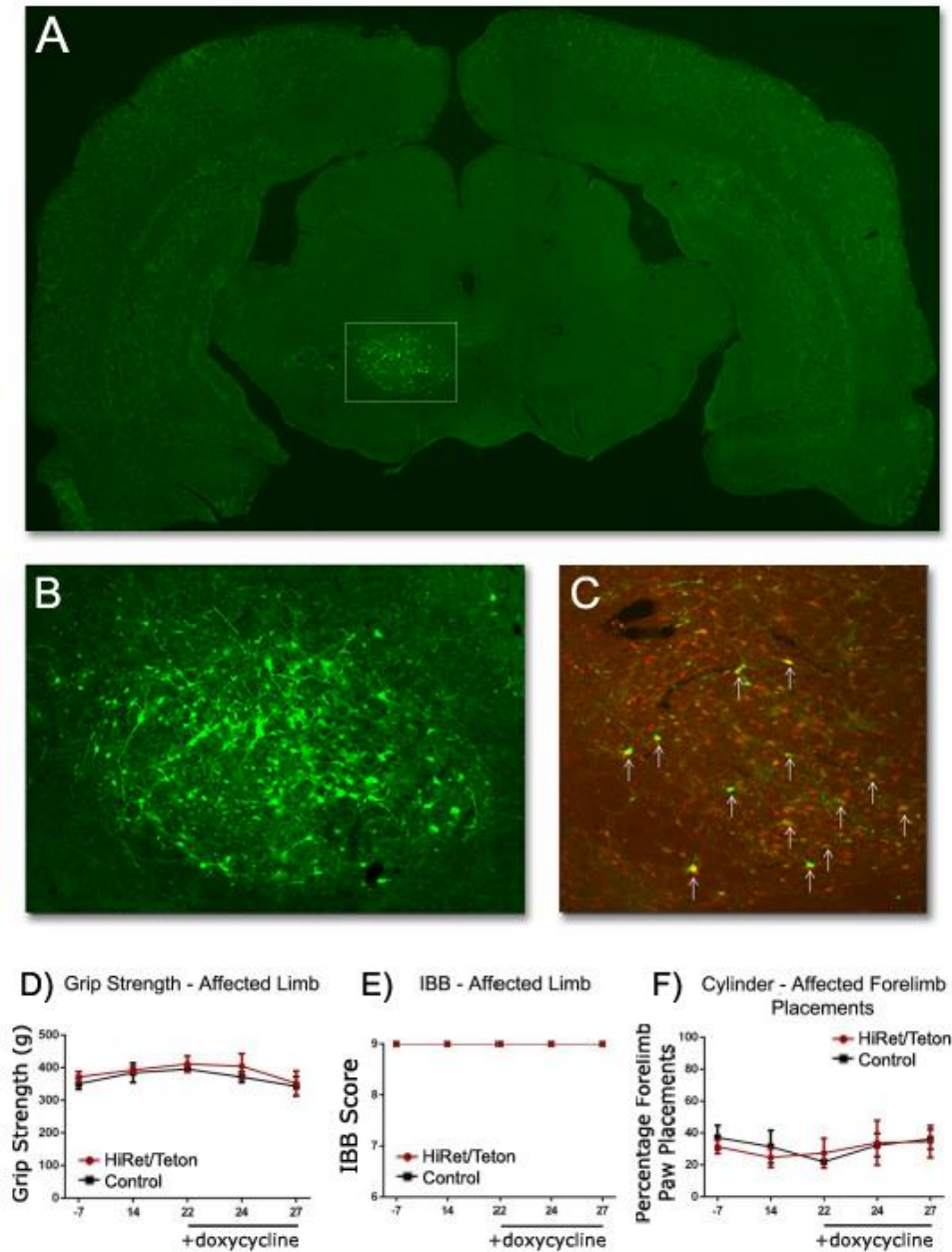


Figure 27. Silencing of the Red Nucleus has no effect on behavior in uninjured animals – A) A coronal section of the midbrain shows robust and specific expression of GFP (green) in neurons of the RN. Boxed area shown in B. B) Greater magnification shows morphology is typically neuronal in cells that express GFP. C) IHC with NeuN (red) confirms that GFP expression occurs in neurons. Arrows highlight doubly-stained cells. D) Force exerted in the grip strength test was not significantly different in the affected limb between animals doubly infected with HiRet and TetOn, and a control group infected with HiRet and saline. E) IBB score was not significantly affected between RST group and control group. F) There is no significant difference in forelimb placements during rearing in the cylinder test between the RST group and control group. Data are mean \pm SEM, n=5, RST group, n=4, control group.

Silencing of a population of neurons in the forelimb motor cortex affects grip strength, but not other behaviors in an uninjured rat

Strong GFP expression was seen in a small population of neurons and their associated axons in the FMC (Figure 28A, higher magnification in B), indicating tetanus toxin expression and neuronal silencing. Silencing this population of neurons resulted in a significant deficit in forelimb grip strength in the presence of doxycycline at two and four days of treatment. This deficit disappeared when doxycycline was removed (Figure 28C). The effect of doxycycline on grip strength deficit diminished by 7 days of treatment. This is consistent with previous findings from the Isa group, who found that deficits in reaching and grasping movements in monkeys using this system resolved after 3 days, despite a constant level of doxycycline in the blood stream (Kinoshita et al., 2012).

Silencing of this population of neurons had no significant effect on fine digit manipulation in the IBB test (Figure 28D) or paw preference as seen in the cylinder test (Figure 28E).

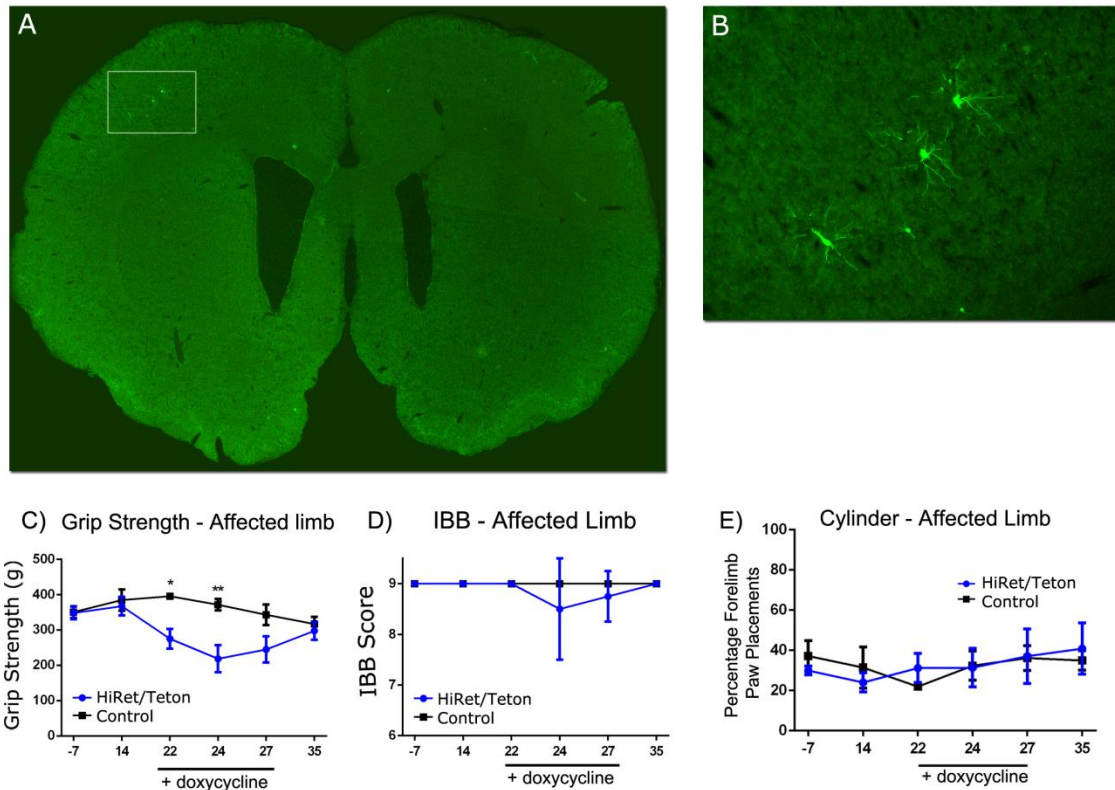


Figure 28. Neuronal silencing of CST neurons affects grip strength – A) A coronal section of the cortex shows GFP expression specific to the FMC. B) Greater magnification shows expression indicative of neurons. C) Maximum force exerted in the grip strength test was significantly reduced in animals experiencing synaptic silencing of the CST after 2 and 4 days of doxycycline application. Recovery was seen one week after doxycycline was withdrawn. D) IBB scores were minorly affected in some animals upon application of doxycycline, but this did not reach significance. E) No behavioral effect was seen in the cylinder test. Data are mean \pm SEM, n=4 each group. * $p < 0.05$.

Discussion

HiRet as a Neuron-Specific Retrograde Tracer

Unlike traditional retrograde tracers, viral retrograde tracers allow genetic manipulation of neurons that innervate a specific region of the spinal cord. Here we show that discrete unilateral injections of HiRet lentivirus into either the cervical or lumbar spinal cord label well-defined locations within the spinal cord and brainstem when compared to previous studies using retrograde chemical tracers. This labeling is

found to be stable *in vivo* for extended time periods (GFP expression has been observed for up to 4 months), making it superior to tracers such as BDA or pseudo-rabies virus, which must be dealt with in a time-sensitive manner. Additionally, no evidence of neuronal cell death in either the brain or spinal cord was seen while using this tracer. HiRet lentivirus uses the rabies G-envelope glycoprotein to enable preferential uptake at synaptic terminals, unlike traditional chemical retrograde tracers that can be taken up by damaged axons or axons en passage (see K. Kobayashi et al., 2016 for review). In this regard, we have observed no neuronal labeling of spinal MNs or DRG neurons after injection of HiRet-GFP into the transiently demyelinated sciatic nerve. However, injection of AAV2-mCherry shows robust labeling of both populations. Thus, this viral vector allows for better definition of pathways that innervate specific regions of the brain or spinal cord and provides an advantage compared to AAVs that are used for retrograde mapping (ex. rAAV2-retro) where uptake by axons en passage needs to be taken into account (Tervo et al., 2016). We have also found no evidence of trans-synaptic transport by this vector. For example, no GFP labeling of neuronal populations that do not make direct synaptic connections into either the cervical or lumbar region was seen, even after increasing injection volume or the time course after injections. These advantages could prove critical not only for mapping of circuits from the brain to the spinal cord, but for studies specifically targeting neuronal populations for silencing or ablation (Tohyama et al., 2017; Y. Liu et al., 2017; Kinoshita et al., 2012).

The ability to use inducible promoters in combination with HiRet also provides an advantage in future studies. During our use of HiRet-TRE-eTeNT-eGFP, we observed neurons specifically labeled throughout their entire length, allowing detailed examination

of dendrites or tracing of axons to their terminals near the injection site to identify their synaptic targets. Thus, this viral labeling procedure allows retrograde labeling as well as anterograde identification of terminals within the same neurons, which no chemical tracer supports.

In the HiRet-GFP tracing study, we examined the utility of a retrogradely transportable lentivirus to map pathways terminating within the lumbar spinal cord. We observed retrograde transport into multiple pathways known to be involved in motor control, primarily within the brainstem and spinal cord. The number and distribution of neurons retrogradely labeled using HiRet lentivirus compared well to those labeled using other methods (ex. fluorogold, microruby) (Liang et al., 2011; Reed et al., 2006). For example, fluorogold tracer injected into multiple mouse cervical spinal cord segments showed average ipsilateral and contralateral neuronal counts of 1,337 and 3,612 for the RN, 1,001 and 532 for the caudal part of the pontine nucleus, and 2,744 and 1,148 for the ventral MRF (Liang et al., 2011). These numbers are comparable to those in the present study considering our injections are localized to specific regions and from either the cervical or lumbar spinal cord. This demonstrates that HiRet can be used to map changes in intraspinal and supraspinal circuit pathways pre- and post-SCI, to highlight neuronal populations potentially involved in spontaneous behavioral recovery or contributing to functional recovery in experimental models.

The lumbar cord contains both the central pattern generator and MNs that connect to the muscles of the hindlimb involved with locomotion (Rossignol, 2000). Thoracic contused animals initially lose the ability to step and bear weight with their hind limbs after a moderately severe (200 kD) injury, but spontaneously recovered some stepping

without coordination by about 4 weeks (Scheff et al., 2003). Spontaneous recovery of hindlimb locomotion often plateaus at this stage, and it is reasonable to assume that plasticity of spared neuronal circuits may contribute and compensate for lost supraspinal input. Application of HiRet-GFP to the area below the lesion allows neurons with synaptic terminals in this area to uptake the virus and express GFP, potentially labeling neuronal populations important to behavioral improvement.

Following injection into the lumbar spinal cord, HiRet-GFP labeled PNs in the cervical and thoracic spinal cord, RN, and discrete reticular and vestibular nuclei in the brainstem. Although few GFP-positive neurons were observed within the somatomotor cortex or RN, we did observe high numbers of neurons within several regions of the reticular formation. The reticular formation consists of a large cluster of nuclei in the brainstem that plays a variety of roles in the rat. Important to locomotion are the fibers of the reticular spinal tract, which run in two main bundles – the medial reticular spinal tract, which originates in the pontine PRF of the pons, and the lateral ReST, which originates in the MRF of the medulla. The MRF contains the NRG, which is known for integration of motor commands from the mesencephalic motor region and other areas (Filli et al., 2014; Zorner et al., 2014).

In normal rat brains, robust labeling of neurons in the caudal part of the PRF and the gigantocellular portion of the medulla was observed. After spinal cord contusion the numbers of GFP-positive neurons within the reticular formation decreased dramatically. Although the majority of connections are lost after injury, reticulospinal fibers have been associated with spontaneous recovery by compensatory sprouting (Zorner et al., 2014; Filli et al., 2014; Ballermann and Fouad, 2006), particularly onto PNs that send their

axons within the lateral and ventral funiculi, which remains partially intact after a contusive injury. Our finding of a small population of neurons with connections below the lesion in both the PRF and MRF after injury support these data.

Numerous studies have indicated that recovery of hindlimb locomotion after SCI is mediated by sprouting of supraspinal axons onto PNs bypassing the lesion (Bareyre et al., 2004; Courtine et al., 2008; van den Brand et al., 2012). As with some reticular axons, these axons travel primarily within the ventral lateral and ventral white matter of the spinal cord. Injections of HiRet-GFP into the lumbar cord of uninjured rats showed dense labeling of both cervical and thoracic PNs. We focused on two types of PNs in this study: the short descending TPNs that connect the thoracic and lumbar segments and the LDPNs, which connect the lumbar and cervical regions (Chung and Coggeshall, 1983; Kostyuk and Vasilenko, 1979; Sherrington and Laslett, 1903). The latter group is thought to synchronize activity between the cervical and lumbar CPGs (Zaporozhets et al., 2006; Miller et al., 1973). The overall numbers of these neurons indicate that there is substantial crosstalk between the various levels of the spinal cord. Depending on the lesion type or location either propriospinal population has been shown to contribute to recovery of locomotion (Bareyre et al., 2004; Courtine et al., 2008; van den Brand et al., 2012; Filli et al., 2014), indicating that either population could act as a relay to send motor commands past a spinal cord lesion. In our study we observed a greater loss of GFP-positive labeled propriospinal neurons within the thoracic compared to the cervical spinal cord. The contusion injury model used may cause higher levels of cell death within thoracic neurons due to their proximity to the lesion site. Indeed, thoracic propriospinal neurons undergo increased cell death and show higher levels of apoptotic markers after thoracic

injury (Siebert et al., 2010; Siebert et al., 2010; Conta Steencken et al., 2011). The relatively low amount of expression that we saw in TPNs after injury could indicate that in our lesion model, spontaneous recovery is more dependent on the cervical population of LDPNs.

In conclusion, HiRet lentivirus provides us with the ability to label neuronal populations within the brain and spinal cord with high fidelity. This viral vector can be utilized as a retrograde tracer to map pathways pre- and post-injury and to target specific neuronal populations. HiRet permits stable, long lasting transgene expression, providing a significant advantage over chemical tracers and neurotoxic retrograde viruses. In addition, this vector may allow detailed and specific analysis of interneuronal circuits that undergo plasticity post-injury.

The HiRet/TetOn system as a Neuronal Silencing Method

In our synaptic silencing experiments, we used the HiRet/TetOn system to label and shutdown neurons of the RN and FMC via their synaptic connections onto propriospinal neurons in the C6-T1 spinal cord in uninjured rats. We found bright and beautifully specific labeling of neurons of the RN with this double vector system. This is worthy of mention because cell labeling via injection into the cell body with a single vector, such as is done with anterograde tracing, can run the risk of diffusing into other nuclei if the target is small. Fluorescent labeling only when neurons are doubly-infected allows for greater specificity because labeled neurons must both take up a virus at their synapse and another at their cell body, making it much less likely that stray neurons will be labeled. Of course, you may get a smaller percentage of labeled cells, as not every cell

within the nucleus will be doubly-infected, but in experiments where specificity is the number one priority, a system such as this is an excellent choice.

When silencing neurons of the RST in the intact rat, we found no effect on paw placement preference in the cylinder test, forelimb strength in the grip strength test, or digit function on the IBB scale. It may be that related interconnected tracts such as the CST can compensate for RST deficit when an animal is uninjured. These tracts are shown to have reciprocal connections in the brain (Tsukahara et al., 1964), and compensatory functional improvements are known to occur when one or the other is lesioned (Goldberger, 1965; Z'Graggen et al., 1998; Evans, B.H., Ingram, W.R., 1939). It is also suggested that these tracts function together to produce skilled forelimb movement (Whishaw et al., 1998), and thus it is possible that neuronal silencing of only RST neurons is not enough to cause discernible deficits in our behavioral tests.

Another possibility is that the RN does not contribute to motor behavior of the forelimb encompassed in the tests we ran in this study. Experiments performing specific lesions to the magnocellular division of the RN revealed only subtle deficits in the arpeggio movement a rat makes when grasping a pellet during forelimb reaching. This subtle deficit was caught using high speed cameras, and was not otherwise observable (Morris et al., 2015). These findings may support Whishaw's idea that behavioral deficits due to ablation of the RN in historical studies have more to do with destruction of passing fibers and adjacent structures than with destruction of the cells of the RN themselves (Whishaw et al., 1992).

In the FMC, we observed labeling in only a small population of neurons, though the labeling was bright and specific to the area of the FMC. The HiRet vector is a

relatively new construct, and thus there has not been extensively studied in CST axons of the rodent, being used mostly in mouse brain and retina, or in primates (Hirano et al., 2013; Tohyama et al., 2017; Kato et al., 2011; Sooksawate et al., 2013; Kinoshita et al., 2012). Throughout our experiments with any HiRet construct, we have never been able to label the CST robustly, though other long descending tracts label well. We suspect that certain receptors needed to permit uptake of HiRet at the synapse are downregulated on mature CST axons. Rabies virus, which contributes envelope glycoproteins to the HiRet vector, is known to interact with acetylcholine receptors (AChRs) in the peripheral nervous system when undergoing endocytosis at neuromuscular junctions (Lentz et al., 1983). However, as rabies virus can also be taken into sensory endings and stretch receptors that do not express AChRs, it is likely that it has several binding partners (Wunner et al., 1984).

Synaptic receptors in the CNS that interact with rabies virus are not entirely known. It is suspected that rabies can interact with neural cell adhesion molecule (NCAM) and p75 neurotrophin receptor (p75^{NTR}) (Tsiang et al., 1991; Tuffereau et al., 1998; Thoulouze et al., 1998). NCAM is known to have differential expression in embryonic, hatchling and adult chick corneas (Mao et al., 2012), and expression of NCAM is downregulated in cultures derived from mouse forebrain (Charles et al., 2000). It is also known that p75^{NTR} is highly downregulated in the majority of the adult nervous system (Meeker and Williams, 2015).

Despite the small population of neurons labeled in the FMC in our study, we did see modest deficits in forelimb grip strength in the presence of doxycycline, which recovered when doxycycline was washed out of the system. It may be that even a small

population of silenced neurons is enough to cause a small deficit in digit wrapping around the metal bars of the grip strength meter, causing the animal to let go more quickly. Studies that use this system in macaques notice deficits in digit manipulation when CST axons are silenced, and it is worth noting that the pattern of deficit found in the previous study is similar to ours – an initial larger deficit in gripping which started to resolve itself even when doxycycline was still present (Kinoshita et al., 2012).

Our studies demonstrate that this double vector system is interesting for two reasons - it creates a beautiful specificity of labeling useful for many applications, and the potential use of the HiRet vector for synaptic shutdown could help illuminate behavioral contribution of spinal tracts if it can be properly controlled. As seen in the pilot study data shown here, the inducibility of the system can be compromised if injected volume is too high. This can be a big problem when using Tetanus toxin, as animals can contract Tetanus. In a collaborative study in cats with the Lemay lab, we noticed that each cat injected with this system exhibited signs of Tetanus, including intense muscle twitching and greatly enlarged muscles (unpublished observations). It is also possible that the effect on behavior is overstated in this case. We theorize that the large volume of Tetanus toxin injected in our first study may have caused direct intake into MNs cells and thus synaptic shutdown. The C-terminal of Tetanus toxin is shown to interact with pre-synaptic MN terminals, which would allow Tetanus toxin to be taken directly into these neurons (Toivonen et al., 2010).

Due to these issues, we have created a HiRet-TRE-DREADDs vector, using the designer receptors activated by designer drugs system (for review, see (D. J. Urban and Roth, 2015)). The concept is the same – cells must be doubly infected and then a drug

applied to the system to fully activate it, the difference being that the DREADDs system, which relies on manufactured receptors and ligands, are not activated by any endogenous molecule, and thus even if the system is leaky there will be no deleterious effect.

CHAPTER 4. EXPLORING THE REGROWTH POTENTIAL OF SPINAL PATHWAYS AFTER INJURY

Introduction

SCI is a devastating life event due to the permanent loss of motor function and sensory input associated with the trauma. The lasting deficits reflect the poor capacity of the CNS to elicit regenerative growth that can repair damaged fibers and restore function. In two related studies in this chapter, we target the PI3K/AKT pathway in an attempt to spur axonal growth. The first study targets neurons of the RST with viral injections of Ras Homolog Enriched in Brain (Rheb) and Signal Transducer and Activator of Transcription 3 (STAT3) after a hemisection lesion. Rheb is a direct activator of mTOR, a downstream molecule of the PI3K pathway. mTOR is a major stimulator of new protein synthesis via *s6* kinases (Laplante and Sabatini, 2012), which allows for axonal extension, and is required for the formation of new growth cones (Swiech et al., 2008). It is highly upregulated after peripheral injury, in which axons generally show greater regeneration (Don et al., 2012), and our lab has previously demonstrated that direct stimulation of mTOR via Rheb promotes peripheral axon regeneration (Y. Liu et al., 2016).

Another important molecule upregulated in regenerating peripheral nerves is STAT3 (Bareyre et al., 2011). STAT3 is a transcription factor shown to stimulate GAP-43 (Dziennis and Alkayed, 2008), and STAT3 phosphorylation is highly upregulated during the conditioning response. Recent studies have shown that STAT3 regulates the initiation of growth, essentially ‘jumpstarting’ the growth process (Bareyre et al., 2011).

It is not yet known how STAT3 initiates growth. It may interact with the PI3k/AKT pathway to encourage cytoskeleton assembly and enhance axonal transport. A study by Sun *et al.* demonstrated that deletion of PTEN and suppressor of cell signaling 3 (SOCS3), the negative upstream regulators of mTOR and STAT3, respectively, caused impressive regeneration in retinal ganglion cells (Sun et al., 2011a).

In a separate study, we target PTEN with small molecule antagonist peptides. AKT is indirectly stimulated via receptor tyrosine kinases (RTKs). When the RTK is bound, PI3K phosphorylates second messenger phosphatidylinositol bisphosphate (PIP2), converting it into phosphatidylinositol triphosphate (PIP3), which then activates phosphoinositide-dependent kinase 1/2 (PDK1/2), which in turn activates AKT (G. Song et al., 2005). PTEN antagonizes the action of PI3K, and catalyzes the conversion of PIP3 back into PIP2, causing suppression of the AKT pathway. Several studies inhibiting the action of PTEN in the CNS have demonstrated greater neuronal survival and some of the most impressive axonal regeneration after injury seen in recent years (Park et al., 2008; Sun et al., 2011a; K. Liu, Lu, Lee, Samara, Willenberg, Sears-Kraxberger, Tedeschi, Park, Jin, Cai, Xu, Connolly, Steward, Zheng and He, 2010a). PTEN inhibition has a demonstrated effect on regrowth of the CST in mice (K. Liu et al., 2010a), including one year after SCI (Du et al., 2015). PTEN is present in both the soma and axonal compartment, including growth cones during axonal extension (Chadborn et al., 2006).

PTEN peptides were administered systemically to animals with moderate contusions to explore their effect on regenerative growth and sprouting of the CST in rats, and their effect on functional recovery of hindlimb locomotion. These peptides target distinct regions of the PTEN protein and represent a selective and efficient non-

transgenic approach to PTEN inhibition that is potentially translatable for patient treatment.

Materials and Methods

Animals

All surgical and animal care protocols were approved by the Temple University Lewis Katz School of Medicine's Institutional Animal Care and Use Committee, and performed per the National Institutes of Health *Guide for the Care and Use of Laboratory Animals*. Female Sprague-Dawley rats (65-75 d, 200-224 g; Harlan Laboratories) were housed two per cage, on a 12-hour light-dark cycle with food and water provided *ad libitum*. Animals were allowed 7 days of acclimatization prior to any experimental procedure. For the mTOR and STAT3 upregulation studies, animals were divided into two groups: 1) eight animals were injected with AAV-Rheb/STAT3/scGFP into the red nucleus, and one week later a unilateral hemisection was performed at T8 spinal level on the contralateral side; 2) eight animals were injected with AAV-scGFP into the red nucleus, and one week later a unilateral hemisection was performed on the contralateral side. For the PTEN antagonist protein studies, 37 animals were divided into five groups. Each group received a 150kD contusion at T8 spinal level. Five days after the contusion, animals were given systemic injections of: 1) PAP1: n = 7, 2) PAP2: n = 7, 3) PAP3: n = 7, 4) PAP4: n = 8, or 5) DMSO: n = 8, twice a day for four weeks. After four weeks, BDA was injected into the motor cortex of all animals to trace CST axons, and two weeks later animals were perfused.

Surgical Procedures

Animals were anesthetized via injection of ketamine (70 mg/kg; i.m.) and xylazine (8 mg/kg; i.p). For the PTEN antagonist peptide study, contusion injuries to the T8 spinal cord and BDA tracer injections into the hindlimb motor cortices were performed. For contusion injuries, a skin incision was made to expose musculature over the T5-T7 vertebral bodies, which will reveal the T7-T9 spinal cord when removed (Gelderd and Chopin, 1977). Musculature was cleared and bilateral laminectomies performed to expose the target. 150kD contusions were carried out with an IHI (Precision Systems, Inc.) at the T8 spinal cord segment. Six weeks after contusion, craniotomies were performed to allow bilateral injection of BDA into the hindlimb motor cortices at equally spaced injection sites between A/P: 1.25-3.75 mm; M/L: 1.0-3.25 mm and D: 2.0 mm to target CST axons (7 μ l per injection; 5 injection sites per side). Following injection surgeries, 14 days were allowed for tracer transport.

For the mTOR/STAT3 upregulation study, stereotactic injections of AAV2-Rheb/STAT3/scGFP were made into the RN as previously described. One week after brain injections, unilateral hemisections were performed at the contralateral T8 spinal level. Musculature was cleared from the T5-T7 area to expose the T8 spinal cord. A few drops of lidocaine were applied directly to the spinal cord tissue as a numbing agent, and spring scissors were used to cut one side of the cord just lateral to the midline. A needle was then passed through the ventral and lateral most aspects of the cut to sever any spared fibers.

PTEN Peptide Preparation and Treatments

PTEN antagonist peptides were prepared as previously described (Ohtake et al., 2014). Briefly, PAPs1-4 were designed to target distinct regions of the PTEN protein, such as the phosphatidylinositol-4,5-bisphosphate (PIP2) binding motif (PAP1), the protein tyrosine phosphatase (PTP) domain (PAP2, amino acids 60-73; PAP3 amino acids 122-136) or the C-terminal tail domain (PAP4) (for binding map see Ohtake et al., 2014]. A transactivator of transcription (TAT) sequence (GRKKRRQRRRC) was added at the C-terminal end of all peptides to facilitate access into cells. Peptides were synthesized by CHI Scientific Inc. (Maynard, MA), and purity was analyzed by high-performance liquid chromatography. Peptides were stored in Dimethyl Sulfoxide (DMSO) (20 mg/ml) at -20°C until needed, wherein they were diluted to the appropriate concentration in sterile saline. Animals were divided into five groups – one control group treated with DMSO, and four groups assigned treatment with one each of the four peptide inhibitors (PAPs 1-4). PAPs were administered twice a day for 30 days beginning five days post contusion (0.1 mL in sterile PBS, 2 times/day; s.q.). All experimenters were blinded to the type of treatment each group of subjects received.

Tissue Processing and Histology

At the completion of each experiment, all animals were sacrificed by injection of Fatal-Plus (Dearborn, MI) and perfused with saline (0.9% NaCl) followed by 4% PFA in 0.1 M phosphate buffer (pH 7.5) to fix the tissue. Brains and spinal cords were promptly dissected and post-fixed in 4% PFA overnight. Tissue was then transferred to 30% sucrose for 2-3 days. To isolate the lesion area for analysis in the PTEN antagonist peptide study, the dura was carefully removed from the spinal cord. Using the center of

the lesion as a guide, tissue was cut 8 mm rostral and 10 mm caudal to create an 18 mm block for later parasagittal sectioning. Additional blocks were cut immediately rostral and caudal to this area for later coronal sectioning; all blocks were cut serially, parasagittal sections at 40 μm , and coronal sections at 30 μm . Sections not immediately stained were placed into cryoprotectant (containing $\text{Na}_2\text{HPO}_4 \cdot \text{H}_2\text{O}$, NaH_2PO_4 , sucrose, PVP-40, and ethylene glycol) for long term storage at -20°C .

Immunofluorescence

Lesion sections were exposed to a tyramide signal amplification (TSA) stain to amplify BDA tracer signal present in CST axons at the lesion area. Sections were first blocked in 5% H_2O_2 /Tris-buffered saline (TBS) and 2% Triton (TX)+0.5% BSA/TBS solutions (independent events of 80 minutes each) to reduce non-specific binding, and then incubated in avidin-biotin complex solution (1:50; 0.3% TX+0.1% BSA/TBS) overnight at 4°C . The next day sections were washed thoroughly (1x 5 min with TBS +0.1% Triton X-100 (TX), 2 x 5 min with TBS, 3 x 10 min with TBS) and then incubated with TSA plus cyanide 3 solution (1:100; PerkinElmer; Waltham, Massachusetts) for 3.5 minutes. This time course was chosen after testing a series of sections for optimal timing, to prevent overexposure and reduce the possibility of false signal. Additional TBS washes were then performed (3 x 5 min with TBS, 2 x 10 min with TBS) and primary antibody was applied to highlight the astrocytic scar and serotonergic axons in the lesion area. Sections were incubated in mouse-anti-GFAP (1:200, MilliporeSigma; Temecula, California) and rabbit-anti-5-hydroxytryptamine (5-HT) (1:4000; MilliporeSigma; Temecula, California) overnight at 4°C . The next day sections were washed thoroughly in TBS and incubated with goat-anti-mouse AlexaFluor 647 (1:200, Invitrogen,

ThermoFischer Scientific; Waltham, MA) and goat-anti-rabbit AlexaFluor 488 secondary antibody (1:200; Jackson ImmunoResearch Laboratories, Inc.; West Grove, PA) in TBS-TX/BSA solution. Every section from the parasagittal blocks was used in order to get a complete picture of CST axons at the lesion site.

Coronal spinal cord sections rostral or caudal to the lesion area were exposed to a 5-HT stain to visualize serotonergic signal in CST axons. 20 sections for each animal were incubated in rabbit-anti-5-HT primary antibody (1:4000; MilliporeSigma; Temecula, California) in a TBS-TX/BSA solution (0.3% TX+0.1% BSA+TBS) overnight at 4°C. The next day sections were washed with TBS and incubated in goat-anti-rabbit AlexaFluor 488 secondary antibody (1:200; Jackson ImmunoResearch Laboratories, Inc.; West Grove, PA) in TBS-TX/BSA solution. Following the 1 hour secondary antibody incubation period, sections were washed and mounted on glass slides.

For the mTOR/STAT3 upregulation study the lesion area sections were stained with GFAP to highlight the astrocytic scar. Floating sections were first washed with 0.1 M PBS to remove cryoprotectant storage solution, then incubated for one hour in 0.3% Triton X-100 and 5% normal goat serum in 0.1 M PBS to block non-specific antigen sites. The tissue was then incubated overnight at 4°C with rabbit-anti-GFAP antibody (1:500, Dako Agilent Pathology Solutions, Santa Clara, CA). The next day primary antibody was washed from the tissue thoroughly with 0.1 M PBS and incubated with goat-anti-rabbit Texas Red (1:400, Jackson Labs, Sacramento, CA).

Following the staining and mounting of every section, photographs were taken using Axiovision software (Carl Zeiss Microscopy; Thornwood, NY).

Photo Analysis

For the PTEN antagonist peptide study, photos of the parasagittal lesion sections were stitched together in Adobe Photoshop to form a complete image of each 18mm section at a standard width, height and resolution. All images of a particular animal were then surveyed to choose a section most representative of the size and shape of the lesion for that animal. Following this, each other complete lesion section was aligned so that the center of the lesion matched the center of the representative image. All areas of axonal expression were traced with a 4 pixel brush on separate layers, and then merged to create a map of TSA signal density. These density maps for each animal were then divided into 2mm blocks and quantified using ImageJ. Each image was converted to binary, skeletonized and then the signal analyzed with the 'measure' tool to create a relative signal density measurement.

Coronal sections stained with 5-HT were surveyed for each animal and the 3 sections most representative of serotonergic fiber expression in that animal were chosen for analysis. These sections were stitched and traced as above, without the alignment step. Each complete image was then brought into Image J and analyzed as indicated above.

Behavioral Tests

BBB hindlimb locomotor test

The hindlimb locomotor test is a measure of success and accuracy of gait in the hind limbs while an animal locomotes across a flat plane. Gross measures such as the ability to step on the plantar surface of the paw, support the body weight and walk with a

coordinated gait can be measured. Additionally, fine motor skills such as stability of the trunk, position of the tail, lateral paw placement and ability to walk without dragging the toes are measured. Animals were analyzed by two investigators trained in this method for a 4 minute time period, and a score was given on the 21 point BBB scale (Basso et al., 1995).

Horizontal Ladder

Assessment for recovery of proprioceptive axons was measured by recording the accuracy of paw placement on a horizontal grid as described by Kunkel-Bagden et al., and modified by the Whishaw group (Kunkel-Bagden et al., 1993; Metz and Whishaw, 2009). Rats are videotaped walking for a minimum of 30 steps across a 6-foot horizontal grid contained randomly spaced pegs, each of which are 4–8 cm apart. The videos are then scored by dividing the number of correct foot placements by the total steps taken, to achieve a percentage of correct steps. Different categories of incorrect placements are also noted (misses, slips and touches), as each is indicative of a slightly different type of deficit.

Statistical analysis

All statistical analysis was performed using GraphPad Prism 6 (GraphPad Software, Inc., La Jolla, CA). Evaluations of axon signal density and behavioral recovery were analyzed by two-way ANOVA followed by a Sidak post-hoc test for statistical significance. Signal density is represented as mean \pm SD, and behavioral recovery as mean \pm SEM.

Results

To determine whether co-stimulation of STAT3 and mTOR proteins would encourage growth in RST axons, AAV-Rheb/STAT3/GFP was injected into the RN. After one week, lateral hemisections were performed at the T8 spinal level. After 4 weeks, animals were perfused and lesion histology performed to investigate GFP signal in RST axons (Figure 29).

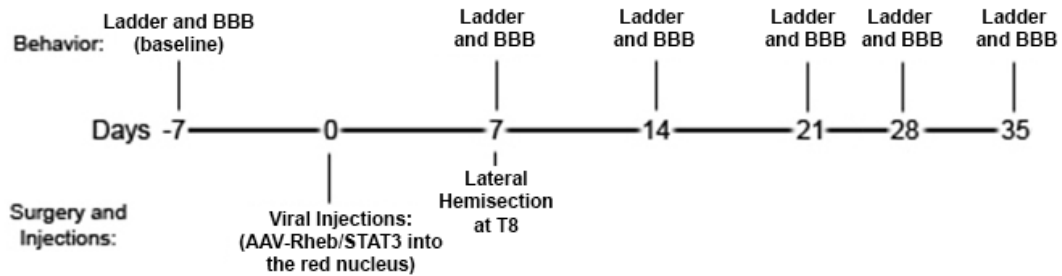


Figure 29. Timeline of mTOR/STAT3 upregulation study

mTOR/STAT3 upregulation modestly increases regrowth of rubrospinal tract axons after injury

A modest amount of regrowth was seen in treated animals, including axonal extension into the lesion cavity (Figure 30A, arrowheads) and limited axon profiles caudal to the lesion (Figure 30A, arrows, higher magnification in B). However, growth extending into the lesion cavity or caudal to the lesion was not robust enough to merit quantification. We did notice, however, that axonal dieback, which is discussed in the next figure, was significantly affected.

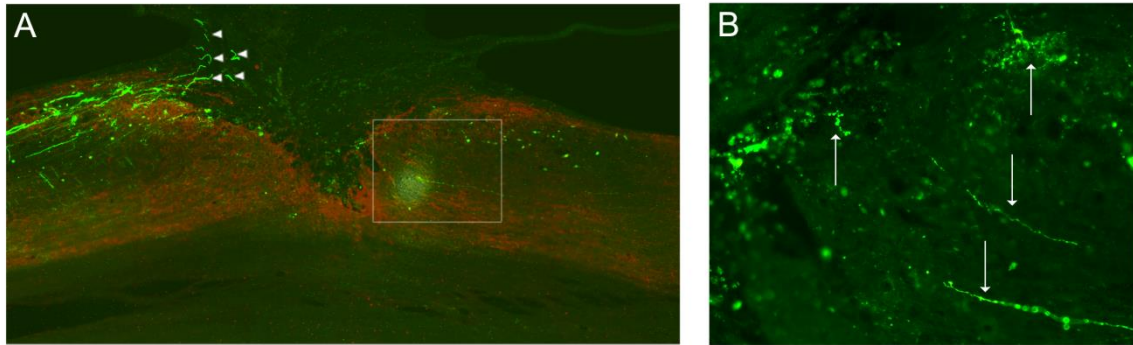


Figure 30. Increased growth of RST axons in animals treated with AAV-Rheb/STAT3 – A) An animal injected with AAV-Rheb/STAT3/scGFP exhibits axonal extension into the lesion cavity (arrowheads), and limited tracing caudal to the lesion (boxed area). B) Higher magnification of the caudal spinal cord shows traced axon profiles (arrows). N = 4 AAV=Rheb/STAT3/scGFP injected, n = 3 control.

mTOR/STAT3 upregulation decreases dieback in RST axons after injury

Looking at the profiles of axons expressing GFP in this study, we noticed a difference in their relative distances from the lesion cavity. In Figure 31, axonal profiles in an untreated animal (A) are further from the cavity than those treated with AAV-Rheb/STAT3 (B). Axonal profiles were quantified in C from 2 mm rostral to the lesion to 2 mm caudal to the lesion, in chunks of 0.5 mm each. Significantly less dieback was seen at 1.5 and 2 mm rostral to the lesion in treated animals, with a trend towards lesser dieback at 0.5 and 1 mm.

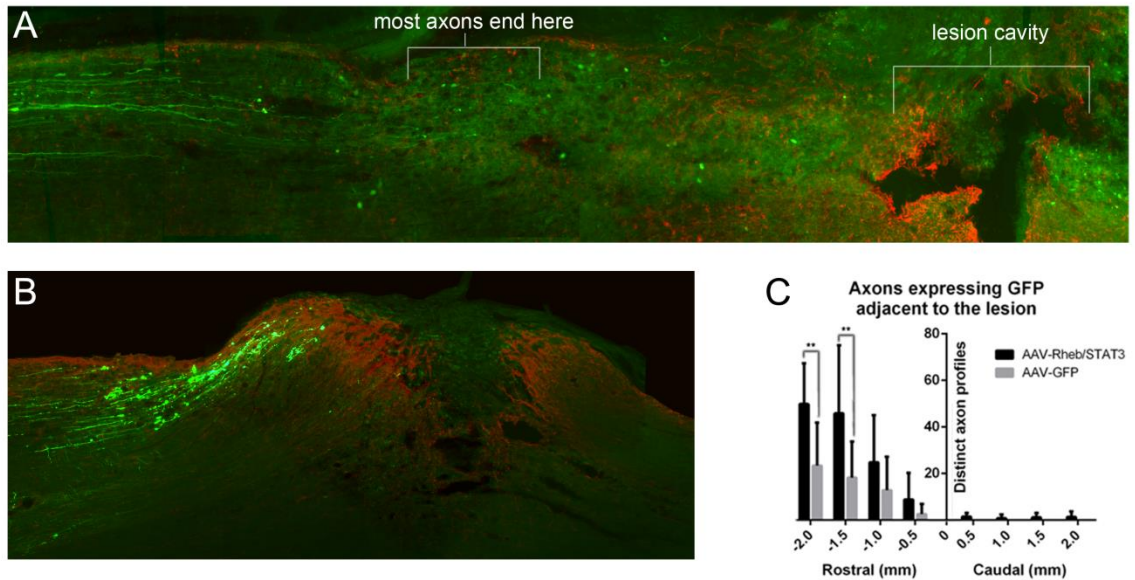


Figure 31. Axonal dieback is decreased in animals treated with a combination of AAV2-Rheb/STAT3 – A) Significant dieback from a lesion center is seen in untreated animals. B) A comparative section in an animal treated with AAV2-Rheb/STAT3 shows axon profiles in closer approximation to a lesion center. C) Quantification of GFP-expressing axons 0-2 mm rostral and caudal to a lesion center demonstrates a significantly higher number of axons between 1.5-2.0 mm rostral to a lesion in treated animals. N = 4 AAV=Rheb/STAT3/scGFP injected, n = 3 control. Green = GFP, Red = GFAP. Comparisons by repeated measures one-way ANOVA, **: p < 0.01, Data are mean \pm SD.

Skilled locomotion in the horizontal ladder test was modestly affected by mTOR/STAT3 upregulation

Two behavioral paradigms were used in this study – the BBB scale, which evaluates over ground locomotion including aspects of balance and posture (Basso et al., 1995), and the horizontal ladder test, which measures limb placement, stepping and interlimb coordination (Metz and Whishaw, 2009). A modest improvement in the percentage of correct steps taken was seen in the horizontal ladder test in animals treated with AAV-Rheb/STAT3, which reached significance at 4 weeks post injury. No significant effect was seen in over ground locomotion in the BBB test (Figure 32).

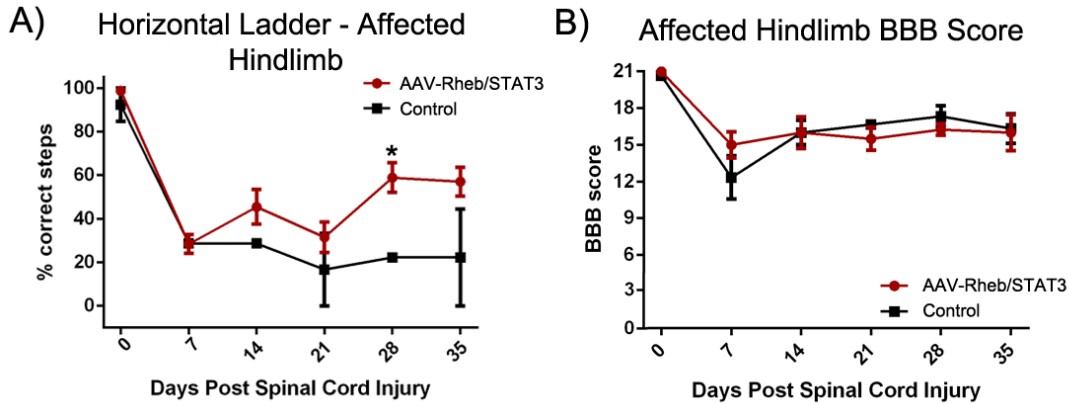


Figure 32. Behavioral assessments show mild proprioceptive recovery in animals treated with a combination of AAV-Rheb/STAT3 – A) A trend towards behavioral recovery of proprioception was seen in animals treated with AAV-Rheb/STAT3 (red line). This was significant at 4 weeks post injury. B) No significant recovery was seen in hindlimb locomotion via the BBB test. N=4 treated, n=3 control. Comparisons in both graphs by two-way ANOVA, Sidak multiple comparisons post-hoc test, * = $p < 0.05$, **** = $p < 0.0001$). Data are mean \pm SEM.

The Effects of PTEN Antagonist Peptides on Growth of Corticospinal Axons in a Contusion Model of Spinal Cord Injury

In order to determine whether inhibition of the PTEN molecule would have an effect on growth of CST axons after injury, we exposed four groups of contused rats to systemic injections of our PTEN antagonist peptides, beginning five days after injury for a period of four weeks. A fifth control group received scrambled peptide. CST axons were then traced via injection of BDA into the motor cortex two weeks prior to perfusion. The BBB behavioral test was performed to test hindlimb locomotor function at 2, 5 and 7 days, and once a week thereafter until completion of the study (Figure 33).

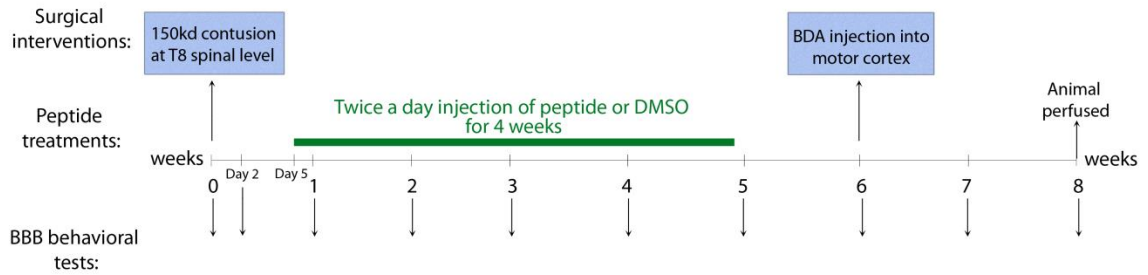


Figure 33. Experimental Timeline of PTEN Antagonist Peptide Study

To demonstrate the totality of BDA expression in CST axons in the spinal cord of our animals, we photographed and traced every section of an area surrounding the contusion and producing composite drawings. In the groups treated with the PAP2 and PAP3 peptides, a subset of animals displayed very robust expression caudal to the contusion when compared to controls (Figure 34). Axon density rostral to the lesion is similar in the three groups (Figure 34A, top row), while expression in individual sections is increased in those treated with PAP2 and PAP3 peptides (Figure 34A, bottom row). Composite drawings demonstrate significantly increased expression caudal to the contusion in these animals (Figure 34B). Axon density is quantified in 2mm blocks in Figure 34C. Notably, robust signal density is seen even at 8-10 mm caudal to the lesion center. A trend towards increased expression is apparent in these groups, though high variability within PAP2 and PAP3 treated animals prevents statistical significance.

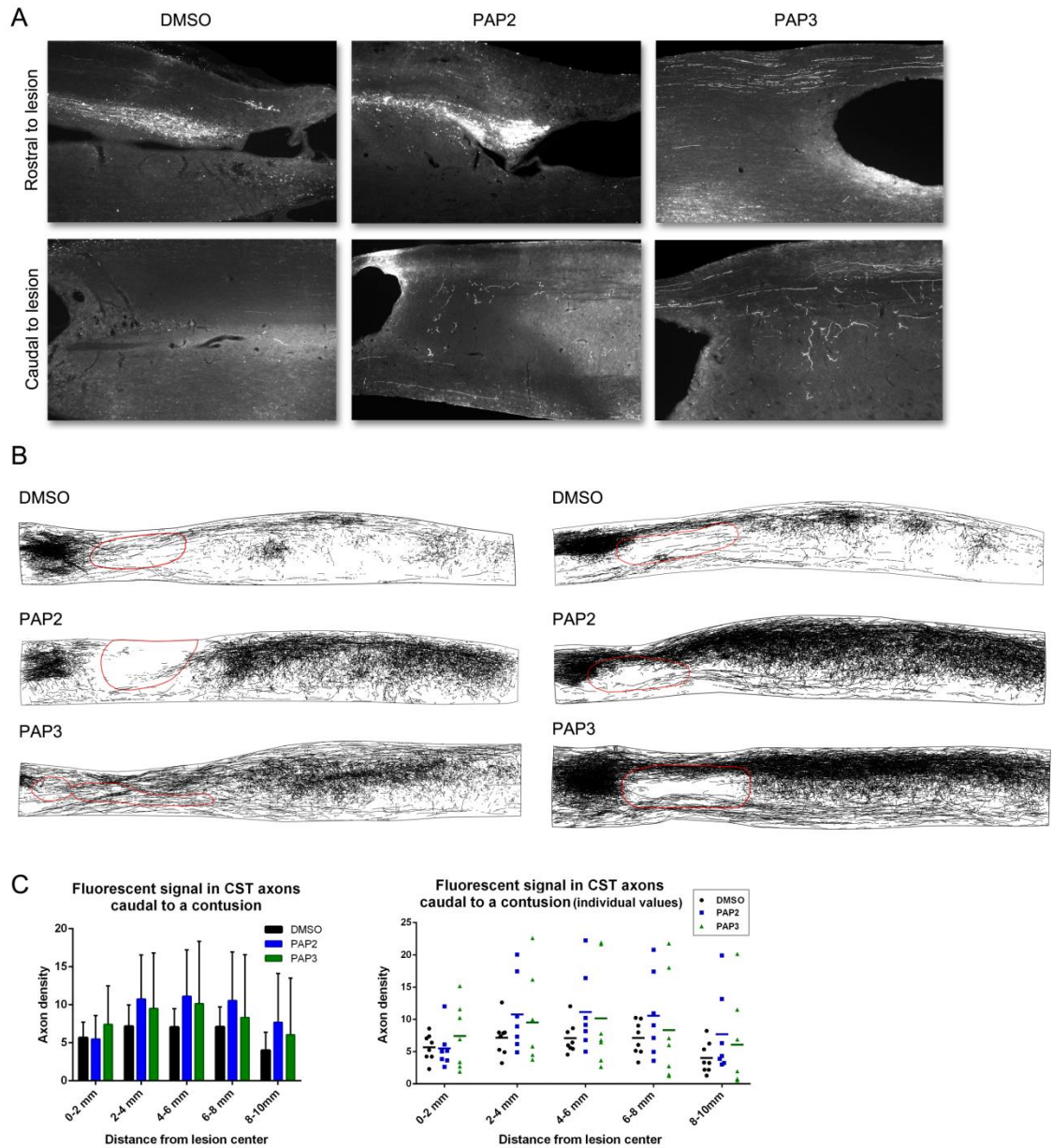


Figure 34 – Increased CST axon density in a subset of animals treated with PAP2 and PAP3 knockdown peptides. A) BDA expression in CST axons rostral (top row) and caudal (bottom row) to a lesion cavity in contused animals. Animals treated with PAP2 (middle column) and PAP3 (right column) display a greater density of axon profiles in the caudal cord. B) Composite drawings of all axon profiles in control animals (top row), and animals treated with PAP2 (middle row) and PAP3 (bottom row). Peptide treated animals demonstrate robust axon density caudal to the lesion area. Areas outlined in red represent the lesion cavity. C) Comparative axon density measurements in these groups expressed in 2mm segments of the caudal cord, as a bar graph with mean values (left) or a scatter plot of individual values (right). PAP2 and PAP3 groups show a trend towards increased growth. N = 7 PAP1 and PAP2 groups, n = 8 DMSO control.

Animals with robust growth demonstrated axon profiles indicative of sprouting or newly regenerating axons

Our composite drawings of axon profiles in those PAP2 and PAP3 treated animals that showed robust BDA expression revealed a pattern of growth indicative of regenerative sprouting. In control animals, axons can be seen traveling in the expected dorsomedial CST territory, with some expansion into more ventromedial territory. In PAP2 and PAP3 treated animals with robust expression, significant expansion into the ventromedial territory may indicate extensive grey matter sprouting. At higher magnification, axon profiles indicative of sprouting or newly regenerating axons were apparent in these animals, such as tortuous growth (Figure 35A), thin, varicose axons with extensive branching (Figure 35B), or axons with multiple dystrophic growth cones (Figure 35C).

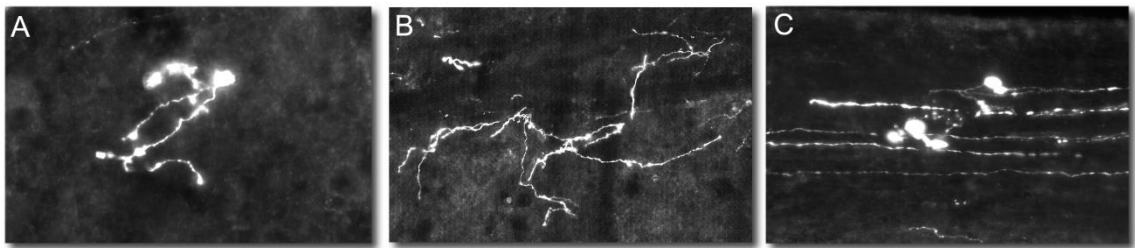


Figure 35 – CST axons in animals treated with PAP2 and PAP3 demonstrated typical profiles of sprouting or regenerative growth. Axon profiles in animals with robust BDA expression caudal to a contusion demonstrated signs of attempted growth such as A) tortuous routes, B) thin, many branched structures and C) multiple dystrophic growth cones

Animals given systemic PAP1 or PAP4 peptides had similar or lesser density of CST axons caudal to a contusion

In contrast with the other treatment groups, animals given systemic PAP1 peptide showed poor BDA expression caudal to a contusion, while animals given PAP4 peptide showed no change (Figure 36). BDA expression in CST axons rostral to the lesion was comparable to controls, though axonal dieback from the lesion center was sometimes apparent in these two groups (Figure 36A, top row). Caudal to a lesion, individual sections had relatively low expression (Figure 36A, bottom row). Composite drawings demonstrate total axon profiles in several animals of each group (Figure 36B). Quantification of axon density reveals a trend towards poor expression in PAP1-treated animals (Figure 36C).

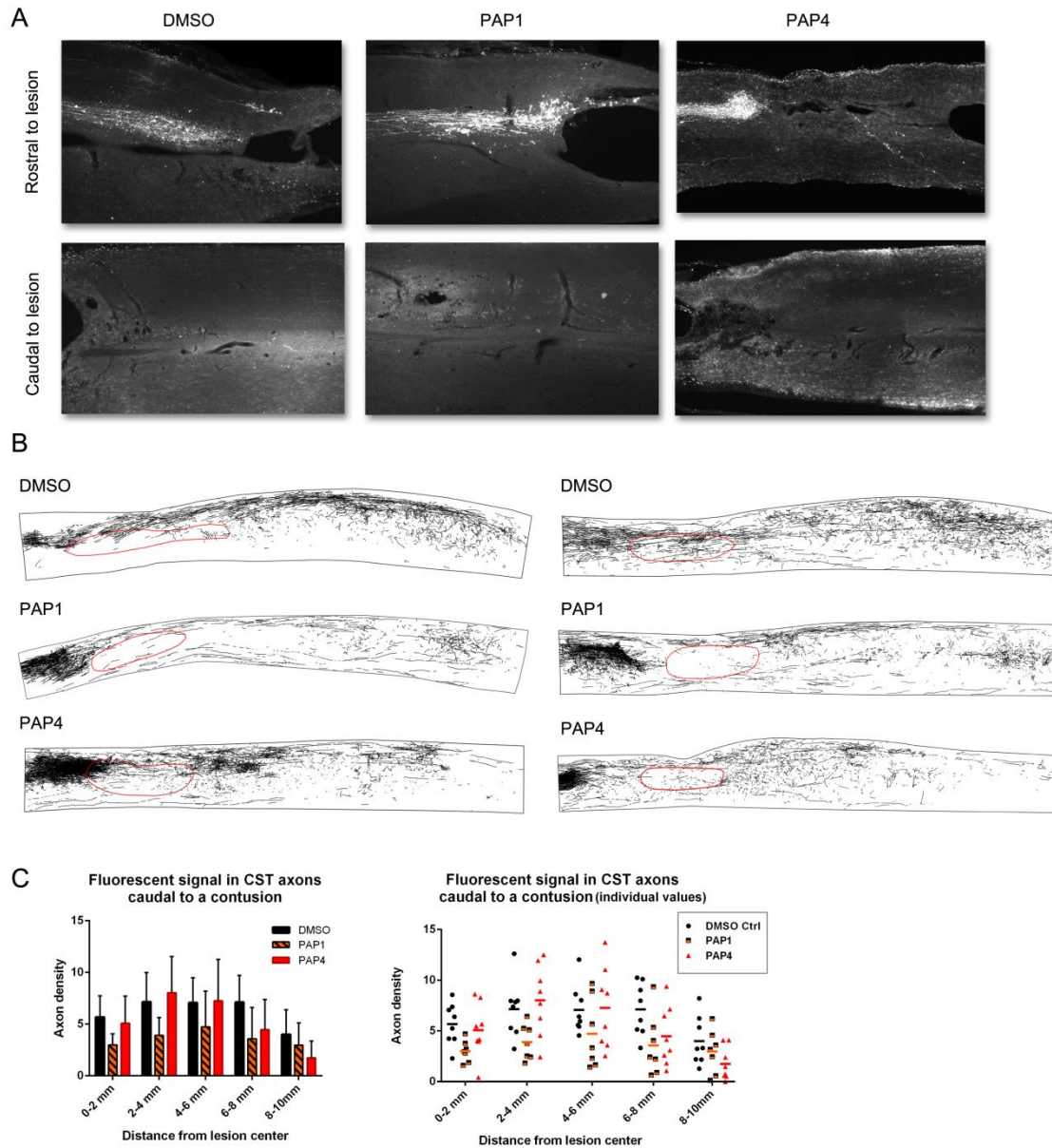


Figure 36. Similar or lesser CST axon density was seen caudal to a contusion in animals treated with PAP1 or PAP4 peptides – A) Similar BDA expression was seen in CST axons rostral to the contusion in controls (top left) versus animals treated with PAP1 (top middle) and PAP4 (top right). Caudal to the contusion, similar expression was seen in controls animals (bottom left) and those treated with the PAP4 peptide (bottom middle). In PAP1-treated animals, a trend towards lesser expression was apparent (bottom right). B) Composite drawings of BDA expression in controls (top row), versus PAP1-treated animals (middle row) and PAP4-treated animals (bottom row). C) Comparative axon density measurements in these three groups show a trend towards decreased growth in animals treated with PAP1 (mean value bar graph on the left, individual value scatter plot on the right). N = 7 PAP1 group, n = 8 PAP4 and DMSO control groups.

Serotonergic Fiber density was not significantly different in animals treated with PTEN knockdown peptides

Neurons that use serotonin as a key neurotransmitter have cell bodies mainly in the raphe nucleus, but their fibers can project throughout the CNS. These neurons have the ability to sprout robustly after various types of CNS injury (Zhou et al., 1995; Inman and Steward, 2003; Sharma et al., 1990; Camand et al., 2004), and are shown to have higher levels of GAP-43 and more active growth cones than cortical neurons (Hawthorne et al., 2011).

We were interested in whether serotonergic fibers would respond to treatment with PTEN antagonist peptides in the injured state, and we thus analyzed fiber density via 5-HT expression in our animal groups. We found no significant difference in 5-HT expression between animals that exhibited robust CST axon density caudal to a contusion and those with poorer density (Figure 37). In Figure 37A, the animal with the poorest CST axon density of those studied (PAP1, top row) has roughly similar 5-HT expression to the animal with the most robust CST axon density (PAP2, bottom row). The pattern of serotonergic fiber expression was also similar between groups at 10mm caudal to the lesion center (Figure 37B), with fibers clustered around MNs in the ventral horn. Quantification of serotonergic fiber density revealed no significant difference in any treatment group (Figure 37C).

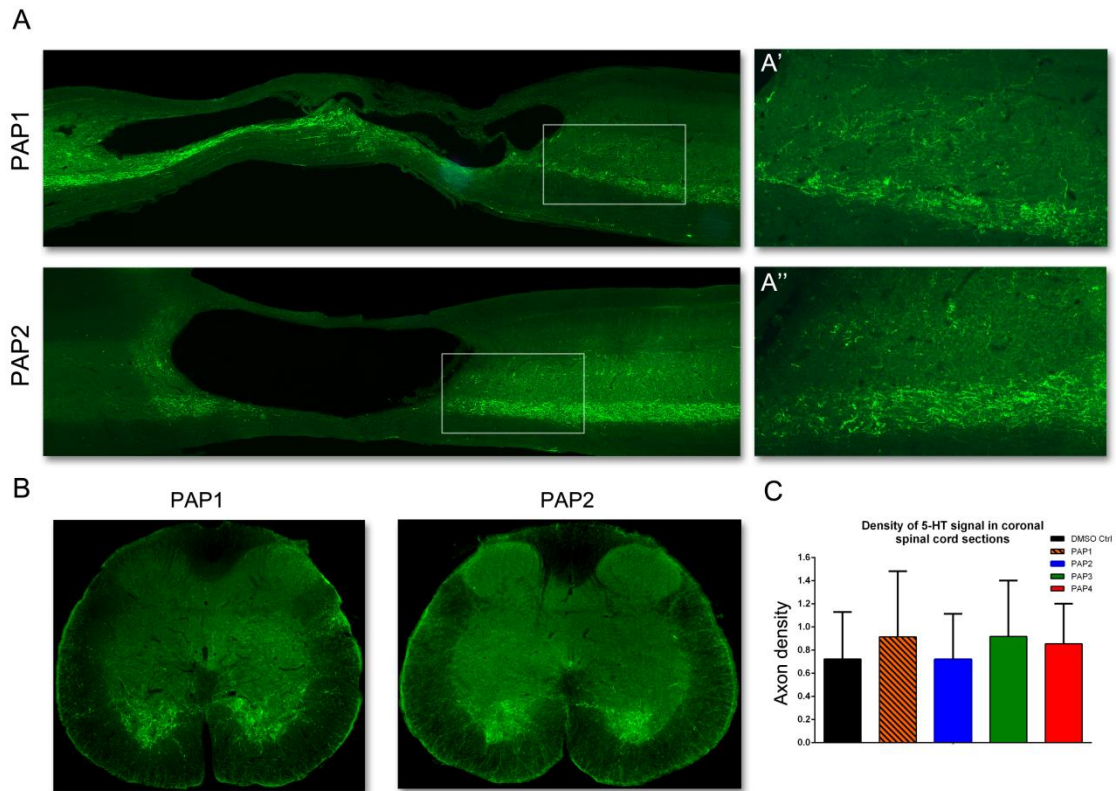


Figure 37. Serotonergic Fiber density was similar in all animal groups studied – A) Lesion areas stained with 5-HT to highlight serotonergic fibers reveal no significant difference in animals with very low BDA expression (PAP1-treated, top row) and those with very high BDA expression (PAP2, bottom row). B) Coronal sections taken 10mm caudal to the center of the contusion reveal a similar expression pattern in the same animals as A. C) Density measurements of fibers expressing 5-HT caudal to a contusion.

No significant behavioral recovery was seen in animals treated with PTEN antagonist peptides

The BBB behavioral test was performed to test hindlimb locomotor function at 2, 5 and 7 days, and once a week thereafter until completion of the study. Animals treated with PAPs showed no significant behavioral improvement in hindlimb locomotion during this time (Figure 38).

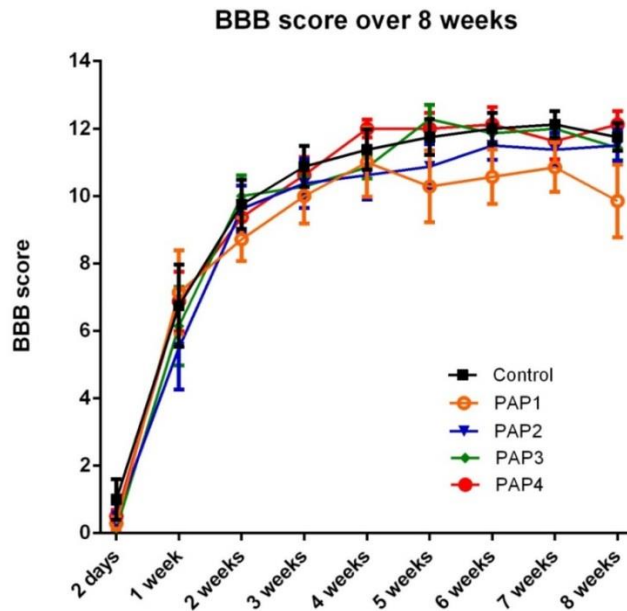


Figure 38. No significant effect was seen on hindlimb locomotion in animals treated with PTEN antagonist peptides

Discussion

Interest in the PI3K/AKT pathway was stimulated by the extensive regeneration seen in the optic nerve via genetic deletion of PTEN in studies by Zhigang He and Kevin Park (Sun et al., 2011b; K. Liu et al., 2010a; Park et al., 2008). The mTOR protein was specifically a target of interest due to its involvement in protein synthesis (X. M. Ma and Blenis, 2009; Sabatini, 2006), and due to studies showing blockade of mTOR via rapamycin abolishes recovery seen during PTEN inhibition (Park et al., 2008). Here we use Rheb to directly stimulate mTOR. At the time of these experiments, few studies were using Rheb as a direct activator, though a few have adopted it since then (D. Wu et al., 2016; D. Wu et al., 2015; M. W. Urban et al., 2018).

In our study, we found modest regeneration of RST fibers extending into lesion cavities, and axon profiles caudal to the lesion in some animals. We also saw a significant effect on the extent of axonal dieback from the edge of a lesion, with treated animals showing more axonal profiles on the rostral lesion edge. We noticed small behavioral differences in correct foot placement in the ladder test in treated animals. Modest improvements such as these are supported by the literature (M. W. Urban et al., 2018; Y. Liu et al., 2016); though direct stimulation of mTOR has not allowed for a level of axonal regrowth seen in the original PTEN knockdown studies. It is quite possible that the growth seen in those original studies relies on multiple branches of PI3K/AKT pathway activation, and thus we decided to move to PTEN inhibition in the next study.

Genetic deletion of PTEN has demonstrated significant axonal regrowth after injury, both in the optic nerve as described in the above papers, and in the CST (K. Liu, Lu, Lee, Samara, Willenberg, Sears-Kraxberger, Tedeschi, Park, Jin, Cai, Xu, Connolly, Steward, Zheng and He, 2010b). Others have explored more clinically relevant methods of inhibition such as knockdown with short-hairpin RNAs or pharmacological blockades such as bisperoxovanadium (bpV), a general phosphatase inhibitor (Ohtake et al., 2014; Park et al., 2008; K. Liu et al., 2010b; Zukor et al., 2013; Sun et al., 2011b; Nakashima et al., 2008; Walker et al., 2012). BpV is being actively explored in nerve regeneration studies (Nakashima et al., 2008; Walker et al., 2012; Walker and Xu, 2014; Walker et al., 2015). However, due to its non-specific targeting, there is a concern about clinical side effects such as lowered blood glucose levels (Scrivens et al., 2003; Drake and Posner, 1998).

In our study we investigate several unique small molecule inhibitors of PTEN, each targeted at a distinct amino acid sequence of the protein. These antagonist peptides are targeted solely to PTEN, alleviating the concern about non-specific side effects. We apply PTEN inhibition to a contusive model of SCI, a combination which has been explored in only the bpV studies mentioned above and a few others (Zukor et al., 2013).

Peptides targeted at the PTEN protein phosphatase domain increased axonal growth and sprouting

We found robust growth and sprouting in a subset of animals treated with the PAP2 and PAP3 antagonist peptides, both of which target the protein tyrosine phosphatase domain of the PTEN molecule. The PAP2 peptide data is consistent with a previous study, where systemic infusion induced CST sprouting and limited CST growth caudal to a lesion in mice with dorsal overhemisections (Ohtake et al., 2014). However, we did see variable levels of growth within these treatment groups, with individual animals showing very dense axon profiles caudal to the contusion, and others showing no significant difference from controls.

One potential explanation for differences in growth is lesion variability. The contusive injury by nature creates variations in the size of the lesion cavity and differences in the number of spared fibers (Basso et al., 1996; Asboth et al., 2018). Our animals treated with PAP2 and PAP3 peptides that had extensive axon signal density caudal to the contusion appeared to have cavities of similar or larger size to controls, including a similar rim of spared tissue. However, past studies have found that individual differences in the arrangement of vasculature, for example, can result in differences in ischemia and secondary tissue loss (Koehn et al., 2016). If sprouting of spared fibers is

the main source of axon signal density caudal to the lesion in this study, animals with a larger number of spared fibers could exhibit a more robust signal.

Serotonergic Fiber density is unaffected by PTEN antagonist peptides

Serotonergic fibers arise mainly from the brainstem raphe nuclei, and run in dispersed bundles neighboring the central gray matter in the spinal cord. Due to their positioning, it is very hard to sever all of them without a complete transection. Serotonin agonists can increase the excitability of MNs in the spinal cord, and can increase motor activity to facilitate weight bearing and treadmill stepping in injured rats and mice (Courtine et al., 2009; Antri et al., 2003; Landry et al., 2006). Previous studies have also reported treatment-related increases in serotonergic axon density below an injury, or growth of these axons into cellular grafts (Lu et al., 2003; Ribotta et al., 2000; Barbeau and Rossignol, 1991; S. Li et al., 2004). Our previous study in mice reported an increase in the density of serotonergic fibers caudal to a dorsal overhemisection lesion in animals treated with our PAP2 and PAP4 peptides (Ohtake et al., 2014).

For these reasons, we measured the density of serotonergic fibers caudal to the lesion in our animals. These fibers were abundant and showed signs of sprouting; however we did not see any significant increase in the density of fibers in any of our animal groups treated with PAPs when compared to DMSO-treated animals.

Conclusions

Despite some variability, the density of CST axons seen caudal to a contusive lesion in our study is an interesting demonstration of a strong intrinsic growth response and may indicate that our PTEN antagonist peptides are a good choice for studies using

multiple growth-promotion strategies. PTEN inhibition has been used to successfully enhance growth in combination with other intrinsic factors such as cAMP treatments (Kurimoto et al., 2010; de Lima et al., 2012), BRAF proto-oncogene (B-RAF) expression (O'Donovan et al., 2014), or suppression of SOCs 3 (Sun et al., 2011a) in optic nerve crush models, or with manipulation of extrinsic factors such as deletion of Nogo in mice (Geoffroy et al., 2015) or delivery of salmon fibrin to a lesion site in a dorsal hemisection in rats (Lewandowski and Steward, 2014). A combinatory strategy in a rat contusion model involving these PTEN peptides may be worth exploring.

CHAPTER 5. DISCUSSION

Insight into the basic organization of brain and spinal cord circuitry, including specifics of their interconnectivity, will help us understand what plastic arrangements these circuits may make after injury and how they are regulated. In pursuit of this goal, we present here several tracing studies exploring the structure, function and connectivity of long descending tracts and propriospinal neurons in a rat model, in both the injured and uninjured states.

AAV vectors were used to demonstrate anterograde tracing in long descending tracts such as the RST, CST and ReST. This is well documented in the literature (for review see (McCown, 2011)). We also found that the self-complimentary version of the AAV vector can transduce neurons at the origin of these tracts more efficiently than ssAAV, with neuronal specificity and bright labeling that does not require histology. Although previous studies have demonstrated scAAV transduction of CNS neurons via strategies such as intramuscular injection and subsequent retrograde transport into MNs (Foust et al., 2009; Kaspar et al., 2003; Boulis et al., 2003; Benkhelifa-Ziyyat et al., 2013), intravenous infection of MNs in neonatal mice (Foust et al., 2010), or direct injections to the sciatic nerve (Hollis et al., 2008) or retina (Yokoi et al., 2007; Natkunarajah et al., 2008), we were the first to demonstrate classic tracing of long descending spinal tracts via injection into nuclei in the brain and brainstem in a rodent model.

We were able to use both GFP and mCherry inserts to achieve the same effect, and found that these vectors could be co-transfected with other anterograde tracers and maintain efficient labeling. scAAV-mCherry had been used in the past in a few studies in

the mouse brain or retina (Koilkonda et al., 2014; Aschauer et al., 2013) and co-transduction was mentioned in a few previously mentioned studies, but again we were the first to describe the use of these vectors in discrete brain nuclei to label long descending spinal tracts in the rat. We also observed that self-complimentary vectors would label axons of descending tracts in injured animals brightly. Our 2014 study was the first to demonstrate use of this vector in a rodent dorsal root crush model (Y. Liu et al., 2014), and the demonstration here of AAV-scGFP expression in RST axons at a lesion site, though unpublished, was among only a few in rodent models at that time.

Considering the excellent labeling and transduction efficiency of scAAV vectors, we believe they are superior tools for tracing studies outlining descending tracts, or for regrowth studies that either require tract tracing to demonstrate their findings, or that are interested in using a transgene small enough to fit into this vector. The use of scAAV has become popular in larger animals, likely due to the lower viral load needed to achieve the required labeling (S. I. Duque et al., 2015; Bucher et al., 2014). In the future it would be worth exploring the addition of other small molecules to self-complimentary vectors. Perhaps the genomic sequences that create the PTEN antagonist peptides used in our studies could be added, so that PTEN inhibition could be achieved in specific populations of neurons. This would be especially useful if any side effects of systemic infusion have been observed.

In our studies exploring retrograde tracing with the HiRet lentiviral vector, we found evidence to support the literature that HiRet can transduce neurons of descending tracts and PNs in the injured or uninjured state via uptake at the synapse. Retrograde tracing with HiRet has been demonstrated in the brains of mice and primates (Kato et al.,

2011; Kato, Kuramochi et al., 2011), or via intramuscular injection, where it successfully transported into MNs (Hirano et al., 2013). The HiRet/TetOn system has also been used for synaptic silencing of C3-C4 PNs, meaning that it can be taken up by some populations of PNs. However, there have not been many studies targeting lumbar connections below a contusive injury with this vector, so our findings should be interesting to the community.

Additionally, since this is a fairly new vector, there have not been many studies looking at transport from cervical PNs to supraspinal areas, especially in the rodent. Studies with classical tracers show connections of the CST, RST and ReST onto these neurons (Mitchell et al., 2016; L. T. Brown, 1974; Kuchler et al., 2002), and thus we expected GFP signal in the RN and FMC. We saw that HiRet transported well to neurons of the RN, but labeled only a very small population in the FMC. We suspect that receptors necessary for intake of HiRet at the synapse, such as NCAM or p75^{NTR}, are only weakly expressed on adult CST neurons (Mao et al., 2012; Charles et al., 2000), and thus this vector may not be a good fit for studies targeted at the CST.

Interestingly, the group that developed HiRet has been continually modifying this vector, and has now released a version that may have better expression in the brain. This vector, which has a modified junction of Rabies Virus Glycoprotein (RVG) and VSV-G segments in the membrane (now termed FUG-E), is also modified to be more specific to neurons, so that it will not infect glia at the injection site (Kato et al., 2014). Considering our findings, we think that HiRet is a superior vector for retrograde transport along the rubro- and reticulospinal tracts, as well as to various populations of PNs. For studies targeting the CST, the new FUG-E modified vector may work more efficiently.

Our HiRet-GFP tracing studies found that neurons of the ReST and cervical LDPNs may contribute to spontaneous recovery after a low thoracic contusion, and that cervical LDPNs may perform midline crossings while sprouting to make new connections. This is supported by data showing compensatory circuit formation of reticulospinal and corticospinal fibers, including midline crossings of the CST (Lemon and Griffiths, 2005; Filli et al., 2014). Comparative studies of TPNs and LDPNs also demonstrated that LDPNs undergo significantly less apoptosis after a thoracic contusion, though this study also reports a downregulation of genes involved with regeneration in this population (Siebert et al., 2010).

It should be noted that the neuronal counts seen in this study contained some degree of variability. This was also true in comparable studies (Liang et al., 2011; Reed et al., 2006) and can be attributed to a number of factors, which can be divided into two main categories – biological and procedural. Biological causes may include interanimal variability, and differential percentage of uptake of the virus. Each animal may have slightly different anatomy, which would affect the number of projections from any given nucleus to the target area. These counts also rely on viral uptake at the synapse, which is likely to have some variability between animals in studies that employ retrograde tracing (unpublished observations). It has been demonstrated that HiRet increases the efficiency of uptake over other lentiviral vectors overall (Hirano et al., 2013), however since traditional lentiviral vectors do not perform retrograde transport well, uptake at the synapse is more difficult to compare.

Procedural causes of variability could include differences in targeting and diffusion at the injection area, variability of fluorescent signal seen due to the IHC

procedure, and variation in the decision processes made during stereological counting. When performing spinal cord injections, slight adjustments of the injection needle up or down may change the laminar targets so that a slightly different population of synapses is being covered. Lentiviral vectors are large particles, and this limits the spread through the extracellular space (Cetin et al., 2006; Lerchner et al., 2014). For example, one microliter of a VSV-G pseudotyped lentivirus injected into the brain had a spread of 1-2 mm away from the injection site (Desmaris et al., 2001; Linterman et al., 2011). Subtle equipment failures such as a partially blocked needle or compromised injector pressure may influence the amount of virus injected and diffused throughout the area. IHC also introduces a degree of variability, as the amount of fluorescence seen on each piece of tissue can vary slightly. Lastly, the stereological counting procedure does require some objective judgements when analyzing tissue. Each neuron within the parameters may have a varying strength of signal, and it is up to the counter to determine what strength of signal constitutes a positive neuron. Every effort is made to minimize the effect of these procedural variations, but the cumulative tally of them does contribute to data spread.

Propriospinal neurons need further study, especially after contusive injury, and our data contributes to the understanding of how they might differentially contribute to spontaneous recovery. A next step might be to use trans-synaptic tracers to highlight connections between supraspinal and PNs after contusion, verifying the exact cells that are restoring active circuits. We initially tried this with an AAV2-mCherry-P2A-WGA vector, which theoretically would allow transfer of WGA to second order neurons during anterograde tracing. However, we could never find a WGA signal in any experiments, despite the mCherry reporter working successfully. Perhaps the use of a different trans-

synaptic tracer could be explored, including retrograde tracer trans-synaptic options (Lanciego and Wouterlood, 2011; Ohara et al., 2009).

When investigating synaptic silencing with the HiRet/TetOn system, we found that HiRet-TRE-eTeNT-eGFP was able to very specifically and brightly transduce neurons of the RN. This is important because, as mentioned in a previous chapter, small nuclei such as the RN can be very challenging to accurately target. The labeling achieved with this system was the most beautifully specific I have encountered in the many times RN labeling was attempted.

In our silencing experiments, we found that the RN had no significant contribution to gross forelimb motor behavior in intact rats. Or, at least, that other undamaged tracts may serve such a parallel function that immediate compensation can occur. This is supported by literature that shows that the CST and RST are intertwined pathways. For example, a direct connection exists between the RN and the motor cortex, and direct stimulation of the cortex excites ipsilateral neurons in the RN (Tsukahara et al., 1964). Studies in cats and macaques find that these pathways can compensate for each other when one is lesioned (Goldberger, 1965; Z'Graggen et al., 1998; Evans, B.H., Ingram, W.R., 1939). It may be that the main function of the RST in gross motor movement is as a kind of backup system, most active when the system is in peril.

It is also worth noting that the behavioral contribution of the RST could be more subtle than the behavioral tests in these experiments can ascertain. The Whishaw groups study examining a discrete lesion to the magnocellular portion of the RN found a behavioral difference in the arpeggio movement of the forepaw when grasping a pellet, which they caught only on high speed camera (Morris et al., 2015).

Our synaptic silencing experiments also targeted the portion of the CST descending from the FMC. We found deficits in grip strength when a small population of CST neurons was silenced. Though the grip strength test can be a measure of the strength of the forelimb muscles, it also relies on digit wrapping – the animal must wrap its fingers across a metal bar and be able to maintain that grip while being pulled. CST involvement in hand dexterity is well documented (J. Duque et al., 2003; Rosso et al., 2013), and it may be that malfunction in even a small population of neurons is enough to weaken grip and affect the test. The data also shows that even with doxycycline in the system, the deficit was beginning to resolve after 4 days. This is a similar result to the experiment in monkeys exploring hand dexterity with the HiRet/TetOn system – after 3 days grip function started to improve, even though levels of doxycycline in the blood remained the same (Kinoshita et al., 2012). Presumably, compensatory circuits were starting to adapt as time progressed.

Synaptic silencing studies described here are of interest because silencing of the RST and CST in the intact rat has not been thoroughly explored. Lesioning studies are obviously valuable, but as outlined in this document, injury changes more than just the function of the targeted tract, and therefore there are many other variables to take into account that can confuse interpretation of the data. Synaptic silencing experiments in undamaged tissue have greater ‘purity’ in this manner, and should be carried out in as many systems as possible. The HiRet vector is a very useful tool for this purpose, though, as discussed in a previous chapter, the DREADDs system may make a better shutdown mechanism than Tetanus toxin until the problems with leakiness and Tetanus are solved. Future studies working with HiRet-DREADDs could target the pathways outlined in our

HiRet-GFP study that may contribute to spontaneous recovery, to ascertain whether silencing of those circuits would abolish that recovery.

In our final set of experiments exploring the PI3k/AKT pathway, we found that upregulation of Rheb and STAT3 can cause modest regeneration of the RST and improve dieback from a lesion site. This combination was more successful in previously mentioned studies in the retina (Sun et al., 2011a). We have found that throughout all of our studies targeting the RST, the growth response of these fibers has been disappointingly modest and highly variable when targeted with only intrinsic growth factors. The best regeneration seen in rubrospinal neurons seems to be during transplant studies that include cocktails of neurotrophins (Y. Liu et al., 1999; Tobias et al., 2003), and it may be that PI3k/AKT pathway manipulation is not the correct target for rubrospinal neurons to achieve their growth potential.

Somewhat more successful was our exploration of the effects of PTEN antagonist peptides on CST neurons. We found significantly higher numbers of axon profiles caudal to a contusive injury in a subset of animals treated with PAPs 2 and 3. This was important for two reasons – the amount of growth seen was substantial in these animals, and knockdown of PTEN has not been thoroughly studied in CST fibers after contusive injury. The CST has often been refractory to regrowth (Thallmair et al., 1998; Cafferty and Strittmatter, 2006; Case and Tessier-Lavigne, 2005), and thus manipulations that demonstrate substantial regrowth are worth noting, even if the results have some variability. As discussed, genetic knockdown of PTEN in the CST has resulted in substantial regrowth in previous studies, and thus our data using a more clinically relevant knockdown strategy and animal model adds to the excitement around this

intervention. PAPs should be explored in combinatorial studies targeting both intrinsic and extrinsic factors in the rat.

REFERENCES CITED

- Intrathecal administration of scAAV9/JeT-GAN for the treatment of giant axonal neuropathy. (2017).
- Gene transfer clinical trial for spinal muscular atrophy type 1. (2017).
- Adjali O, Marodon G, Steinberg M, Mongellaz C, Thomas-Vaslin V, Jacquet C, Taylor N, Klatzmann D (2005) In vivo correction of ZAP-70 immunodeficiency by intrathymic gene transfer. *J Clin Invest (United States)* 115:2287-2295.
- Adler CE, Fetter RD, Bargmann CI (2006) UNC-6/netrin induces neuronal asymmetry and defines the site of axon formation. *Nat Neurosci (United States)* 9:511-518.
- Ahuja CS, Martin AR, Fehlings M (2016) Recent advances in managing a spinal cord injury secondary to trauma. *F1000Res (England)* 5:10.12688/f1000research.7586.1. eCollection 2016.
- Ahuja CS, Wilson JR, Nori S, Kotter MRN, Druschel C, Curt A, Fehlings MG (2017) Traumatic spinal cord injury. *Nat Rev Dis Primers (England)* 3:17018.
- Aigner L, Arber S, Kapfhammer JP, Laux T, Schneider C, Botteri F, Brenner HR, Caroni P (1995) Overexpression of the neural growth-associated protein GAP-43 induces nerve sprouting in the adult nervous system of transgenic mice. *Cell (United States)* 83:269-278.
- Allan SM, Rothwell NJ (2001) Cytokines and acute neurodegeneration. *Nat Rev Neurosci (England)* 2:734-744.
- Allen AR (1911) Surgery of experimental lesion of spinal cord equivalent to crush injury of fracture dislocation of spinal column: A preliminary report. *The Journal of the American Medical Association* 57:878.
- Allocca M, Doria M, Petrillo M, Colella P, Garcia-Hoyos M, Gibbs D, Kim SR, Maguire A, Rex TS, Di Vicino U, Cuttillo L, Sparrow JR, Williams DS, Bennett J, Auricchio A (2008) Serotype-dependent packaging of large genes in adeno-associated viral vectors results in effective gene delivery in mice. *J Clin Invest (United States)* 118:1955-1964.
- Alstermark B, Pinter MJ, Sasaki S (1992) Descending pathways mediating disynaptic excitation of dorsal neck motoneurons in the cat: Brain stem relay. *Neurosci Res (Ireland)* 15:42-57.

- Alstermark B, Kummel H, Pinter MJ, Tantisira B (1987) Branching and termination of C3-C4 propriospinal neurones in the cervical spinal cord of the cat. *Neurosci Lett (Ireland)* 74:291-296.
- Anderson KD, Gunawan A, Steward O (2007) Spinal pathways involved in the control of forelimb motor function in rats. *Exp Neurol (United States)* 206:318-331.
- Anderson MA, Burda JE, Ren Y, Ao Y, O'Shea TM, Kawaguchi R, Coppola G, Khakh BS, Deming TJ, Sofroniew MV (2016) Astrocyte scar formation aids central nervous system axon regeneration. *Nature (England)* 532:195-200.
- Anderson PN, Campbell G, Zhang Y, Lieberman AR (1998) Cellular and molecular correlates of the regeneration of adult mammalian CNS axons into peripheral nerve grafts. *Prog Brain Res (Netherlands)* 117:211-232.
- Antal M, Sholomenko GN, Moschovakis AK, Storm-Mathisen J, Heizmann CW, Hunziker W (1992) The termination pattern and postsynaptic targets of rubrospinal fibers in the rat spinal cord: A light and electron microscopic study. *J Comp Neurol (United States)* 325:22-37.
- Antri M, Mouffle C, Orsal D, Barthe JY (2003) 5-HT_{1A} receptors are involved in short- and long-term processes responsible for 5-HT-induced locomotor function recovery in chronic spinal rat. *Eur J Neurosci (France)* 18:1963-1972.
- Armantrout E (2017) Nerve conduction studies and needle electromyography. In: *Orthopaedic physical therapy secrets Nerve conduction studies and needle electromyography.*
- Asboth L, Friedli L, Beauparlant J, Martinez-Gonzalez C, Anil S, Rey E, Baud L, Pidpruzhnykova G, Anderson MA, Shkorbatova P, Batti L, Pages S, Kreider J, Schneider BL, Barraud Q, Courtine G (2018) Cortico-reticulo-spinal circuit reorganization enables functional recovery after severe spinal cord contusion. *Nat Neurosci (United States)* 21:576-588.
- Aschauer DF, Kreuz S, Rumpel S (2013) Analysis of transduction efficiency, tropism and axonal transport of AAV serotypes 1, 2, 5, 6, 8 and 9 in the mouse brain. *PLoS One (United States)* 8:e76310.
- Atchison RW, Casto BC, Hammon WM (1965) Adenovirus-associated defective virus particles. *Science (United States)* 149:754-756.
- Ayuso E, Mingozzi F, Montane J, Leon X, Anguela XM, Haurigot V, Edmonson SA, Africa L, Zhou S, High KA, Bosch F, Wright JF (2010) High AAV vector purity results in serotype- and tissue-independent enhancement of transduction efficiency. *Gene Ther (England)* 17:503-510.

- Azzouz M, Hottinger A, Paterna JC, Zurn AD, Aebischer P, Bueler H (2000) Increased motoneuron survival and improved neuromuscular function in transgenic ALS mice after intraspinal injection of an adeno-associated virus encoding bcl-2. *Hum Mol Genet (England)* 9:803-811.
- Bacon SJ, Smith AD (1993) A monosynaptic pathway from an identified vasomotor centre in the medial prefrontal cortex to an autonomic area in the thoracic spinal cord. *Neuroscience (United States)* 54:719-728.
- Ballermann M, Fouad K (2006) Spontaneous locomotor recovery in spinal cord injured rats is accompanied by anatomical plasticity of reticulospinal fibers. *Eur J Neurosci (France)* 23:1988-1996.
- Bambakidis NC, Miller RH (2004) Transplantation of oligodendrocyte precursors and sonic hedgehog results in improved function and white matter sparing in the spinal cords of adult rats after contusion. *Spine J (United States)* 4:16-26.
- Barbeau H, Rossignol S (1991) Initiation and modulation of the locomotor pattern in the adult chronic spinal cat by noradrenergic, serotonergic and dopaminergic drugs. *Brain Res (Netherlands)* 546:250-260.
- Bareyre FM, Schwab ME (2003) Inflammation, degeneration and regeneration in the injured spinal cord: Insights from DNA microarrays. *Trends Neurosci (England)* 26:555-563.
- Bareyre FM, Garzorz N, Lang C, Misgeld T, Buning H, Kerschensteiner M (2011) In vivo imaging reveals a phase-specific role of STAT3 during central and peripheral nervous system axon regeneration. *Proc Natl Acad Sci U S A (United States)* 108:6282-6287.
- Bareyre FM, Kerschensteiner M, Raineteau O, Mettenleiter TC, Weinmann O, Schwab ME (2004) The injured spinal cord spontaneously forms a new intraspinal circuit in adult rats. *Nat Neurosci (United States)* 7:269-277.
- Bartus RT, Baumann TL, Siffert J, Herzog CD, Alterman R, Boulis N, Turner DA, Stacy M, Lang AE, Lozano AM, Olanow CW (2013) Safety/feasibility of targeting the substantia nigra with AAV2-neurturin in parkinson patients. *Neurology (United States)* 80:1698-1701.
- Basso DM, Beattie MS, Bresnahan JC (1996) Graded histological and locomotor outcomes after spinal cord contusion using the NYU weight-drop device versus transection. *Exp Neurol (United States)* 139:244-256.
- Basso DM, Beattie MS, Bresnahan JC (1995) A sensitive and reliable locomotor rating scale for open field testing in rats. *J Neurotrauma (United States)* 12:1-21.

- Beattie MS, Farooqui AA, Bresnahan JC (2000) Review of current evidence for apoptosis after spinal cord injury. *J Neurotrauma (United States)* 17:915-925.
- Belhaj-Saif A, Cheney PD (2000) Plasticity in the distribution of the red nucleus output to forearm muscles after unilateral lesions of the pyramidal tract. *J Neurophysiol (United States)* 83:3147-3153.
- Benkhelifa-Ziyyat S, Besse A, Roda M, Duque S, Astord S, Carcenac R, Marais T, Barkats M (2013) Intramuscular scAAV9-SMN injection mediates widespread gene delivery to the spinal cord and decreases disease severity in SMA mice. *Mol Ther (United States)* 21:282-290.
- Benowitz LI, Lewis ER (1983) Increased transport of 44,000- to 49,000-dalton acidic proteins during regeneration of the goldfish optic nerve: A two-dimensional gel analysis. *J Neurosci (United States)* 3:2153-2163.
- Blesch A, Tuszynski MH (2009) Spinal cord injury: Plasticity, regeneration and the challenge of translational drug development. *Trends Neurosci (England)* 32:41-47.
- Blight AR (2004) Just one word: Plasticity. *Nat Neurosci (United States)* 7:206-208.
- Blight AR (1991) Morphometric analysis of blood vessels in chronic experimental spinal cord injury: Hypervascularity and recovery of function. *J Neurol Sci (Netherlands)* 106:158-174.
- Borras T, Xue W, Choi VW, Bartlett JS, Li G, Samulski RJ, Chisolm SS (2006) Mechanisms of AAV transduction in glaucoma-associated human trabecular meshwork cells. *J Gene Med (England)* 8:589-602.
- Bouard D, Alazard-Dany D, Cosset FL (2009) Viral vectors: From virology to transgene expression. *Br J Pharmacol (England)* 157:153-165.
- Boulis NM, Willmarth NE, Song DK, Feldman EL, Imperiale MJ (2003) Intraneural colchicine inhibition of adenoviral and adeno-associated viral vector remote spinal cord gene delivery. *Neurosurgery (United States)* 52:381-7; discussion 387.
- Brandt HM, Apkarian AV (1992) Biotin-dextran: A sensitive anterograde tracer for neuroanatomic studies in rat and monkey. *J Neurosci Methods (Netherlands)* 45:35-40.
- Bresnahan JC (1978) An electron-microscopic analysis of axonal alterations following blunt contusion of the spinal cord of the rhesus monkey (*macaca mulatta*). *J Neurol Sci (Netherlands)* 37:59-82.

- Brichta AM, Grant G (1985) Cytoarchitectural organization of the spinal cord. In: The rat nervous system. vol. 2, hindbrain and spinal cord Cytoarchitectural organization of the spinal cord. pp293. Academic Press.
- Brosamle C, Schwab ME (1997) Cells of origin, course, and termination patterns of the ventral, uncrossed component of the mature rat corticospinal tract. *J Comp Neurol (United States)* 386:293-303.
- Brown BD, Cantore A, Annoni A, Sergi LS, Lombardo A, Della Valle P, D'Angelo A, Naldini L (2007) A microRNA-regulated lentiviral vector mediates stable correction of hemophilia B mice. *Blood (United States)* 110:4144-4152.
- Brown LT (1974) Rubrospinal projections in the rat. *J Comp Neurol (United States)* 154:169-187.
- Brown TG (1914) On the nature of the fundamental activity of the nervous centres; together with an analysis of the conditioning of rhythmic activity in progression, and a theory of the evolution of function in the nervous system. *J Physiol (England)* 48:18-46.
- Bruehlmeier M, Dietz V, Leenders KL, Roelcke U, Missimer J, Curt A (1998) How does the human brain deal with a spinal cord injury? *Eur J Neurosci (France)* 10:3918-3922.
- Bucher T, Dubreil L, Colle MA, Maquigneau M, Deniaud J, Ledevin M, Moullier P, Joussemet B (2014) Intracisternal delivery of AAV9 results in oligodendrocyte and motor neuron transduction in the whole central nervous system of cats. *Gene Ther (England)* 21:522-528.
- Bunge RP, Puckett WR, Hiester ED (1997) Observations on the pathology of several types of human spinal cord injury, with emphasis on the astrocyte response to penetrating injuries. *Adv Neurol (United States)* 72:305-315.
- Bunge RP, Puckett WR, Becerra JL, Marcillo A, Quencer RM (1993) Observations on the pathology of human spinal cord injury. A review and classification of 22 new cases with details from a case of chronic cord compression with extensive focal demyelination. *Adv Neurol (United States)* 59:75-89.
- Bush MS, Tonge DA, Woolf C, Gordon-Weeks PR (1996) Expression of a developmentally regulated, phosphorylated isoform of microtubule-associated protein 1B in regenerating axons of the sciatic nerve. *Neuroscience (United States)* 73:553-563.
- Cafferty WB, Strittmatter SM (2006) The nogo-nogo receptor pathway limits a spectrum of adult CNS axonal growth. *J Neurosci (United States)* 26:12242-12250.

- Cai D, Qiu J, Cao Z, McAtee M, Bregman BS, Filbin MT (2001) Neuronal cyclic AMP controls the developmental loss in ability of axons to regenerate. *J Neurosci (United States)* 21:4731-4739.
- Cajal RY (1909) *System nerveux de l'homme et des vertebres*. Maloine.
- Cajal SRY, DeFelipe J, Jones EG (1991) *Cajal's degeneration and regeneration of the nervous system*. Oxford Scholarship.
- Camand E, Morel MP, Faissner A, Sotelo C, Dusart I (2004) Long-term changes in the molecular composition of the glial scar and progressive increase of serotonergic fibre sprouting after hemisection of the mouse spinal cord. *Eur J Neurosci (France)* 20:1161-1176.
- Canedo A (1997) Primary motor cortex influences on the descending and ascending systems. *Prog Neurobiol (England)* 51:287-335.
- Carmel JB, Martin JH (2014) Motor cortex electrical stimulation augments sprouting of the corticospinal tract and promotes recovery of motor function. *Front Integr Neurosci (Switzerland)* 8:51.
- Caroni P, Aigner L, Schneider C (1997) Intrinsic neuronal determinants locally regulate extrasynaptic and synaptic growth at the adult neuromuscular junction. *J Cell Biol (United States)* 136:679-692.
- Case LC, Tessier-Lavigne M (2005) Regeneration of the adult central nervous system. *Curr Biol (England)* 15:R749-53.
- Cetin A, Komai S, Eliava M, Seeburg PH, Osten P (2006) Stereotaxic gene delivery in the rodent brain. *Nat Protoc (England)* 1:3166-3173.
- Chadborn NH, Ahmed AI, Holt MR, Prinjha R, Dunn GA, Jones GE, Eickholt BJ (2006) PTEN couples Sema3A signalling to growth cone collapse. *J Cell Sci (England)* 119:951-957.
- Chamberlin NL, Du B, de Lacalle S, Saper CB (1998) Recombinant adeno-associated virus vector: Use for transgene expression and anterograde tract tracing in the CNS. *Brain Res (Netherlands)* 793:169-175.
- Charles P, Hernandez MP, Stankoff B, Aigrot MS, Colin C, Rougon G, Zalc B, Lubetzki C (2000) Negative regulation of central nervous system myelination by polysialylated-neural cell adhesion molecule. *Proc Natl Acad Sci U S A (United States)* 97:7585-7590.

- Cheema SS, Rustioni A, Whitsel BL (1984) Light and electron microscopic evidence for a direct corticospinal projection to superficial laminae of the dorsal horn in cats and monkeys. *J Comp Neurol (United States)* 225:276-290.
- Chen Y, He Y, DeVivo MJ (2016) Changing demographics and injury profile of new traumatic spinal cord injuries in the united states, 1972-2014. *Arch Phys Med Rehabil (United States)* 97:1610-1619.
- Chung K, Coggeshall RE (1983) Propriospinal fibers in the rat. *J Comp Neurol (United States)* 217:47-53.
- Cizkova D, Rosocha J, Vanicky I, Jergova S, Cizek M (2006) Transplants of human mesenchymal stem cells improve functional recovery after spinal cord injury in the rat. *Cell Mol Neurobiol (United States)* 26:1167-1180.
- Clement N, Knop DR, Byrne BJ (2009) Large-scale adeno-associated viral vector production using a herpesvirus-based system enables manufacturing for clinical studies. *Hum Gene Ther (United States)* 20:796-806.
- Conforti L, Gilley J, Coleman MP (2014) Wallerian degeneration: An emerging axon death pathway linking injury and disease. *Nat Rev Neurosci (England)* 15:394-409.
- Conta Steencken AC, Stelzner DJ (2010) Loss of propriospinal neurons after spinal contusion injury as assessed by retrograde labeling. *Neuroscience (United States)* 170:971-980.
- Conta Steencken AC, Smirnov I, Stelzner DJ (2011) Cell survival or cell death: Differential vulnerability of long descending and thoracic propriospinal neurons to low thoracic axotomy in the adult rat. *Neuroscience (United States)* 194:359-371.
- Conta AC, Stelzner DJ (2004) Differential vulnerability of propriospinal tract neurons to spinal cord contusion injury. *J Comp Neurol (United States)* 479:347-359.
- Courtine G, Song B, Roy RR, Zhong H, Herrmann JE, Ao Y, Qi J, Edgerton VR, Sofroniew MV (2008) Recovery of supraspinal control of stepping via indirect propriospinal relay connections after spinal cord injury. *Nat Med (United States)* 14:69-74.
- Courtine G, Gerasimenko Y, van den Brand R, Yew A, Musienko P, Zhong H, Song B, Ao Y, Ichiyama RM, Lavrov I, Roy RR, Sofroniew MV, Edgerton VR (2009) Transformation of nonfunctional spinal circuits into functional states after the loss of brain input. *Nat Neurosci (United States)* 12:1333-1342.
- Crowe MJ, Bresnahan JC, Shuman SL, Masters JN, Beattie MS (1997) Apoptosis and delayed degeneration after spinal cord injury in rats and monkeys. *Nat Med (United States)* 3:73-76.

- Croyle MA, Callahan SM, Auricchio A, Schumer G, Linse KD, Wilson JM, Brunner LJ, Kobinger GP (2004) PEGylation of a vesicular stomatitis virus G pseudotyped lentivirus vector prevents inactivation in serum. *J Virol (United States)* 78:912-921.
- Davies SJ, Goucher DR, Doller C, Silver J (1999) Robust regeneration of adult sensory axons in degenerating white matter of the adult rat spinal cord. *J Neurosci (United States)* 19:5810-5822.
- De la Monte SM, Federoff HJ, Ng SC, Grabczyk E, Fishman MC (1989) GAP-43 gene expression during development: Persistence in a distinctive set of neurons in the mature central nervous system. *Brain Res Dev Brain Res (Netherlands)* 46:161-168.
- de Lima S, Koriyama Y, Kurimoto T, Oliveira JT, Yin Y, Li Y, Gilbert HY, Fagiolini M, Martinez AM, Benowitz L (2012) Full-length axon regeneration in the adult mouse optic nerve and partial recovery of simple visual behaviors. *Proc Natl Acad Sci U S A (United States)* 109:9149-9154.
- Deng YB, Liu Y, Zhu WB, Bi XB, Wang YZ, Ye MH, Zhou GQ (2008) The co-transplantation of human bone marrow stromal cells and embryo olfactory ensheathing cells as a new approach to treat spinal cord injury in a rat model. *Cytotherapy (England)* 10:551-564.
- DePolo NJ, Reed JD, Sheridan PL, Townsend K, Sauter SL, Jolly DJ, Dubensky TW, Jr (2000) VSV-G pseudotyped lentiviral vector particles produced in human cells are inactivated by human serum. *Mol Ther (United States)* 2:218-222.
- Desmaris N, Bosch A, Salaun C, Petit C, Prevost MC, Tordo N, Perrin P, Schwartz O, de Rocquigny H, Heard JM (2001) Production and neurotropism of lentivirus vectors pseudotyped with lyssavirus envelope glycoproteins. *Mol Ther (United States)* 4:149-156.
- Ditunno JF, Little JW, Tessler A, Burns AS (2004) Spinal shock revisited: A four-phase model. *Spinal Cord (England)* 42:383-395.
- Dohrmann GJ, Panjabi MM (1976) "Standardized" spinal cord trauma: Biomechanical parameters and lesion volume. *Surg Neurol (United States)* 6:263-267.
- Dohrmann GJ, Panjabi MM, Banks D (1978) Biomechanics of experimental spinal cord trauma. *J Neurosurg (United States)* 48:993-1001.
- Domeniconi M, Cao Z, Spencer T, Sivasankaran R, Wang K, Nikulina E, Kimura N, Cai H, Deng K, Gao Y, He Z, Filbin M (2002) Myelin-associated glycoprotein interacts with the Nogo66 receptor to inhibit neurite outgrowth. *Neuron (United States)* 35:283-290.

- Don AS, Tsang CK, Kazdoba TM, D'Arcangelo G, Young W, Zheng XF (2012) Targeting mTOR as a novel therapeutic strategy for traumatic CNS injuries. *Drug Discov Today (England)* 17:861-868.
- Dong JY, Fan PD, Frizzell RA (1996) Quantitative analysis of the packaging capacity of recombinant adeno-associated virus. *Hum Gene Ther (United States)* 7:2101-2112.
- Drake PG, Posner BI (1998) Insulin receptor-associated protein tyrosine phosphatase(s): Role in insulin action. *Mol Cell Biochem (Netherlands)* 182:79-89.
- Du K, Zheng S, Zhang Q, Li S, Gao X, Wang J, Jiang L, Liu K (2015) Pten deletion promotes regrowth of corticospinal tract axons 1 year after spinal cord injury. *J Neurosci (United States)* 35:9754-9763.
- Duque J, Thonnard JL, Vandermeeren Y, Sebire G, Cosnard G, Olivier E (2003) Correlation between impaired dexterity and corticospinal tract dysgenesis in congenital hemiplegia. *Brain (England)* 126:732-747.
- Duque SI, Arnold WD, Odermatt P, Li X, Porensky PN, Schmelzer L, Meyer K, Kolb SJ, Schumperli D, Kaspar BK, Burghes AH (2015) A large animal model of spinal muscular atrophy and correction of phenotype. *Ann Neurol (United States)* 77:399-414.
- Dziennis S, Alkayed NJ (2008) Role of signal transducer and activator of transcription 3 in neuronal survival and regeneration. *Rev Neurosci (Germany)* 19:341-361.
- Emery E, Aldana P, Bunge MB, Puckett W, Srinivasan A, Keane RW, Bethea J, Levi AD (1998) Apoptosis after traumatic human spinal cord injury. *J Neurosurg (United States)* 89:911-920.
- Erturk A, Hellal F, Enes J, Bradke F (2007) Disorganized microtubules underlie the formation of retraction bulbs and the failure of axonal regeneration. *J Neurosci (United States)* 27:9169-9180.
- Evans, B.H., Ingram, W.R. (1939) The effects of combined red nucleus and pyramidal lesions in cats. *Journal of Comparative Neurology* 70:.
- Evarts EV, Tanji J (1976) Reflex and intended responses in motor cortex pyramidal tract neurons of monkey. *J Neurophysiol (United States)* 39:1069-1080.
- Falconer JC, Narayana PA, Bhattacharjee M, Liu SJ (1996) Characterization of an experimental spinal cord injury model using waveform and morphometric analysis. *Spine (Phila Pa 1976) (United States)* 21:104-112.

- Faulkner JR, Herrmann JE, Woo MJ, Tansey KE, Doan NB, Sofroniew MV (2004) Reactive astrocytes protect tissue and preserve function after spinal cord injury. *J Neurosci (United States)* 24:2143-2155.
- Fawcett JW et al (2007) Guidelines for the conduct of clinical trials for spinal cord injury as developed by the ICCP panel: Spontaneous recovery after spinal cord injury and statistical power needed for therapeutic clinical trials. *Spinal Cord (England)* 45:190-205.
- Fernandes KJ, Fan DP, Tsui BJ, Cassar SL, Tetzlaff W (1999) Influence of the axotomy to cell body distance in rat rubrospinal and spinal motoneurons: Differential regulation of GAP-43, tubulins, and neurofilament-M. *J Comp Neurol (United States)* 414:495-510.
- Ferrari FK, Samulski T, Shenk T, Samulski RJ (1996) Second-strand synthesis is a rate-limiting step for efficient transduction by recombinant adeno-associated virus vectors. *J Virol (United States)* 70:3227-3234.
- Filbin MT (2003) Myelin-associated inhibitors of axonal regeneration in the adult mammalian CNS. *Nat Rev Neurosci (England)* 4:703-713.
- Filli L, Schwab ME (2015) Structural and functional reorganization of propriospinal connections promotes functional recovery after spinal cord injury. *Neural Regen Res (India)* 10:509-513.
- Filli L, Engmann AK, Zorner B, Weinmann O, Moraitis T, Gullo M, Kasper H, Schneider R, Schwab ME (2014) Bridging the gap: A reticulo-propriospinal detour bypassing an incomplete spinal cord injury. *J Neurosci (United States)* 34:13399-13410.
- Fink RP, Heimer L (1967) Two methods for selective silver impregnation of degenerating axons and their synaptic endings in the central nervous system. *Brain Res (Netherlands)* 4:369-374.
- Fisher KJ, Gao GP, Weitzman MD, DeMatteo R, Burda JF, Wilson JM (1996) Transduction with recombinant adeno-associated virus for gene therapy is limited by leading-strand synthesis. *J Virol (United States)* 70:520-532.
- Fitch MT, Silver J (2008) CNS injury, glial scars, and inflammation: Inhibitory extracellular matrices and regeneration failure. *Exp Neurol (United States)* 209:294-301.
- Flynn JR, Graham BA, Galea MP, Callister RJ (2011) The role of propriospinal interneurons in recovery from spinal cord injury. *Neuropharmacology (England)* 60:809-822.

- Fouad K, Pedersen V, Schwab ME, Brosamle C (2001) Cervical sprouting of corticospinal fibers after thoracic spinal cord injury accompanies shifts in evoked motor responses. *Curr Biol (England)* 11:1766-1770.
- Foust KD, Nurre E, Montgomery CL, Hernandez A, Chan CM, Kaspar BK (2009) Intravascular AAV9 preferentially targets neonatal neurons and adult astrocytes. *Nat Biotechnol (United States)* 27:59-65.
- Foust KD, Wang X, McGovern VL, Braun L, Bevan AK, Haidet AM, Le TT, Morales PR, Rich MM, Burghes AH, Kaspar BK (2010) Rescue of the spinal muscular atrophy phenotype in a mouse model by early postnatal delivery of SMN. *Nat Biotechnol (United States)* 28:271-274.
- Fu H, Samulski RJ, McCown TJ, Picornell YJ, Fletcher D, Muenzer J (2002) Neurological correction of lysosomal storage in a mucopolysaccharidosis IIIB mouse model by adeno-associated virus-mediated gene delivery. *Mol Ther (United States)* 5:42-49.
- Fujito Y, Aoki M (1995) Monosynaptic rubrospinal projections to distal forelimb motoneurons in the cat. *Exp Brain Res (Germany)* 105:181-190.
- Fukata Y, Itoh TJ, Kimura T, Menager C, Nishimura T, Shiromizu T, Watanabe H, Inagaki N, Iwamatsu A, Hotani H, Kaibuchi K (2002) CRMP-2 binds to tubulin heterodimers to promote microtubule assembly. *Nat Cell Biol (England)* 4:583-591.
- Ganem D, Nussbaum AL, Davoli D, Fareed GC (1976) Propagation of a segment of bacteriophage lambda-DNA in monkey cells after covalent linkage to a defective simian virus 40 genome. *Cell (United States)* 7:349-359.
- Geed S, van Kan PLE (2017) Grasp-based functional coupling between reach- and grasp-related components of forelimb muscle activity. *J Mot Behav (United States)* 49:312-328.
- Gelderd JB, Chopin SF (1977) The vertebral level of origin of spinal nerves in the rat. *Anat Rec (United States)* 188:45-47.
- Gensel JC, Tovar CA, Hamers FP, Deibert RJ, Beattie MS, Bresnahan JC (2006) Behavioral and histological characterization of unilateral cervical spinal cord contusion injury in rats. *J Neurotrauma (United States)* 23:36-54.
- Gensert JM, Goldman JE (1997) Endogenous progenitors remyelinate demyelinated axons in the adult CNS. *Neuron (United States)* 19:197-203.
- Geoffroy CG, Lorenzana AO, Kwan JP, Lin K, Ghassemi O, Ma A, Xu N, Creger D, Liu K, He Z, Zheng B (2015) Effects of PTEN and nogo codeletion on corticospinal axon sprouting and regeneration in mice. *J Neurosci (United States)* 35:6413-6428.

- Gilbert PF, Thach WT (1977) Purkinje cell activity during motor learning. *Brain Res (Netherlands)* 128:309-328.
- Goff SP, Berg P (1976) Construction of hybrid viruses containing SV40 and lambda phage DNA segments and their propagation in cultured monkey cells. *Cell (United States)* 9:695-705.
- Goldberger ME (1965) The extrapyramidal systems of the spinal cord: Results of combined spinal and cortical lesions in the macaque. *J Comp Neurol (United States)* 124:161-174.
- GrandPre T, Nakamura F, Vartanian T, Strittmatter SM (2000) Identification of the nogo inhibitor of axon regeneration as a reticulon protein. *Nature (England)* 403:439-444.
- Grieger JC, Samulski RJ (2005) Packaging capacity of adeno-associated virus serotypes: Impact of larger genomes on infectivity and postentry steps. *J Virol (United States)* 79:9933-9944.
- Guertin DA, Sabatini DM (2007) Defining the role of mTOR in cancer. *Cancer Cell (United States)* 12:9-22.
- Guertin DA, Sabatini DM (2005) An expanding role for mTOR in cancer. *Trends Mol Med (England)* 11:353-361.
- Guertin PA (2013) Central pattern generator for locomotion: Anatomical, physiological, and pathophysiological considerations. *Front Neurol (Switzerland)* 3:183.
- Guest JD, Rao A, Olson L, Bunge MB, Bunge RP (1997) The ability of human schwann cell grafts to promote regeneration in the transected nude rat spinal cord. *Exp Neurol (United States)* 148:502-522.
- Guth L, Zhang Z, Steward O (1999) The unique histopathological responses of the injured spinal cord. implications for neuroprotective therapy. *Ann N Y Acad Sci (United States)* 890:366-384.
- Han Z, Berendzen K, Zhong L, Surolia I, Chouthai N, Zhao W, Maina N, Srivastava A, Stacpoole PW (2008) A combined therapeutic approach for pyruvate dehydrogenase deficiency using self-complementary adeno-associated virus serotype-specific vectors and dichloroacetate. *Mol Genet Metab (United States)* 93:381-387.
- Hannila SS, Filbin MT (2008) The role of cyclic AMP signaling in promoting axonal regeneration after spinal cord injury. *Exp Neurol (United States)* 209:321-332.
- Harrison M, O'Brien A, Adams L, Cowin G, Ruitenberg MJ, Sengul G, Watson C (2013) Vertebral landmarks for the identification of spinal cord segments in the mouse. *Neuroimage (United States)* 68:22-29.

- Hawthorne AL, Hu H, Kundu B, Steinmetz MP, Wylie CJ, Deneris ES, Silver J (2011) The unusual response of serotonergic neurons after CNS injury: Lack of axonal dieback and enhanced sprouting within the inhibitory environment of the glial scar. *J Neurosci (United States)* 31:5605-5616.
- Hay N (2005) The akt-mTOR tango and its relevance to cancer. *Cancer Cell (United States)* 8:179-183.
- Hermonat PL, Quirk JG, Bishop BM, Han L (1997) The packaging capacity of adeno-associated virus (AAV) and the potential for wild-type-plus AAV gene therapy vectors. *FEBS Lett (England)* 407:78-84.
- Herzog RW, Hagstrom JN, Kung SH, Tai SJ, Wilson JM, Fisher KJ, High KA (1997) Stable gene transfer and expression of human blood coagulation factor IX after intramuscular injection of recombinant adeno-associated virus. *Proc Natl Acad Sci U S A (United States)* 94:5804-5809.
- Hiersemenzel LP, Curt A, Dietz V (2000) From spinal shock to spasticity: Neuronal adaptations to a spinal cord injury. *Neurology (United States)* 54:1574-1582.
- Higashikawa F, Chang L (2001) Kinetic analyses of stability of simple and complex retroviral vectors. *Virology (United States)* 280:124-131.
- Hill CE, Beattie MS, Bresnahan JC (2001) Degeneration and sprouting of identified descending supraspinal axons after contusive spinal cord injury in the rat. *Exp Neurol (United States)* 171:153-169.
- Hirano M, Kato S, Kobayashi K, Okada T, Yaginuma H, Kobayashi K (2013) Highly efficient retrograde gene transfer into motor neurons by a lentiviral vector pseudotyped with fusion glycoprotein. *PLoS One (United States)* 8:e75896.
- Holaday JW, Faden AI (1983) Spinal shock and injury: Experimental therapeutic approaches. *Adv Shock Res (United States)* 10:95-98.
- Hollis ER, 2nd, Kadoya K, Hirsch M, Samulski RJ, Tuszynski MH (2008) Efficient retrograde neuronal transduction utilizing self-complementary AAV1. *Mol Ther (United States)* 16:296-301.
- Holstege G (1987) Anatomical evidence for an ipsilateral rubrospinal pathway and for direct rubrospinal projections to motoneurons in the cat. *Neurosci Lett (Ireland)* 74:269-274.
- Houle JD, Tom VJ, Mayes D, Wagoner G, Phillips N, Silver J (2006) Combining an autologous peripheral nervous system "bridge" and matrix modification by chondroitinase allows robust, functional regeneration beyond a hemisection lesion of the adult rat spinal cord. *J Neurosci (United States)* 26:7405-7415.

- Ingram WR, Ranson SW, Hannett FI (1932) The direct stimulation of the red nucleus in cats. *J Neurol Psychopathol (England)* 12:219-230.
- Inman DM, Steward O (2003) Ascending sensory, but not other long-tract axons, regenerate into the connective tissue matrix that forms at the site of a spinal cord injury in mice. *J Comp Neurol (United States)* 462:431-449.
- Irvine KA, Ferguson AR, Mitchell KD, Beattie SB, Beattie MS, Bresnahan JC (2010) A novel method for assessing proximal and distal forelimb function in the rat: The irvine, beatties and bresnahan (IBB) forelimb scale. *J Vis Exp (United States)* (46). pii: 2246. doi:10.3791/2246.
- Irvine KA, Ferguson AR, Mitchell KD, Beattie SB, Lin A, Stuck ED, Huie JR, Nielson JL, Talbott JF, Inoue T, Beattie MS, Bresnahan JC (2014) The irvine, beatties, and bresnahan (IBB) forelimb recovery scale: An assessment of reliability and validity. *Front Neurol (Switzerland)* 5:116.
- Jain S, Gupta R (2007) Neural blockade with neurolytic agents. In: Pain management Neural blockade with neurolytic agents.
- Jankowska E, Jukes MG, Lund S, Lundberg A (1967) The effect of DOPA on the spinal cord. 6. half-centre organization of interneurons transmitting effects from the flexor reflex afferents. *Acta Physiol Scand (England)* 70:389-402.
- Janson C, McPhee S, Bilaniuk L, Haselgrove J, Testaiuti M, Freese A, Wang DJ, Shera D, Hurh P, Rupin J, Saslow E, Goldfarb O, Goldberg M, Larijani G, Sharrar W, Liouterman L, Camp A, Kolodny E, Samulski J, Leone P (2002) Clinical protocol. gene therapy of canavan disease: AAV-2 vector for neurosurgical delivery of aspartoacylase gene (ASPA) to the human brain. *Hum Gene Ther (United States)* 13:1391-1412.
- Jaumard NV, Leung J, Gokhale AJ, Guarino BB, Welch WC, Winkelstein BA (2015) Relevant anatomic and morphological measurements of the rat spine: Considerations for rodent models of human spine trauma. *Spine (Phila Pa 1976) (United States)* 40:E1084-92.
- Jin Y, Fischer I, Tessler A, Houle JD (2002) Transplants of fibroblasts genetically modified to express BDNF promote axonal regeneration from supraspinal neurons following chronic spinal cord injury. *Exp Neurol (United States)* 177:265-275.
- Joosten EA, Gribnau AA, Dederen PJ (1987) An anterograde tracer study of the developing corticospinal tract in the rat: Three components. *Brain Res (Netherlands)* 433:121-130.

- Joosten EA, Schuitman RL, Vermelis ME, Dederen PJ (1992) Postnatal development of the ipsilateral corticospinal component in rat spinal cord: A light and electron microscopic anterograde HRP study. *J Comp Neurol (United States)* 326:133-146.
- Jung M, Petrusch B, Stuermer CA (1997) Axon-regenerating retinal ganglion cells in adult rats synthesize the cell adhesion molecule L1 but not TAG-1 or SC-1. *Mol Cell Neurosci (United States)* 9:116-131.
- Kalil K, Skene JH (1986) Elevated synthesis of an axonally transported protein correlates with axon outgrowth in normal and injured pyramidal tracts. *J Neurosci (United States)* 6:2563-2570.
- Kamber D, Erez H, Spira ME (2009) Local calcium-dependent mechanisms determine whether a cut axonal end assembles a retarded endbulb or competent growth cone. *Exp Neurol (United States)* 219:112-125.
- Kaplitt MG, Leone P, Samulski RJ, Xiao X, Pfaff DW, O'Malley KL, During MJ (1994) Long-term gene expression and phenotypic correction using adeno-associated virus vectors in the mammalian brain. *Nat Genet (United States)* 8:148-154.
- Kaplitt MG, Feigin A, Tang C, Fitzsimons HL, Mattis P, Lawlor PA, Bland RJ, Young D, Strybing K, Eidelberg D, During MJ (2007) Safety and tolerability of gene therapy with an adeno-associated virus (AAV) borne GAD gene for parkinson's disease: An open label, phase I trial. *Lancet (England)* 369:2097-2105.
- Kaspar BK, Llado J, Sherkat N, Rothstein JD, Gage FH (2003) Retrograde viral delivery of IGF-1 prolongs survival in a mouse ALS model. *Science (United States)* 301:839-842.
- Kato S, Kobayashi K, Kobayashi K (2014) Improved transduction efficiency of a lentiviral vector for neuron-specific retrograde gene transfer by optimizing the junction of fusion envelope glycoprotein. *J Neurosci Methods (Netherlands)* 227:151-158.
- Kato S, Kuramochi M, Kobayashi K, Fukabori R, Okada K, Uchigashima M, Watanabe M, Tsutsui Y, Kobayashi K (2011) Selective neural pathway targeting reveals key roles of thalamostriatal projection in the control of visual discrimination. *J Neurosci (United States)* 31:17169-17179.
- Kato S, Kobayashi K, Inoue K, Kuramochi M, Okada T, Yaginuma H, Morimoto K, Shimada T, Takada M, Kobayashi K (2011) A lentiviral strategy for highly efficient retrograde gene transfer by pseudotyping with fusion envelope glycoprotein. *Hum Gene Ther (United States)* 22:197-206.
- Katz LC, Iarovici DM (1990) Green fluorescent latex microspheres: A new retrograde tracer. *Neuroscience (United States)* 34:511-520.

- Katz LC, Burkhalter A, Dreyer WJ (1984) Fluorescent latex microspheres as a retrograde neuronal marker for in vivo and in vitro studies of visual cortex. *Nature (England)* 310:498-500.
- Kawata K, Morimoto T, Ohashi T, Tsujimoto S, Hoshida T, Tsunoda S, Sakaki T (1993) Experimental study of acute spinal cord injury: A histopathological study. *No Shinkei Geka (Japan)* 21:45-51.
- Keefe KM, Sheikh IS, Smith GM (2017) Targeting neurotrophins to specific populations of neurons: NGF, BDNF, and NT-3 and their relevance for treatment of spinal cord injury. *Int J Mol Sci (Switzerland)* 18:10.3390/ijms18030548.
- Kelamangalath L, Tang X, Bezik K, Sterling N, Son YJ, Smith GM (2015) Neurotrophin selectivity in organizing topographic regeneration of nociceptive afferents. *Exp Neurol (United States)* 271:262-278.
- Kells AP, Hadaczek P, Yin D, Bringas J, Varenika V, Forsayeth J, Bankiewicz KS (2009) Efficient gene therapy-based method for the delivery of therapeutics to primate cortex. *Proc Natl Acad Sci U S A (United States)* 106:2407-2411.
- Kennedy PR (1979) The rubro-olivo-cerebellar teaching circuit. *Med Hypotheses (United States)* 5:799-807.
- Khan T, Havey RM, Sayers ST, Patwardhan A, King WW (1999) Animal models of spinal cord contusion injuries. *Lab Anim Sci (United States)* 49:161-172.
- Kilmer SL, Carlsen RC (1984) Forskolin activation of adenylate cyclase in vivo stimulates nerve regeneration. *Nature (England)* 307:455-457.
- Kim BG, Dai HN, McAtee M, Vicini S, Bregman BS (2006) Remodeling of synaptic structures in the motor cortex following spinal cord injury. *Exp Neurol (United States)* 198:401-415.
- Kinoshita M, Matsui R, Kato S, Hasegawa T, Kasahara H, Isa K, Watakabe A, Yamamori T, Nishimura Y, Alstermark B, Watanabe D, Kobayashi K, Isa T (2012) Genetic dissection of the circuit for hand dexterity in primates. *Nature (England)* 487:235-238.
- Kirshblum S, Millis S, McKinley W, Tulskey D (2004) Late neurologic recovery after traumatic spinal cord injury. *Arch Phys Med Rehabil (United States)* 85:1811-1817.
- Kjell J, Olson L (2016) Rat models of spinal cord injury: From pathology to potential therapies. *Dis Model Mech (England)* 9:1125-1137.

- Kobayashi K, Kato S, Inoue K, Takada M, Kobayashi K (2016) Altering entry site preference of lentiviral vectors into neuronal cells by pseudotyping with envelope glycoproteins. *Methods Mol Biol (United States)* 1382:175-186.
- Kobayashi NR, Fan DP, Giehl KM, Bedard AM, Wiegand SJ, Tetzlaff W (1997) BDNF and NT-4/5 prevent atrophy of rat rubrospinal neurons after cervical axotomy, stimulate GAP-43 and Talpha1-tubulin mRNA expression, and promote axonal regeneration. *J Neurosci (United States)* 17:9583-9595.
- Koehn LM, Noor NM, Dong Q, Er SY, Rash LD, King GF, Dziegielewska KM, Saunders NR, Habgood MD (2016) Selective inhibition of ASIC1a confers functional and morphological neuroprotection following traumatic spinal cord injury. *F1000Res (England)* 5:1822.
- Koilkonda R, Yu H, Talla V, Porciatti V, Feuer WJ, Hauswirth WW, Chiodo V, Erger KE, Boye SL, Lewin AS, Conlon TJ, Renner L, Neuringer M, Detrisac C, Guy J (2014) LHON gene therapy vector prevents visual loss and optic neuropathy induced by G11778A mutant mitochondrial DNA: Biodistribution and toxicology profile. *Invest Ophthalmol Vis Sci (United States)* 55:7739-7753.
- Kostyuk PG, Vasilenko DA (1979) Spinal interneurons. *Annu Rev Physiol (United States)* 41:115-126.
- Kristensson K, Lycke E, Sjostrand J (1970) Transport of herpes simplex virus in peripheral nerves. *Acta Physiol Scand Suppl (England)* 357:13-14.
- Kromer LF (1987) Nerve growth factor treatment after brain injury prevents neuronal death. *Science (United States)* 235:214-216.
- Kuchler M, Fouad K, Weinmann O, Schwab ME, Raineteau O (2002) Red nucleus projections to distinct motor neuron pools in the rat spinal cord. *J Comp Neurol (United States)* 448:349-359.
- Kunkel-Bagden E, Dai HN, Bregman BS (1993) Methods to assess the development and recovery of locomotor function after spinal cord injury in rats. *Exp Neurol (United States)* 119:153-164.
- Kurimoto T, Yin Y, Omura K, Gilbert HY, Kim D, Cen LP, Moko L, Kugler S, Benowitz LI (2010) Long-distance axon regeneration in the mature optic nerve: Contributions of oncomodulin, cAMP, and pten gene deletion. *J Neurosci (United States)* 30:15654-15663.
- Kwon BK, Borisoff JF, Tetzlaff W (2002) Molecular targets for therapeutic intervention after spinal cord injury. *Mol Interv (United States)* 2:244-258.

- Lanciego JL, Wouterlood FG (2011) A half century of experimental neuroanatomical tracing. *J Chem Neuroanat (Netherlands)* 42:157-183.
- Landry ES, Lapointe NP, Rouillard C, Levesque D, Hedlund PB, Guertin PA (2006) Contribution of spinal 5-HT_{1A} and 5-HT₇ receptors to locomotor-like movement induced by 8-OH-DPAT in spinal cord-transected mice. *Eur J Neurosci (France)* 24:535-546.
- Laplante M, Sabatini DM (2012) mTOR signaling in growth control and disease. *Cell (United States)* 149:274-293.
- Lee H, McKeon RJ, Bellamkonda RV (2010) Sustained delivery of thermostabilized chABC enhances axonal sprouting and functional recovery after spinal cord injury. *Proc Natl Acad Sci U S A (United States)* 107:3340-3345.
- Lemon RN (2008) Descending pathways in motor control. *Annu Rev Neurosci (United States)* 31:195-218.
- Lemon RN, Griffiths J (2005) Comparing the function of the corticospinal system in different species: Organizational differences for motor specialization? *Muscle Nerve (United States)* 32:261-279.
- Lentz TL, Burrage TG, Smith AL, Tignor GH (1983) The acetylcholine receptor as a cellular receptor for rabies virus. *Yale J Biol Med (United States)* 56:315-322.
- Lerchner W, Corgiat B, Der Minassian V, Saunders RC, Richmond BJ (2014) Injection parameters and virus dependent choice of promoters to improve neuron targeting in the nonhuman primate brain. *Gene Ther (England)* 21:233-241.
- Levy WJ, Jr, Amassian VE, Traad M, Cadwell J (1990) Focal magnetic coil stimulation reveals motor cortical system reorganized in humans after traumatic quadriplegia. *Brain Res (Netherlands)* 510:130-134.
- Lewandowski G, Steward O (2014) AAVshRNA-mediated suppression of PTEN in adult rats in combination with salmon fibrin administration enables regenerative growth of corticospinal axons and enhances recovery of voluntary motor function after cervical spinal cord injury. *J Neurosci (United States)* 34:9951-9962.
- LeWitt PA et al (2011) AAV2-GAD gene therapy for advanced parkinson's disease: A double-blind, sham-surgery controlled, randomised trial. *Lancet Neurol (England)* 10:309-319.
- Li M, Shibata A, Li C, Braun PE, McKerracher L, Roder J, Kater SB, David S (1996) Myelin-associated glycoprotein inhibits neurite/axon growth and causes growth cone collapse. *J Neurosci Res (United States)* 46:404-414.

- Li S, Liu BP, Budel S, Li M, Ji B, Walus L, Li W, Jirik A, Rabacchi S, Choi E, Worley D, Sah DW, Pepinsky B, Lee D, Relton J, Strittmatter SM (2004) Blockade of nogo-66, myelin-associated glycoprotein, and oligodendrocyte myelin glycoprotein by soluble nogo-66 receptor promotes axonal sprouting and recovery after spinal injury. *J Neurosci (United States)* 24:10511-10520.
- Liang H, Paxinos G, Watson C (2012) The red nucleus and the rubrospinal projection in the mouse. *Brain Struct Funct (Germany)* 217:221-232.
- Liang H, Paxinos G, Watson C (2011) Projections from the brain to the spinal cord in the mouse. *Brain Struct Funct (Germany)* 215:159-186.
- Linterman KS, Palmer DN, Kay GW, Barry LA, Mitchell NL, McFarlane RG, Black MA, Sands MS, Hughes SM (2011) Lentiviral-mediated gene transfer to the sheep brain: Implications for gene therapy in batten disease. *Hum Gene Ther (United States)* 22:1011-1020.
- Liu K, Lu Y, Lee JK, Samara R, Willenberg R, Sears-Kraxberger I, Tedeschi A, Park KK, Jin D, Cai B, Xu B, Connolly L, Steward O, Zheng B, He Z (2010a) PTEN deletion enhances the regenerative ability of adult corticospinal neurons. *Nat Neurosci (United States)* 13:1075-1081.
- Liu K, Lu Y, Lee JK, Samara R, Willenberg R, Sears-Kraxberger I, Tedeschi A, Park KK, Jin D, Cai B, Xu B, Connolly L, Steward O, Zheng B, He Z (2010b) PTEN deletion enhances the regenerative ability of adult corticospinal neurons. *Nat Neurosci (United States)* 13:1075-1081.
- Liu Y, Keefe K, Tang X, Lin S, Smith GM (2014) Use of self-complementary adeno-associated virus serotype 2 as a tracer for labeling axons: Implications for axon regeneration. *PLoS One (United States)* 9:e87447.
- Liu Y, Kim D, Himes BT, Chow SY, Schallert T, Murray M, Tessler A, Fischer I (1999) Transplants of fibroblasts genetically modified to express BDNF promote regeneration of adult rat rubrospinal axons and recovery of forelimb function. *J Neurosci (United States)* 19:4370-4387.
- Liu Y, Kelamangalath L, Kim H, Han SB, Tang X, Zhai J, Hong JW, Lin S, Son YJ, Smith GM (2016) NT-3 promotes proprioceptive axon regeneration when combined with activation of the mTor intrinsic growth pathway but not with reduction of myelin extrinsic inhibitors. *Exp Neurol (United States)* 283:73-84.
- Liu Y, Wang X, Li W, Zhang Q, Li Y, Zhang Z, Zhu J, Chen B, Williams PR, Zhang Y, Yu B, Gu X, He Z (2017) A sensitized IGF1 treatment restores corticospinal axon-dependent functions. *Neuron (United States)* 95:817-833.e4.

- Liu ZH, Yip PK, Adams L, Davies M, Lee JW, Michael GJ, Priestley JV, Michael-Titus AT (2015) A single bolus of docosahexaenoic acid promotes neuroplastic changes in the innervation of spinal cord interneurons and motor neurons and improves functional recovery after spinal cord injury. *J Neurosci (United States)* 35:12733-12752.
- Lo Bianco C, Schneider BL, Bauer M, Sajadi A, Brice A, Iwatsubo T, Aebischer P (2004) Lentiviral vector delivery of parkin prevents dopaminergic degeneration in an alpha-synuclein rat model of parkinson's disease. *Proc Natl Acad Sci U S A (United States)* 101:17510-17515.
- Lu P, Jones LL, Snyder EY, Tuszynski MH (2003) Neural stem cells constitutively secrete neurotrophic factors and promote extensive host axonal growth after spinal cord injury. *Exp Neurol (United States)* 181:115-129.
- Lumb AB (2017) *Nunn's applied respiratory physiology*.
- Luppi PH, Fort P, Jouviet M (1990) Iontophoretic application of unconjugated cholera toxin B subunit (CTb) combined with immunohistochemistry of neurochemical substances: A method for transmitter identification of retrogradely labeled neurons. *Brain Res (Netherlands)* 534:209-224.
- Ma XM, Blenis J (2009) Molecular mechanisms of mTOR-mediated translational control. *Nat Rev Mol Cell Biol (England)* 10:307-318.
- Ma YH, Zhang Y, Cao L, Su JC, Wang ZW, Xu AB, Zhang SC (2010) Effect of neurotrophin-3 genetically modified olfactory ensheathing cells transplantation on spinal cord injury. *Cell Transplant (United States)* 19:167-177.
- MacLaren RE, Groppe M, Barnard AR, Cottrill CL, Tolmachova T, Seymour L, Clark KR, During MJ, Cremers FP, Black GC, Lotery AJ, Downes SM, Webster AR, Seabra MC (2014) Retinal gene therapy in patients with choroideremia: Initial findings from a phase 1/2 clinical trial. *Lancet (England)* 383:1129-1137.
- Maeda Y, Ikeda U, Ogasawara Y, Urabe M, Takizawa T, Saito T, Colosi P, Kurtzman G, Shimada K, Ozawa K (1997) Gene transfer into vascular cells using adeno-associated virus (AAV) vectors. *Cardiovasc Res (England)* 35:514-521.
- Maguire AM et al (2008) Safety and efficacy of gene transfer for leber's congenital amaurosis. *N Engl J Med (United States)* 358:2240-2248.
- Malik P, Arumugam PI, Yee JK, Puthenveetil G (2005) Successful correction of the human cooley's anemia beta-thalassemia major phenotype using a lentiviral vector flanked by the chicken hypersensitive site 4 chromatin insulator. *Ann N Y Acad Sci (United States)* 1054:238-249.

- Mandel RJ (2010) CERE-110, an adeno-associated virus-based gene delivery vector expressing human nerve growth factor for the treatment of alzheimer's disease. *Curr Opin Mol Ther (England)* 12:240-247.
- Mandel RJ, Spratt SK, Snyder RO, Leff SE (1997) Midbrain injection of recombinant adeno-associated virus encoding rat glial cell line-derived neurotrophic factor protects nigral neurons in a progressive 6-hydroxydopamine-induced degeneration model of parkinson's disease in rats. *Proc Natl Acad Sci U S A (United States)* 94:14083-14088.
- Mao X, Schwend T, Conrad GW (2012) Expression and localization of neural cell adhesion molecule and polysialic acid during chick corneal development. *Invest Ophthalmol Vis Sci (United States)* 53:1234-1243.
- Marino RJ, Ditunno JF, Jr, Donovan WH, Maynard F, Jr (1999) Neurologic recovery after traumatic spinal cord injury: Data from the model spinal cord injury systems. *Arch Phys Med Rehabil (United States)* 80:1391-1396.
- Marks WJ, Jr et al (2010) Gene delivery of AAV2-neurturin for parkinson's disease: A double-blind, randomised, controlled trial. *Lancet Neurol (England)* 9:1164-1172.
- Marr RA, Guan H, Rockenstein E, Kindy M, Gage FH, Verma I, Masliah E, Hersch LB (2004) Neprilysin regulates amyloid beta peptide levels. *J Mol Neurosci (United States)* 22:5-11.
- Martin D, Schoenen J, Delree P, Rigo JM, Rogister B, Leprince P, Moonen G (1993) Syngeneic grafting of adult rat DRG-derived schwann cells to the injured spinal cord. *Brain Res Bull (United States)* 30:507-514.
- Massion J (1967) The mammalian red nucleus. *Physiol Rev (United States)* 47:383-436.
- Matsushita M (1970) The axonal pathways of spinal neurons in the cat. *J Comp Neurol (United States)* 138:391-417.
- McCarty DM (2008) Self-complementary AAV vectors; advances and applications. *Mol Ther (United States)* 16:1648-1656.
- McCarty DM, Monahan PE, Samulski RJ (2001) Self-complementary recombinant adeno-associated virus (scAAV) vectors promote efficient transduction independently of DNA synthesis. *Gene Ther (England)* 8:1248-1254.
- McCown TJ (2011) Adeno-associated virus (AAV) vectors in the CNS. *Curr Gene Ther (Netherlands)* 11:181-188.
- McKeon RJ, Schreiber RC, Rudge JS, Silver J (1991) Reduction of neurite outgrowth in a model of glial scarring following CNS injury is correlated with the expression of

- inhibitory molecules on reactive astrocytes. *J Neurosci (United States)* 11:3398-3411.
- Meeker RB, Williams KS (2015) The p75 neurotrophin receptor: At the crossroad of neural repair and death. *Neural Regen Res (India)* 10:721-725.
- Menei P, Montero-Menei C, Whittemore SR, Bunge RP, Bunge MB (1998) Schwann cells genetically modified to secrete human BDNF promote enhanced axonal regrowth across transected adult rat spinal cord. *Eur J Neurosci (France)* 10:607-621.
- Menetrey D, de Pommery J, Roudier F (1985) Propriospinal fibers reaching the lumbar enlargement in the rat. *Neurosci Lett (Ireland)* 58:257-261.
- Metz GA, Whishaw IQ (2009) The ladder rung walking task: A scoring system and its practical application. *J Vis Exp (United States)* (28). pii: 1204. doi:10.3791/1204.
- Metz GA, Merkler D, Dietz V, Schwab ME, Fouad K (2000) Efficient testing of motor function in spinal cord injured rats. *Brain Res (Netherlands)* 883:165-177.
- Miller S, Reitsma DJ, van der Meche FG (1973) Functional organization of long ascending propriospinal pathways linking lumbo-sacral and cervical segments in the cat. *Brain Res (Netherlands)* 62:169-188.
- Ming GL, Song HJ, Berninger B, Holt CE, Tessier-Lavigne M, Poo MM (1997) cAMP-dependent growth cone guidance by netrin-1. *Neuron (United States)* 19:1225-1235.
- Mitchell EJ, McCallum S, Dewar D, Maxwell DJ (2016) Corticospinal and reticulospinal contacts on cervical commissural and long descending propriospinal neurons in the adult rat spinal cord; evidence for powerful reticulospinal connections. *PLoS One (United States)* 11:e0152094.
- Morcuende S, Delgado-Garcia JM, Ugolini G (2002) Neuronal premotor networks involved in eyelid responses: Retrograde transneuronal tracing with rabies virus from the orbicularis oculi muscle in the rat. *J Neurosci (United States)* 22:8808-8818.
- Morris R, Vallester KK, Newton SS, Kearsley AP, Whishaw IQ (2015) The differential contributions of the parvocellular and the magnocellular subdivisions of the red nucleus to skilled reaching in the rat. *Neuroscience (United States)* 295:48-57.
- Muir GD, Whishaw IQ (2000) Red nucleus lesions impair overground locomotion in rats: A kinetic analysis. *Eur J Neurosci (France)* 12:1113-1122.
- Nakagawa H, Ninomiya T, Yamashita T, Takada M (2015) Reorganization of corticospinal tract fibers after spinal cord injury in adult macaques. *Sci Rep (England)* 5:11986.

- Nakashima A, Maruki Y, Imamura Y, Kondo C, Kawamata T, Kawanishi I, Takata H, Matsuura A, Lee KS, Kikkawa U, Ohsumi Y, Yonezawa K, Kamada Y (2008) The yeast tor signaling pathway is involved in G2/M transition via polo-kinase. *PLoS One (United States)* 3:e2223.
- Nathwani AC et al (2011) Adenovirus-associated virus vector-mediated gene transfer in hemophilia B. *N Engl J Med (United States)* 365:2357-2365.
- Natkunarahaj M, Trittibach P, McIntosh J, Duran Y, Barker SE, Smith AJ, Nathwani AC, Ali RR (2008) Assessment of ocular transduction using single-stranded and self-complementary recombinant adeno-associated virus serotype 2/8. *Gene Ther (England)* 15:463-467.
- Nauta WJ (1952) Selective silver impregnation of degenerating axons in the central nervous system. *Stain Technol (United States)* 27:175-179.
- Neumann S, Woolf CJ (1999) Regeneration of dorsal column fibers into and beyond the lesion site following adult spinal cord injury. *Neuron (United States)* 23:83-91.
- Neumann S, Bradke F, Tessier-Lavigne M, Basbaum AI (2002) Regeneration of sensory axons within the injured spinal cord induced by intraganglionic cAMP elevation. *Neuron (United States)* 34:885-893.
- Nishimura Y, Isa T (2009) Compensatory changes at the cerebral cortical level after spinal cord injury. *Neuroscientist (United States)* 15:436-444.
- Nogradi A, Vrbova G (1994) The use of embryonic spinal cord grafts to replace identified motoneuron pools depleted by a neurotoxic lectin, volkensin. *Exp Neurol (United States)* 129:130-141.
- Novikova LN, Novikov LN, Kellerth JO (2000) Survival effects of BDNF and NT-3 on axotomized rubrospinal neurons depend on the temporal pattern of neurotrophin administration. *Eur J Neurosci (France)* 12:776-780.
- Nussbaum AL, Davoli D, Ganem D, Fareed GC (1976) Construction and propagation of a defective simian virus 40 genome bearing an operator from bacteriophage lambda. *Proc Natl Acad Sci U S A (United States)* 73:1068-1072.
- O'Donovan KJ, Ma K, Guo H, Wang C, Sun F, Han SB, Kim H, Wong JK, Charron J, Zou H, Son YJ, He Z, Zhong J (2014) B-RAF kinase drives developmental axon growth and promotes axon regeneration in the injured mature CNS. *J Exp Med (United States)* 211:801-814.
- Ogawa Y, Sawamoto K, Miyata T, Miyao S, Watanabe M, Nakamura M, Bregman BS, Koike M, Uchiyama Y, Toyama Y, Okano H (2002) Transplantation of in vitro-expanded fetal neural progenitor cells results in neurogenesis and functional

- recovery after spinal cord contusion injury in adult rats. *J Neurosci Res (United States)* 69:925-933.
- Ohara S, Inoue K, Yamada M, Yamawaki T, Koganezawa N, Tsutsui K, Witter MP, Iijima T (2009) Dual transneuronal tracing in the rat entorhinal-hippocampal circuit by intracerebral injection of recombinant rabies virus vectors. *Front Neuroanat (Switzerland)* 3:1.
- Ohtake Y, Park D, Abdul-Muneer PM, Li H, Xu B, Sharma K, Smith GM, Selzer ME, Li S (2014) The effect of systemic PTEN antagonist peptides on axon growth and functional recovery after spinal cord injury. *Biomaterials (Netherlands)* 35:4610-4626.
- Ojano-Dirain C, Glushakova LG, Zhong L, Zolotukhin S, Muzyczka N, Srivastava A, Stacpoole PW (2010) An animal model of PDH deficiency using AAV8-siRNA vector-mediated knockdown of pyruvate dehydrogenase E1 alpha. *Mol Genet Metab (United States)* 101:183-191.
- Okada S, Nakamura M, Katoh H, Miyao T, Shimazaki T, Ishii K, Yamane J, Yoshimura A, Iwamoto Y, Toyama Y, Okano H (2006) Conditional ablation of Stat3 or Socs3 discloses a dual role for reactive astrocytes after spinal cord injury. *Nat Med (United States)* 12:829-834.
- Okada S, Ishii K, Yamane J, Iwanami A, Ikegami T, Katoh H, Iwamoto Y, Nakamura M, Miyoshi H, Okano HJ, Contag CH, Toyama Y, Okano H (2005) In vivo imaging of engrafted neural stem cells: Its application in evaluating the optimal timing of transplantation for spinal cord injury. *Faseb J (United States)* 19:1839-1841.
- Onifer SM, Smith GM, Fouad K (2011) Plasticity after spinal cord injury: Relevance to recovery and approaches to facilitate it. *Neurotherapeutics (United States)* 8:283-293.
- Orlovsky GN (1972) Activity of rubrospinal neurons during locomotion. *Brain Res (Netherlands)* 46:99-112.
- Park KK, Liu K, Hu Y, Smith PD, Wang C, Cai B, Xu B, Connolly L, Kramvis I, Sahin M, He Z (2008) Promoting axon regeneration in the adult CNS by modulation of the PTEN/mTOR pathway. *Science (United States)* 322:963-966.
- Pawliuk R, Westerman KA, Fabry ME, Payen E, Tighe R, Bouhassira EE, Acharya SA, Ellis J, London IM, Eaves CJ, Humphries RK, Beuzard Y, Nagel RL, Lebourch P (2001) Correction of sickle cell disease in transgenic mouse models by gene therapy. *Science (United States)* 294:2368-2371.

- Pineau I, Lacroix S (2007) Proinflammatory cytokine synthesis in the injured mouse spinal cord: Multiphasic expression pattern and identification of the cell types involved. *J Comp Neurol (United States)* 500:267-285.
- Plant GW, Christensen CL, Oudega M, Bunge MB (2003) Delayed transplantation of olfactory ensheathing glia promotes sparing/regeneration of supraspinal axons in the contused adult rat spinal cord. *J Neurotrauma (United States)* 20:1-16.
- Prinjha R, Moore SE, Vinson M, Blake S, Morrow R, Christie G, Michalovich D, Simmons DL, Walsh FS (2000) Inhibitor of neurite outgrowth in humans. *Nature (England)* 403:383-384.
- Qi HX, Stepniowska I, Kaas JH (2000) Reorganization of primary motor cortex in adult macaque monkeys with long-standing amputations. *J Neurophysiol (United States)* 84:2133-2147.
- Qiu J, Cai D, Filbin MT (2002) A role for cAMP in regeneration during development and after injury. *Prog Brain Res (Netherlands)* 137:381-387.
- Raineteau O, Schwab ME (2001) Plasticity of motor systems after incomplete spinal cord injury. *Nat Rev Neurosci (England)* 2:263-273.
- Raineteau O, Fouad K, Bareyre FM, Schwab ME (2002) Reorganization of descending motor tracts in the rat spinal cord. *Eur J Neurosci (France)* 16:1761-1771.
- Reed WR, Shum-Siu A, Onifer SM, Magnuson DS (2006) Inter-enlargement pathways in the ventrolateral funiculus of the adult rat spinal cord. *Neuroscience (United States)* 142:1195-1207.
- Reid JM, Flumerfelt BA, Gwyn DG (1975) An ultrastructural study of the red nucleus in the rat. *J Comp Neurol (United States)* 162:363-385.
- Reiner A, Veenman CL, Medina L, Jiao Y, Del Mar N, Honig MG (2000) Pathway tracing using biotinylated dextran amines. *J Neurosci Methods (Netherlands)* 103:23-37.
- Rexed B (1952) The cytoarchitectonic organization of the spinal cord in the cat. *J Comp Neurol (United States)* 96:414-495.
- Ribotta MG, Provencher J, Feraboli-Lohnherr D, Rossignol S, Privat A, Orsal D (2000) Activation of locomotion in adult chronic spinal rats is achieved by transplantation of embryonic raphe cells reinnervating a precise lumbar level. *J Neurosci (United States)* 20:5144-5152.
- Richardson PM, Issa VM, Aguayo AJ (1984) Regeneration of long spinal axons in the rat. *J Neurocytol (United States)* 13:165-182.

- Rivlin AS, Tator CH (1978) Effect of duration of acute spinal cord compression in a new acute cord injury model in the rat. *Surg Neurol (United States)* 10:38-43.
- Roger M, Cadusseau J (1987) Anatomical evidence of a reciprocal connection between the posterior thalamic nucleus and the parvocellular division of the red nucleus in the rat. A combined retrograde and anterograde study. *Neuroscience (United States)* 21:573-583.
- Romero MI, Rangappa N, Garry MG, Smith GM (2001) Functional regeneration of chronically injured sensory afferents into adult spinal cord after neurotrophin gene therapy. *J Neurosci (United States)* 21:8408-8416.
- Rosenzweig ES, McDonald JW (2004) Rodent models for treatment of spinal cord injury: Research trends and progress toward useful repair. *Curr Opin Neurol (England)* 17:121-131.
- Rosenzweig ES, Courtine G, Jindrich DL, Brock JH, Ferguson AR, Strand SC, Nout YS, Roy RR, Miller DM, Beattie MS, Havton LA, Bresnahan JC, Edgerton VR, Tuszynski MH (2010) Extensive spontaneous plasticity of corticospinal projections after primate spinal cord injury. *Nat Neurosci (United States)* 13:1505-1510.
- Rossignol S (2000) Locomotion and its recovery after spinal injury. *Curr Opin Neurobiol (England)* 10:708-716.
- Rosso C, Valabregue R, Attal Y, Vargas P, Gaudron M, Baronnet F, Bertasi E, Humbert F, Peskine A, Perlberg V, Benali H, Lehericy S, Samson Y (2013) Contribution of corticospinal tract and functional connectivity in hand motor impairment after stroke. *PLoS One (United States)* 8:e73164.
- Ruitenbergh MJ, Levison DB, Lee SV, Verhaagen J, Harvey AR, Plant GW (2005) NT-3 expression from engineered olfactory ensheathing glia promotes spinal sparing and regeneration. *Brain (England)* 128:839-853.
- Ruschel J, Hellal F, Flynn KC, Dupraz S, Elliott DA, Tedeschi A, Bates M, Sliwinski C, Brook G, Dobrindt K, Peitz M, Brustle O, Norenberg MD, Blesch A, Weidner N, Bunge MB, Bixby JL, Bradke F (2015) Axonal regeneration. systemic administration of epothilone B promotes axon regeneration after spinal cord injury. *Science (United States)* 348:347-352.
- Ryan DA, Mastrangelo MA, Narrow WC, Sullivan MA, Federoff HJ, Bowers WJ (2010) Abeta-directed single-chain antibody delivery via a serotype-1 AAV vector improves learning behavior and pathology in alzheimer's disease mice. *Mol Ther (United States)* 18:1471-1481.
- Sabatini DM (2006) mTOR and cancer: Insights into a complex relationship. *Nat Rev Cancer (England)* 6:729-734.

- Salganik M, Hirsch ML, Samulski RJ (2015) Adeno-associated virus as a mammalian DNA vector. *Microbiol Spectr (United States)* 3:10.1128/microbiolspec.MDNA3-0052-2014.
- Samulski RJ, Muzyczka N (2014) AAV-mediated gene therapy for research and therapeutic purposes. *Annu Rev Virol (United States)* 1:427-451.
- Sasaki M, Radtke C, Tan AM, Zhao P, Hamada H, Houkin K, Honmou O, Kocsis JD (2009) BDNF-hypersecreting human mesenchymal stem cells promote functional recovery, axonal sprouting, and protection of corticospinal neurons after spinal cord injury. *J Neurosci (United States)* 29:14932-14941.
- Schaden H, Stuermer CA, Bahr M (1994) GAP-43 immunoreactivity and axon regeneration in retinal ganglion cells of the rat. *J Neurobiol (United States)* 25:1570-1578.
- Scheff SW, Rabchevsky AG, Fugaccia I, Main JA, Lumppp JE, Jr (2003) Experimental modeling of spinal cord injury: Characterization of a force-defined injury device. *J Neurotrauma (United States)* 20:179-193.
- Schmued LC, Fallon JH (1986) Fluoro-gold: A new fluorescent retrograde axonal tracer with numerous unique properties. *Brain Res (Netherlands)* 377:147-154.
- Schnell L, Schneider R, Kolbeck R, Barde YA, Schwab ME (1994) Neurotrophin-3 enhances sprouting of corticospinal tract during development and after adult spinal cord lesion. *Nature (England)* 367:170-173.
- Schreyer DJ, Skene JH (1991) Fate of GAP-43 in ascending spinal axons of DRG neurons after peripheral nerve injury: Delayed accumulation and correlation with regenerative potential. *J Neurosci (United States)* 11:3738-3751.
- Schreyer DJ, Jones EG (1982) Growth and target finding by axons of the corticospinal tract in prenatal and postnatal rats. *Neuroscience (United States)* 7:1837-1853.
- Schwab ME, Strittmatter SM (2014) Nogo limits neural plasticity and recovery from injury. *Curr Opin Neurobiol (England)* 27:53-60.
- Schwab ME, Bartholdi D (1996) Degeneration and regeneration of axons in the lesioned spinal cord. *Physiol Rev (United States)* 76:319-370.
- Scrivens PJ, Alaoui-Jamali MA, Giannini G, Wang T, Loignon M, Batist G, Sandor VA (2003) Cdc25A-inhibitory properties and antineoplastic activity of bisperoxovanadium analogues. *Mol Cancer Ther (United States)* 2:1053-1059.

- Shaner NC, Campbell RE, Steinbach PA, Giepmans BN, Palmer AE, Tsien RY (2004) Improved monomeric red, orange and yellow fluorescent proteins derived from *discosoma* sp. red fluorescent protein. *Nat Biotechnol (United States)* 22:1567-1572.
- Sharma HS, Westman J, Olsson Y, Johansson O, Dey PK (1990) Increased 5-hydroxytryptamine immunoreactivity in traumatized spinal cord. an experimental study in the rat. *Acta Neuropathol (Germany)* 80:12-17.
- Sherrington CS, Laslett EE (1903) Observations on some spinal reflexes and the interconnection of spinal segments. *J Physiol (England)* 29:58-96.
- Shieh JY, Leong SK, Wong WC (1983) Origin of the rubrospinal tract in neonatal, developing, and mature rats. *J Comp Neurol (United States)* 214:79-86.
- Shimizu I, Oppenheim RW, O'Brien M, Shneiderman A (1990) Anatomical and functional recovery following spinal cord transection in the chick embryo. *J Neurobiol (United States)* 21:918-937.
- Siebert JR, Middleton FA, Stelzner DJ (2010) Long descending cervical propriospinal neurons differ from thoracic propriospinal neurons in response to low thoracic spinal injury. *BMC Neurosci (England)* 11:148-2202-11-148.
- Siebert JR, Middleton FA, Stelzner DJ (2010) Intrinsic response of thoracic propriospinal neurons to axotomy. *BMC Neurosci (England)* 11:69-2202-11-69.
- Siegel CS, Fink KL, Strittmatter SM, Cafferty WB (2015) Plasticity of intact rubral projections mediates spontaneous recovery of function after corticospinal tract injury. *J Neurosci (United States)* 35:1443-1457.
- Simard JM, Tsymbalyuk O, Ivanov A, Ivanova S, Bhatta S, Geng Z, Woo SK, Gerzanich V (2007) Endothelial sulfonylurea receptor 1-regulated NC ca-ATP channels mediate progressive hemorrhagic necrosis following spinal cord injury. *J Clin Invest (United States)* 117:2105-2113.
- Skene JH (1989) Axonal growth-associated proteins. *Annu Rev Neurosci (United States)* 12:127-156.
- Skene JH, Willard M (1981) Axonally transported proteins associated with axon growth in rabbit central and peripheral nervous systems. *J Cell Biol (United States)* 89:96-103.
- Smith DS, Skene JH (1997) A transcription-dependent switch controls competence of adult neurons for distinct modes of axon growth. *J Neurosci (United States)* 17:646-658.

- Snyder RO, Miao CH, Patijn GA, Spratt SK, Danos O, Nagy D, Gown AM, Winther B, Meuse L, Cohen LK, Thompson AR, Kay MA (1997) Persistent and therapeutic concentrations of human factor IX in mice after hepatic gene transfer of recombinant AAV vectors. *Nat Genet (United States)* 16:270-276.
- Song G, Ouyang G, Bao S (2005) The activation of akt/PKB signaling pathway and cell survival. *J Cell Mol Med (England)* 9:59-71.
- Song G, Cechvala C, Resnick DK, Dempsey RJ, Rao VL (2001) GeneChip analysis after acute spinal cord injury in rat. *J Neurochem (England)* 79:804-815.
- Song HJ, Ming GL, Poo MM (1997) cAMP-induced switching in turning direction of nerve growth cones. *Nature (England)* 388:275-279.
- Sooksawate T, Isa K, Matsui R, Kato S, Kinoshita M, Kobayashi K, Watanabe D, Kobayashi K, Isa T (2013) Viral vector-mediated selective and reversible blockade of the pathway for visual orienting in mice. *Front Neural Circuits (Switzerland)* 7:162.
- Sroga JM, Jones TB, Kigerl KA, McGaughy VM, Popovich PG (2003) Rats and mice exhibit distinct inflammatory reactions after spinal cord injury. *J Comp Neurol (United States)* 462:223-240.
- Stanton GB (1980) Topographical organization of ascending cerebellar projections from the dentate and interposed nuclei in macaca mulatta: An anterograde degeneration study. *J Comp Neurol (United States)* 190:699-731.
- Sterling P, Kuypers HG (1968) Anatomical organization of the brachial spinal cord of the cat. 3. the propriospinal connections. *Brain Res (Netherlands)* 7:419-443.
- Steward O, Zheng B, Banos K, Yee KM (2007) Response to: Kim et al., "axon regeneration in young adult mice lacking nogo-A/B." *neuron* 38, 187-199. *Neuron (United States)* 54:191-195.
- Strong MK, Blanco JE, Anderson KD, Lewandowski G, Steward O (2009) An investigation of the cortical control of forepaw gripping after cervical hemisection injuries in rats. *Exp Neurol (United States)* 217:96-107.
- Stys PK, Hubatsch DA, Leppanen LL (1998) Effects of K⁺ channel blockers on the anoxic response of CNS myelinated axons. *Neuroreport (England)* 9:447-453.
- Sun F, Park KK, Belin S, Wang D, Lu T, Chen G, Zhang K, Yeung C, Feng G, Yankner BA, He Z (2011a) Sustained axon regeneration induced by co-deletion of PTEN and SOCS3. *Nature (England)* 480:372-375.

- Sun F, Park KK, Belin S, Wang D, Lu T, Chen G, Zhang K, Yeung C, Feng G, Yankner BA, He Z (2011b) Sustained axon regeneration induced by co-deletion of PTEN and SOCS3. *Nature (England)* 480:372-375.
- Swiech L, Perycz M, Malik A, Jaworski J (2008) Role of mTOR in physiology and pathology of the nervous system. *Biochim Biophys Acta (Netherlands)* 1784:116-132.
- Taccola G, Sayenko D, Gad P, Gerasimenko Y, Edgerton VR (2018) And yet it moves: Recovery of volitional control after spinal cord injury. *Prog Neurobiol (England)* 160:64-81.
- Takahashi Y, Nakajima Y (1996) Dermatomes in the rat limbs as determined by antidromic stimulation of sensory C-fibers in spinal nerves. *Pain (United States)* 67:197-202.
- Takami T, Oudega M, Bates ML, Wood PM, Kleitman N, Bunge MB (2002) Schwann cell but not olfactory ensheathing glia transplants improve hindlimb locomotor performance in the moderately contused adult rat thoracic spinal cord. *J Neurosci (United States)* 22:6670-6681.
- Takenobu Y, Hayashi T, Moriwaki H, Nagatsuka K, Naritomi H, Fukuyama H (2013) Motor recovery and microstructural change in rubro-spinal tract in subcortical stroke. *Neuroimage Clin (Netherlands)* 4:201-208.
- Tang XQ, Heron P, Mashburn C, Smith GM (2007) Targeting sensory axon regeneration in adult spinal cord. *J Neurosci (United States)* 27:6068-6078.
- Tator CH, Fehlings MG (1991) Review of the secondary injury theory of acute spinal cord trauma with emphasis on vascular mechanisms. *J Neurosurg (United States)* 75:15-26.
- Tee AR, Blenis J (2005) mTOR, translational control and human disease. *Semin Cell Dev Biol (England)* 16:29-37.
- Tenenbaum L, Chtarto A, Lehtonen E, Velu T, Brotchi J, Levivier M (2004) Recombinant AAV-mediated gene delivery to the central nervous system. *J Gene Med (England)* 6 Suppl 1:S212-22.
- Terashima T (1995) Anatomy, development and lesion-induced plasticity of rodent corticospinal tract. *Neurosci Res (Ireland)* 22:139-161.
- Tervo DG, Hwang BY, Viswanathan S, Gaj T, Lavzin M, Ritola KD, Lindo S, Michael S, Kuleshova E, Ojala D, Huang CC, Gerfen CR, Schiller J, Dudman JT, Hantman AW, Looger LL, Schaffer DV, Karpova AY (2016) A designer AAV variant permits

- efficient retrograde access to projection neurons. *Neuron (United States)* 92:372-382.
- Tetzlaff W, Alexander SW, Miller FD, Bisby MA (1991) Response of facial and rubrospinal neurons to axotomy: Changes in mRNA expression for cytoskeletal proteins and GAP-43. *J Neurosci (United States)* 11:2528-2544.
- Tetzlaff W, Okon EB, Karimi-Abdolrezaee S, Hill CE, Sparling JS, Plemel JR, Plunet WT, Tsai EC, Baptiste D, Smithson LJ, Kawaja MD, Fehlings MG, Kwon BK (2011) A systematic review of cellular transplantation therapies for spinal cord injury. *J Neurotrauma (United States)* 28:1611-1682.
- Thallmair M, Metz GA, Z'Graggen WJ, Raineteau O, Kartje GL, Schwab ME (1998) Neurite growth inhibitors restrict plasticity and functional recovery following corticospinal tract lesions. *Nat Neurosci (United States)* 1:124-131.
- Thoulouze MI, Lafage M, Schachner M, Hartmann U, Cremer H, Lafon M (1998) The neural cell adhesion molecule is a receptor for rabies virus. *J Virol (United States)* 72:7181-7190.
- Tobias CA, Shumsky JS, Shibata M, Tuszynski MH, Fischer I, Tessler A, Murray M (2003) Delayed grafting of BDNF and NT-3 producing fibroblasts into the injured spinal cord stimulates sprouting, partially rescues axotomized red nucleus neurons from loss and atrophy, and provides limited regeneration. *Exp Neurol (United States)* 184:97-113.
- Tohyama T, Kinoshita M, Kobayashi K, Isa K, Watanabe D, Kobayashi K, Liu M, Isa T (2017) Contribution of propriospinal neurons to recovery of hand dexterity after corticospinal tract lesions in monkeys. *Proc Natl Acad Sci U S A (United States)* 114:604-609.
- Toivonen JM, Olivan S, Osta R (2010) Tetanus toxin C-fragment: The courier and the cure? *Toxins (Basel) (Switzerland)* 2:2622-2644.
- Tom VJ, Steinmetz MP, Miller JH, Doller CM, Silver J (2004) Studies on the development and behavior of the dystrophic growth cone, the hallmark of regeneration failure, in an in vitro model of the glial scar and after spinal cord injury. *J Neurosci (United States)* 24:6531-6539.
- Topka H, Cohen LG, Cole RA, Hallett M (1991) Reorganization of corticospinal pathways following spinal cord injury. *Neurology (United States)* 41:1276-1283.
- Trojanowski JQ, Gonatas JO, Gonatas NK (1982) Horseradish peroxidase (HRP) conjugates of cholera toxin and lectins are more sensitive retrogradely transported markers than free HRP. *Brain Res (Netherlands)* 231:33-50.

- Tsiang H, Ceccaldi PE, Lycke E (1991) Rabies virus infection and transport in human sensory dorsal root ganglia neurons. *J Gen Virol (England)* 72 (Pt 5):1191-1194.
- Tsukahara N, Toyama K, Kosaka K (1964) Intracellularly recorded responses of red nucleus neurones during antidromic and orthodromic activation. *Experientia (Switzerland)* 20:632-633.
- Tuffereau C, Benejean J, Blondel D, Kieffer B, Flamand A (1998) Low-affinity nerve-growth factor receptor (P75NTR) can serve as a receptor for rabies virus. *Embo J (England)* 17:7250-7259.
- Tuszynski MH, Steward O (2012) Concepts and methods for the study of axonal regeneration in the CNS. *Neuron (United States)* 74:777-791.
- Tuszynski MH, Gabriel K, Gage FH, Suhr S, Meyer S, Rosetti A (1996) Nerve growth factor delivery by gene transfer induces differential outgrowth of sensory, motor, and noradrenergic neurites after adult spinal cord injury. *Exp Neurol (United States)* 137:157-173.
- Ugolini G (1995) Specificity of rabies virus as a transneuronal tracer of motor networks: Transfer from hypoglossal motoneurons to connected second-order and higher order central nervous system cell groups. *J Comp Neurol (United States)* 356:457-480.
- Urban DJ, Roth BL (2015) DREADDs (designer receptors exclusively activated by designer drugs): Chemogenetic tools with therapeutic utility. *Annu Rev Pharmacol Toxicol (United States)* 55:399-417.
- Urban MW, Ghosh B, Strojny LR, Block CG, Blazejewski SM, Wright MC, Smith GM, Lepore AC (2018) Cell-type specific expression of constitutively-active rheb promotes regeneration of bulbospinal respiratory axons following cervical SCI. *Exp Neurol (United States)* 303:108-119.
- van den Brand R, Heutschi J, Barraud Q, DiGiovanna J, Bartholdi K, Huerlimann M, Friedli L, Vollenweider I, Moraud EM, Duis S, Dominici N, Micera S, Musienko P, Courtine G (2012) Restoring voluntary control of locomotion after paralyzing spinal cord injury. *Science (United States)* 336:1182-1185.
- Vanicky I, Urdzikova L, Saganova K, Cizkova D, Galik J (2001) A simple and reproducible model of spinal cord injury induced by epidural balloon inflation in the rat. *J Neurotrauma (United States)* 18:1399-1407.
- Veenman CL, Reiner A, Honig MG (1992) Biotinylated dextran amine as an anterograde tracer for single- and double-labeling studies. *J Neurosci Methods (Netherlands)* 41:239-254.

- Verma P, Chierzi S, Codd AM, Campbell DS, Meyer RL, Holt CE, Fawcett JW (2005) Axonal protein synthesis and degradation are necessary for efficient growth cone regeneration. *J Neurosci (United States)* 25:331-342.
- Wagner JA, Messner AH, Moran ML, Daifuku R, Kouyama K, Desch JK, Manley S, Norbash AM, Conrad CK, Friberg S, Reynolds T, Guggino WB, Moss RB, Carter BJ, Wine JJ, Flotte TR, Gardner P (1999) Safety and biological efficacy of an adeno-associated virus vector-cystic fibrosis transmembrane regulator (AAV-CFTR) in the cystic fibrosis maxillary sinus. *Laryngoscope (United States)* 109:266-274.
- Walker CL, Xu XM (2014) PTEN inhibitor bisperoxovanadium protects oligodendrocytes and myelin and prevents neuronal atrophy in adult rats following cervical hemiconus spinal cord injury. *Neurosci Lett (Ireland)* 573:64-68.
- Walker CL, Walker MJ, Liu NK, Risberg EC, Gao X, Chen J, Xu XM (2012) Systemic bisperoxovanadium activates akt/mTOR, reduces autophagy, and enhances recovery following cervical spinal cord injury. *PLoS One (United States)* 7:e30012.
- Walker CL, Wang X, Bullis C, Liu NK, Lu Q, Fry C, Deng L, Xu XM (2015) Biphasic bisperoxovanadium administration and schwann cell transplantation for repair after cervical contusive spinal cord injury. *Exp Neurol (United States)* 264:163-172.
- Wall PD, Lidieth M (1997) Five sources of a dorsal root potential: Their interactions and origins in the superficial dorsal horn. *J Neurophysiol (United States)* 78:860-871.
- Wang G, Slepishkin V, Zabner J, Keshavjee S, Johnston JC, Sauter SL, Jolly DJ, Dubensky TW, Jr, Davidson BL, McCray PB, Jr (1999) Feline immunodeficiency virus vectors persistently transduce nondividing airway epithelia and correct the cystic fibrosis defect. *J Clin Invest (United States)* 104:R55-62.
- Wang KC, Koprivica V, Kim JA, Sivasankaran R, Guo Y, Neve RL, He Z (2002) Oligodendrocyte-myelin glycoprotein is a nogo receptor ligand that inhibits neurite outgrowth. *Nature (England)* 417:941-944.
- Wang X, Smith GM, Xu XM (2011) Preferential and bidirectional labeling of the rubrospinal tract with adenovirus-GFP for monitoring normal and injured axons. *J Neurotrauma (United States)* 28:635-647.
- Wang Z, Ma HI, Li J, Sun L, Zhang J, Xiao X (2003) Rapid and highly efficient transduction by double-stranded adeno-associated virus vectors in vitro and in vivo. *Gene Ther (England)* 10:2105-2111.
- Wanner IB, Anderson MA, Song B, Levine J, Fernandez A, Gray-Thompson Z, Ao Y, Sofroniew MV (2013) Glial scar borders are formed by newly proliferated, elongated astrocytes that interact to corral inflammatory and fibrotic cells via

- STAT3-dependent mechanisms after spinal cord injury. *J Neurosci (United States)* 33:12870-12886.
- Waters RL, Yakura JS, Adkins RH, Sie I (1992) Recovery following complete paraplegia. *Arch Phys Med Rehabil (United States)* 73:784-789.
- Watson C, Paxinos G (2007) *The rat brain in stereotactic coordinates*. Academic Press, Inc.
- Watson C, Paxinos G, Kayalioglu G, Heise C (2009) Atlas of the rat spinal cord. In: *The spinal cord Atlas of the rat spinal cord*. pp238-306.
- Weidner N, Blesch A, Grill RJ, Tuszynski MH (1999) Nerve growth factor-hypersecreting schwann cell grafts augment and guide spinal cord axonal growth and remyelinate central nervous system axons in a phenotypically appropriate manner that correlates with expression of L1. *J Comp Neurol (United States)* 413:495-506.
- West MJ, Slomianka L, Gundersen HJ (1991) Unbiased stereological estimation of the total number of neurons in the subdivisions of the rat hippocampus using the optical fractionator. *Anat Rec (United States)* 231:482-497.
- Whishaw IQ, Gorny B, Sarna J (1998) Paw and limb use in skilled and spontaneous reaching after pyramidal tract, red nucleus and combined lesions in the rat: Behavioral and anatomical dissociations. *Behav Brain Res (Netherlands)* 93:167-183.
- Whishaw IQ, Pellis SM, Pellis VC (1992) A behavioral study of the contributions of cells and fibers of passage in the red nucleus of the rat to postural righting, skilled movements, and learning. *Behav Brain Res (Netherlands)* 52:29-44.
- Whishaw IQ, Tomie JA, Ladowsky RL (1990) Red nucleus lesions do not affect limb preference or use, but exacerbate the effects of motor cortex lesions on grasping in the rat. *Behav Brain Res (Netherlands)* 40:131-144.
- Victorin K, Bjorklund A (1992) Axon outgrowth from grafts of human embryonic spinal cord in the lesioned adult rat spinal cord. *Neuroreport (England)* 3:1045-1048.
- Williams PT, Kim S, Martin JH (2014) Postnatal maturation of the red nucleus motor map depends on rubrospinal connections with forelimb motor pools. *J Neurosci (United States)* 34:4432-4441.
- Williams RR, Pearse DD, Tresco PA, Bunge MB (2012) The assessment of adeno-associated vectors as potential intrinsic treatments for brainstem axon regeneration. *J Gene Med (England)* 14:20-34.

- Wu D, Klaw MC, Connors T, Kholodilov N, Burke RE, Tom VJ (2015) Expressing constitutively active rheb in adult neurons after a complete spinal cord injury enhances axonal regeneration beyond a chondroitinase-treated glial scar. *J Neurosci (United States)* 35:11068-11080.
- Wu D, Klaw MC, Kholodilov N, Burke RE, Detloff MR, Cote MP, Tom VJ (2016) Expressing constitutively active rheb in adult dorsal root ganglion neurons enhances the integration of sensory axons that regenerate across a chondroitinase-treated dorsal root entry zone following dorsal root crush. *Front Mol Neurosci (Switzerland)* 9:49.
- Wu J, Zhao W, Zhong L, Han Z, Li B, Ma W, Weigel-Kelley KA, Warrington KH, Srivastava A (2007) Self-complementary recombinant adeno-associated viral vectors: Packaging capacity and the role of rep proteins in vector purity. *Hum Gene Ther (United States)* 18:171-182.
- Wunner WH, Reagan KJ, Koprowski H (1984) Characterization of saturable binding sites for rabies virus. *J Virol (United States)* 50:691-697.
- Xiao X, Li J, Samulski RJ (1998) Production of high-titer recombinant adeno-associated virus vectors in the absence of helper adenovirus. *J Virol (United States)* 72:2224-2232.
- Xiao X, Li J, McCown TJ, Samulski RJ (1997) Gene transfer by adeno-associated virus vectors into the central nervous system. *Exp Neurol (United States)* 144:113-124.
- Xu D, McCarty D, Fernandes A, Fisher M, Samulski RJ, Juliano RL (2005) Delivery of MDR1 small interfering RNA by self-complementary recombinant adeno-associated virus vector. *Mol Ther (United States)* 11:523-530.
- Yang X, Haurigot V, Zhou S, Luo G, Couto LB (2010) Inhibition of hepatitis C virus replication using adeno-associated virus vector delivery of an exogenous anti-hepatitis C virus microRNA cluster. *Hepatology (United States)* 52:1877-1887.
- Ye JH, Houle JD (1997) Treatment of the chronically injured spinal cord with neurotrophic factors can promote axonal regeneration from supraspinal neurons. *Exp Neurol (United States)* 143:70-81.
- Yokoi K, Kachi S, Zhang HS, Gregory PD, Spratt SK, Samulski RJ, Campochiaro PA (2007) Ocular gene transfer with self-complementary AAV vectors. *Invest Ophthalmol Vis Sci (United States)* 48:3324-3328.
- Yoshimura T, Kawano Y, Arimura N, Kawabata S, Kikuchi A, Kaibuchi K (2005) GSK-3beta regulates phosphorylation of CRMP-2 and neuronal polarity. *Cell (United States)* 120:137-149.

- Zaporozhets E, Cowley KC, Schmidt BJ (2006) Propriospinal neurons contribute to bulbospinal transmission of the locomotor command signal in the neonatal rat spinal cord. *J Physiol (England)* 572:443-458.
- Zareen N, Shinozaki M, Ryan D, Alexander H, Amer A, Truong DQ, Khadka N, Sarkar A, Naeem S, Bikson M, Martin JH (2017) Motor cortex and spinal cord neuromodulation promote corticospinal tract axonal outgrowth and motor recovery after cervical contusion spinal cord injury. *Exp Neurol (United States)* 297:179-189.
- Z'Graggen WJ, Metz GA, Kartje GL, Thallmair M, Schwab ME (1998) Functional recovery and enhanced corticofugal plasticity after unilateral pyramidal tract lesion and blockade of myelin-associated neurite growth inhibitors in adult rats. *J Neurosci (United States)* 18:4744-4757.
- Zhou FC, Azmitia EC, Bledsoe S (1995) Rapid serotonergic fiber sprouting in response to ibotenic acid lesion in the striatum and hippocampus. *Brain Res Dev Brain Res (Netherlands)* 84:89-98.
- Ziembra KS, Chaudhry N, Rabchevsky AG, Jin Y, Smith GM (2008) Targeting axon growth from neuronal transplants along preformed guidance pathways in the adult CNS. *J Neurosci (United States)* 28:340-348.
- Zincarelli C, Soltys S, Rengo G, Rabinowitz JE (2008) Analysis of AAV serotypes 1-9 mediated gene expression and tropism in mice after systemic injection. *Mol Ther (United States)* 16:1073-1080.
- Zorner B, Bachmann LC, Filli L, Kapitza S, Gullo M, Bolliger M, Starkey ML, Rothlisberger M, Gonzenbach RR, Schwab ME (2014) Chasing central nervous system plasticity: The brainstem's contribution to locomotor recovery in rats with spinal cord injury. *Brain (England)* 137:1716-1732.
- Zukor K, Belin S, Wang C, Keelan N, Wang X, He Z (2013) Short hairpin RNA against PTEN enhances regenerative growth of corticospinal tract axons after spinal cord injury. *J Neurosci (United States)* 33:15350-15361.